THE UNIVERSITY OF HULL

Introducing an Effect of Climate Change into Global Models

of Rain Fade on Telecommunications Links

being a Thesis submitted for the Degree of

Doctor of Philosophy in Electronic Engineering

In the University of Hull

by

CHANNA RANATUNGA

(BSc)

October 2014

Acknowledgements

I would like to commend my utmost gratitude to Dr. Kevin Paulson, my supervisor, whose sincerity, guidance and encouragement I will never forget and has immensely helped me to finish this work: without your help I would have gained nothing, THANK YOU SIR, for the enormous amount of time that you have invested on me.

I would also like to extend my gratitude to my second supervisor Dr. Timothy Billerby, Mr. N. G. Riley, the School of Engineering and the Graduate School.

Secondly, my upmost thanks and appreciation goes to my loving parents, for their belief in me and allowing me to be aspiring as I wanted. It was under their guidance that I gained so much drive and an ability to tackle challenges head on. Also my two sisters, my in-laws and all my friends: thank you all for standing beside me with continual motivation and your support during the past three years. Special thanks goes to Simon, Himani, Yashodh and Rasika for proofing this thesis.

Finally, and most importantly, I would like to thank my wife Nadee: your support, encouragement, endurance and abiding love were distinctly the core upon which the past seven years of my life have been built. The tolerance of my intermittent unrefined moods is a testimony in itself to your unwavering loyalty and love. THANK YOU!

Abstract

Rain attenuation limits the performance of microwave telecommunication links functioning above approximately 5 GHz. Recent studies have revealed that over the last twenty years the occurrence of rain, at intensities that cause outage on terrestrial links, has experienced a strongly increasing trend in the UK. Globally, the height of rain events has also been observed to increase, which may compound increasing trends in rain fade experienced by Earth-Space communication systems. These climatic changes are almost certainly having significant effect on the performance of existing radio systems, and need to be taken into consideration when planning future systems. The International Telecommunication Union – Radio Section (ITU-R), maintains a set of internationally accepted models for the engineering and regulation of radio systems globally. Although under constant revision, these models assume that atmospheric fading is stationary. This assumption is inherent in the way models are tested.

In this project, a method is developed to estimate global trends in one of the most fundamental parameters to the ITU-R models: the one-minute rain rate exceeded for 0.01% of an average year. This method introduces climate change into the ITU-R model of this parameter: Rec. ITU-R P.837. The new model is tested using a method that does not make a stationary climate assumption. Salonen-Poiares Baptista distribution, which is the fundamental method for developing ITU-R Rec. P.837 has been tested using UK Environment Agency data, but no correlations was found between measured annual accumulations and distribution parameters. Nonetheless a link was found between mean annual total precipitations (M_T) and rain exceeded at larger time percentages such as; 0.1% and 1%.

Table of Contents

CHAPTER 6: A Method to Estimate Trends in Distributions of One-Minute Rain Rates Globally   76

CHAPTER 7: Conclusion and Future Outlook   99

List of Figures

List of Tables

Notation

A	Attenuation level in dB
$A_{0.01}$	Attenuation exceeded for 0.01% of the time in dB
$f(R)$	Annual rain rate probability density function
M_C	Mean annual convective rain accumulation in mm
M_S	Mean annual stratiform rain accumulation in mm
M_T	Mean annual total rain accumulation in mm
P_0	The probability of a one-minute interval experiencing rain
$F(R)$	Complementary cumulative probability distribution or rain rate
P_R	Probability of rain
P_{r6}	Probability of rainy 6-hours periods (%)
R	Rain rate in mm/hr
$R_{0.01\%}$	Rain rate exceeded for 0.01% of the time in mm/hr
γ_R	Specific attenuation of rain in dB/km
Λ	Slope of the drop size distribution
β	Convective fraction
λ	Wavelength

Glossary of Terms

CAMRa	-	Chibolton Advanced Meteorological Radar
CCDF	-	Complimentary Cumulative Distribution Function
dB	-	Decibels
DBSG3	-	ITU-R Study Group 3 Dataset
DMSP	-	Defence Meteorological Satellite Program
DSD	-	Drop Size Distribution
DWD	-	National Meteorological Service of Germany
EA	-	UK Environment Agency
ECMWF	-	European Centre for Medium-Range Weather Forecast
EHF	-	Extremely High Frequency
FMT	-	Fade Mitigation Techniques
GOES	-	Geostationary Operational Environmental Satellite
GPCC	-	Global Precipitation Climatology Centre
GPCP	-	Global Precipitation Climatology Project
IPCC	-	Intergovernmental Panel on Climate Change
IR	-	Infrared
ITU-R	-	International Telecommunication Union - Radio section
JAXA	-	Japan Aerospace Exploration Agency
JMA	-	Japan Meteorological Agency
LEO	-	Low Earth Orbit
METEOSAT	-	Meteorological Satellite
MLE	-	Maximum Likelihood Estimate
MPE	-	Multi Sensor Precipitation Estimate
MTSAT	-	Multifunctional Transport Satellite

NAO	-	North Atlantic Oscillation
NASA	-	National Aeronautics and Space Administration
NCAR	-	National Centre for Atmospheric Research
NCDC	-	National Climate Data Centre
NCEP	-	National Centre for Environmental Prediction
NOAA	-	National Oceanic and Atmospheric Administration
NWP	-	Numerical Weather Predictions
PR	-	Precipitation Radar
QoS	-	Quality of Service
RADAR	-	Radio Detection and Ranging Sector
SGM	-	Satellite Gauge Model
SHF	-	Super High Frequency
SPB	-	Salonen-Poiares Baptista
SSM/I	-	Special Sensor Microwave/Imager
TMI	-	TRMM Microwave Imager
TRMM	-	Tropical Rainfall Measuring Mission
UKCIP	-	United Kingdom Climate Impacts Program
UKEA	-	United Kingdom Environment Agency
UTC	-	Coordinated Universal Time
VASClimO	-	Variability Analysis of Surface Climate Observation
WCRP	-	World Climate Research Program
WMO	-	World Meteorological Organization
ZDI	-	Zero Degree Isotherm

CHAPTER 1

Introduction

Extreme weather conditions affect agriculture, the economy and society due to occasional severe incidents such as heat waves, storms and flooding as a result of heavy rainfall (Maraun et al., 2009). The incidence of excessive precipitation has shown steady trends in many regions around the globe over the last few decades (Trenberth et al., 2007), and further rise associated with global warming are predicted (Meehl et al., 2007). Osborn and Hulme (Osborn et al., 2000) and Maraun, Osborn and Gillett (Maraun et al., 2008) studied the decadal variation of the daily precipitation intensity distribution in the UK and discovered increasing trends in severe precipitation during winter and a smaller increase during the spring and autumn seasons. Significant trends in heavy precipitation events due to climate change in UK, have been identified by UKCIP09 (Jenkins et al., 2009) and the Intergovernmental Panel on Climate Change (IPCC) (Solomon et al., 2007) over the last few decades.

Current ITU−R recommendations assume a stationary climate in prognostic propagation models, model validation and in the methods used to analyse data. All these models and processes may need to be adapted or replaced with methods consistent with known climate trends.

Over the years, many empirical studies have been carried out to identify the possibility of predicting rain attenuation statistics on earth-space paths and terrestrial links. When designing and constructing telecommunication systems, it is critical to be able to accurately predict the probability of fade at outage levels. For systems operating at frequencies above approximately 5 GHz, the dominant

fade mechanism leading to outage is scattering and absorption by hydrometeors i.e. atmospheric particles composed of water, ice and air. The fade distribution is required to set fade margin levels needed to overcome dynamic rain attenuation (Mandeep, 2009). The fade margin is the extra power broadcast to compensate for rain fading and is required for a link to provide the essential Quality of Service (QoS) in terms of capacity and availability. Inaccurate predictions of fade distributions have significant economic costs due to the unreliability of links with low fade margins or the lower packing density of links with high fade margins. The use of a fade margin is the most basic of Fade Mitigation Techniques (FMTs). Other FMTs, for example adaptive coding or modulation or power control, can help maintain QoS when links are available but have little effect during outage (Pasagopoulos et al., 2004).

1.1 Research Motivation

Current ITU-R models and the verification process make the implicit assumption that climatic parameters relevant to propagation are stationary over time. A recent study by Paulson (Paulson, 2010) that analysed UK rain gauge data spanning twenty years, revealed that there is an apparent increasing trend in the incidence of rain rates associated with outage on terrestrial links. The study concludes that observed increasing trends in the incidence of rain rates at outage levels have almost certainly resulted in a doubling or tripling of outage rates on terrestrial links over the last twenty years. Furthermore, it is reasonable to expect these trends to continue into the coming decades. Later papers identified trends in rain height as another climate trend with direct effects on link fade distributions. Paulson and Al-Mreri (Paulson and Al-Mreri, 2011a, Paulson and Al-Mreri, 2011b) identified global trends in rain height and considered the effects on terrestrial and Earth-space links, respectively. Paulson (Paulson, 2011a) considered the combined effects of trends in rain height and in the incidence of rain at outage levels. In the UK these two trends reinforce and lead to greater expected increasing trends in fade.

It is important that the performance of telecommunications systems can be predicted over their lifetime, typically around 30 years. This is required for the business case for new telecommunications systems to be plausible and for appropriate fade mitigation techniques (FMTs) to be implemented. Uncertainty in future performance leads to expensive over-engineering, or viable telecommunications systems not being developed due to inaccurate return on investment projections. This suggests that observed climate trends need to be

integrated into existing ITU-R fade models. The principal aim of this project is to critically analyse global trends in rain distributions.

1.2 Climate Change Scenarios

The recent Intergovernmental Panel on Climate Change (IPCC) report: "Climate Change 2013: The Physical Science Basis" (Stocker et al., 2013) presents clear and strong conclusions after a global assessment of climate change evidence. The report concluded that the warming in the climate system is unequivocal, with clear evidence of warming atmosphere and sea, rising seas levels, increase of greenhouse gasses and melting snow and ice. As an example, it states that the interval 1983-2012 was likely the warmest 30 years in the Northern Hemisphere for the last 1,400 years. Following are some of the main conclusions made in the IPCC climate change:

- "Heat waves are likely to occur frequently and will last for long periods"
- "Extreme precipitation events will likely become more intense and more frequent by end of the century"
- "A nearly ice free arctic ocean before mid-century is likely "

Figure 1.1 compares the Best-Case and Worst-Case scenarios for global climate change acquired from the IPCC Climate Change 2013 report. In the map, the scenario on the left assumes instantaneous global reductions in fossil fuel usage and the scenario on the right assumes "business as usual" just continues.
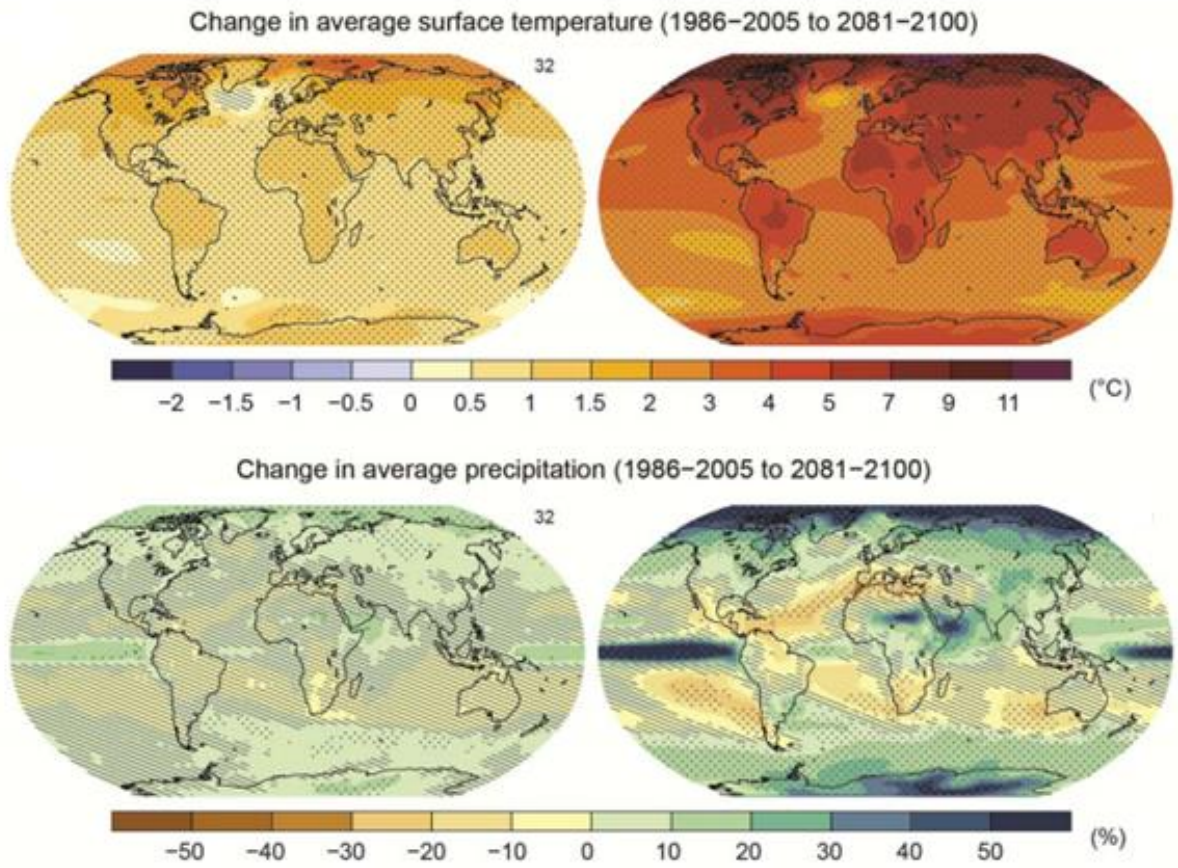
Figure 1.1 Best-Case and Worst-Case scenarios for global climate change (Stocker et al., 2013)

1.3   Increasing Rain Height

Paulson and Al-Mreri (Paulson and Al-Mreri, 2011a) in 2011 discovered rising ZDI (Zero Degree Isotherm) height trends in northern Europe of 8 to 10 meters per year and stated that these trends are likely to increase rain fading on Earth-Space links. It is also understood that general global warming is correlated with ZDI height increase. In 2000 Harris, Bowman and Shin (Harris et al., 2000) performed a comparison of freezing-level altitudes acquired from the National Centres for Environmental Prediction (NCEP) reanalysis data with Tropical Rainfall Measuring Mission (TRMM) precipitation radar data. The study has revealed that positive ZDI height variance is linked to increasing Earth temperature, while Diaz and Graham (Diaz and Graham, 1996) observed a connection between ZDI height and topical sea-surface temperature.

Furthermore, a study carried out by Bradley, Keimig, Diaz and Hardy (Bradley et al., 2009) showed that there was a 30-year increasing tendency in ZDI height in tropical regions with inclines up to 6 m/year. In 2011 Paulson and Al-Mreri investigated trends in rain height and the effects on global satellite telecommunications (Paulson and Al-Mreri, 2011b). The study has looked into NOAA reanalysis data, which yields strong evidence of increasing ZDI height as large as 11 meters per year. The study further suggests that these trends would have increased the rain height by 100m to 200m over regions of global economic importance, in the last 20 years. Over a twenty year period this would cause a 10%-20% increase in rain fading in dB on Earth-space links. This period needs to be taken in the context of the thirty year design-launch-operate-decommission life cycle of a satellite telecommunications system. Furthermore, it states that the

United Kingdom is experiencing a height increase in ZDI and occurrence of heavy precipitation, which will compound increases in rain fading.

1.4   Research Objectives

1. To review internationally recognised models for rain effects on telecommunications links;

2. To identify and analyse current knowledge of trends in rain parameters that affect telecommunications;

3. To critically analyse existing global databases of rain parameters and rain effects on telecommunication;

4. Analyse methods to introduce non-stationary climate parameters into international propagation models;

5. Develop a method to predict trends in rain distributions globally;

6. Validate predictions against known trends in the UK;

7. Suggest a new global rain rate distribution prognostic model (Rec. ITU-R P.837-6) including trends in rain rates.

1.5   Summary of Contributions

During a typical 30 years of a communication systems lifecycle, it is apparent that it will experience many climatic trends and changes. Therefore it is vital that these climate changes and trends are taking into consideration when planning and constructing telecommunication systems. The work in this theses has reviewed and analysed the existing internationally recognized rain fade models to identify current best knowledge of trends in rain parameters that effects telecommunications. Furthermore currently existing global precipitation datasets are critically analysed. The main focus and the objective of this research work has been to explore the introduction of non-stationary or climate trends in to global propagation models.

Major outcome of this work has been the development of a method to predict trends in rain rate distributions globally. Since there is no trend information or guidance currently included in ITU-R Rec. P.837-6, a revised version is proposed with this thesis. The proposed method is tested using known trends over UK. The widely accepted Salonen-Poiares Baptista method has never been tested before. However in this thesis the Salonen-Poiares Baptista distribution is tested using UK environment agency data. The results suggests that there are limitations in Salonen-Poiares Baptista method specifically that it cannot be integrated and therefore distribution cannot be methodically linked with rain accumulations.

1.6 Thesis Outline

This thesis represents a review of research undertaken during three years of study. A brief introduction of research motivation and main objectives have been provided in the previous section. Chapter 2 reviews hydrometeor fade mechanisms. Chapter 3 looks into rain fade modelling including a critical analysis of current ITU-R recommendations. Chapter 4 describes meteorological measurement techniques and examines the existing global databases of rain parameters, particularly reanalysis datasets. Chapter 5 reviews the steps required to estimate one-minute rain rate parameters using Numerical Weather Prediction (NWP) data. Chapter 6 describes a method for estimating global trends in distribution of one-minute rain rates. Chapter 7 summarises the research and conclusions made. Future areas of research are proposed, based on this project's results.

CHAPTER 2

Rain Effects on Microwave Links

Microwave telecommunication links such as Terrestrial and Earth-Space Satellite links, functioning within the EHF (Extremely High Frequency) band (30 GHz – 300 GHz) offer larger bandwidth and high capacity that are require, for applications such as multimedia services. The growing number of users and the increasing complexity of multimedia services, have driven a demand for capacity that has pressured regulators to search higher frequency bands for greater bandwidth. Nonetheless, most of the atmospheric fade mechanisms are frequency dependent and higher frequencies are generally associated with higher losses. Rain attenuation is the dominant fade mechanism on fixed links operating above 5 GHz. Attenuation can be caused by other hydrometeor parameters such as cloud, fog and sleet (wet snow). Scintillation due to refraction through a turbulent atmosphere leads to rapid fading and enhancement. Furthermore, absorption by atmospheric gasses and multipath effects such as ducting also contributes to fade distributions and could be the largest fade mechanism in certain circumstances and for short times. At low EHF frequencies, the wavelength becomes similar in size to large raindrops, and the scattering by drops becomes large. For instance, on the SHF-EHF boundary of 30 GHz, wavelengths are around 10 mm compared to typical raindrop diameters in the range 1 to 8 mm.

Telecommunications engineers use average annual rain statistics to determine the fade margins necessary for a link to achieve the desired availability, typically

99.99% or 99.999% of an average year. The rain rate distribution for any point on Earth may be obtained from Rec. ITU-R P.837-6 (ITU:Rec.P.837-6, 2012), with the caveat that if local rain data is available then statistics derived from these can (and probably should) be used. One of the more important input parameters to annual fade distribution models, for both terrestrial and Earth-space links, is the one-minute rain rate exceeded 0.01% or 0.001% of an average year, depending upon the target availability. These parameters are determined by the extreme rain rates that occur for only 50 minutes, or 5 minutes, in an average year. They exhibit large year-to-year and site-to-site variability, as the rain events that lead to these rain rates are rare, small in area and short in duration. To estimate these parameters to useful accuracy requires at least ten years of point rain data, although rain field data from meteorological radars can provide estimates from shorter duration datasets due to spatial averaging.

2.1 Earth-Space Communication links

Radio communication between Earth and satellites may employ high frequencies as the path through the attenuating troposphere is often short. Due to the link elevation, interference is often a minor issue compared to terrestrial links. Often in commercial Earth-Space telecommunication systems, the satellites are located in geostationary orbit above the equator where the angular velocity of the satellite is equal to the rotation of the earth. The large orbit radius permits a large areal coverage, without the hefty expenses of constructing and maintaining terrestrial networks. A significant parameter when dealing with hydrometeor fade on Earth-Space links is the rain height. The ZDI (Zero Degree Isotherm) height is closely related to rain height. For a stratified, rainy atmosphere, the Earth-Space path

passes through three regions. Near the earth surface, rain will consist entirely of liquid particles and specific attenuation will be close to that predicted by Rec. ITU-R P.838-3 (ITU:Rec.P.838-3, 2005). In the melting layer, due to the presence of large mixed phase particles, specific attenuation associate many times with rain rate of the equivalent intensity. Above the melting layer, all hydrometeors particles will be frozen and specific attenuation at EHF frequencies is close to zero. Rec. ITU-R P.618-11 (ITU:Rec.P.618-11, 2013) includes the effects of melting layer by assuming rain exists up to an altitude known as rain height, assumed in Rec. ITU-R P.837-6 (ITU:Rec.P.837-6, 2012) to be 360m above the ZDI. Average annual rain height can vary from close to the Earth's surface to 5 km, depending on regions and seasonal variations.

2.2 Scattering and Drop Size Distribution

The rain fade experienced by a radio communication link depends on system parameters i.e. frequency and polarisation; link geometry i.e. elevation angle, orientation, link length; and on precipitation parameters such as rain rate and drop size distribution determined by the climate and orography. Hydrometeors cause fading predominantly by scattering radio power out of the beam so it does not reach the receiver. Other effects are less important, such as depolarisation due to asymmetry of drops and by absorption of power. Hydrometeor attenuation is the dominant fade mechanism leading to outage and system unavailability on fixed terrestrial links operating above 5 GHz.

2.2.1   Rain Scattering

Rain drops scatter and absorb the radio wave energy. The Rayleigh scattering model is applicable when the hydrometeor particle is much smaller than the wavelength of the radio wave. The theory predicts that the energy of the incident radio wave is scattered with a radiation pattern similar to that of dipole, and the amount of energy scattered is proportional to a scattering cross-sectional area defined to be $\dfrac{D^3}{\lambda}$, where D is the diameter of the particle and λ is the wavelength.

The more complex Mie scattering model is used when the size of hydrometeor particles are similar to the wavelength. Mie scattering theory can only be applied to spherical objects and therefore it becomes increasingly inaccurate for larger rain drops and is not applicable to most sleet particles. Mie scattering predicts larger peaks in forward and backward scattering directions than the Rayleigh scattering. However the Rayleigh scattering model can be used for most rain scattering effects on microwave links. Figure 2.1 illustrates the Rayleigh and Mie scattering models.
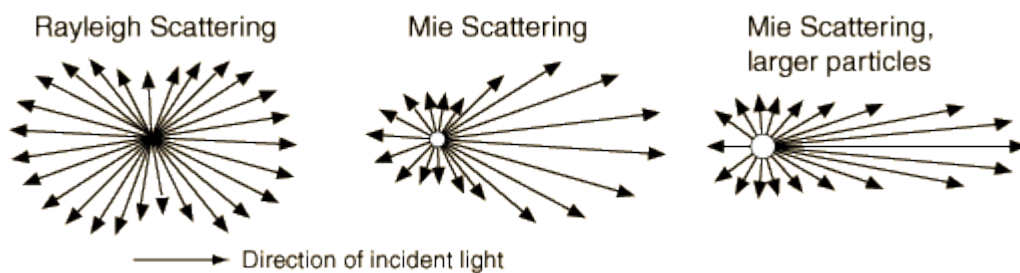
Figure 2.1 Rayleigh and Mie scattering models

(http://hyperphysics.phy-astr.gsu.edu/hbase/atmos/blusky.html)

2.2.2 The Drop Size Distribution

The Drop Size Distribution (DSD) varies in time and space, with rainfall rate as well as with the geographic location. The same rainfall rate can be produced by a range of different drop size distributions. DSD is determined by very complex coalescence and drop break-up processes in the rain column and depends upon many factors including precipitation type, cloud type and wind share. Therefore it is a difficult task to formulate a single DSD model, which describes the actual rain drop size distribution for all rain types and locations. Nevertheless, it is vital to have drop size distribution model so that it can be used to model the attenuation. The distribution of different sizes of raindrops has been studied and modelled since the beginning of the 1940's (Laws and Parsons, 1943, Marshall and Palmer, 1948). In early stages the measurement of DSD was achieved using flour pallets or blotting paper methods. However, more advanced equipment has been designed and built to measure DSD, such as well-known drop impact disdrometer by Joss and Waldvogel (Joss and Waldvogel, 1977) and, more recently, an optical disdrometer (Lempio et al., 2007) was presented. DSD express the number of drops per unit volume and per unit size interval. If all the drops fall at their terminal velocity in still air, the rainfall rate (mm/h) is related to the DSD by;

$$R = C \int_{D_{min}}^{D_{max}} D^3(D)N(D)dD \tag{2.1}$$

The shape of the Drop Size Distribution is often assumed to be exponential (Marshall and Palmer, 1948, Waldvogel, 1974) or a Gamma function (Ulbrich, 1983). Both of these distributions have exponential large drop tails but vary in the proportion of small drops. Some of the variation in the size of the small drop

distribution may be due to the systematic measurement errors related with the distribution measuring instruments.

The Marshall-Palmer exponential DSD is given by:

$$N(D) = N_0 \exp(-\Lambda D), \tag{2.2}$$

where N_0 is the Marshall-Palmer scale parameter and it is approximately 8000 $\text{cm}^{-1}\text{m}^{-3}$.

The value of Λ is given by:

$$\Lambda = 4.1 R^{-0.21}, \tag{2.3}$$

where R is the rainfall rate in mm/hr

It is usually assumed that for the larger sample volumes, exponential DSD models are sufficient. When the sample volumes become smaller, usually for ground based instruments and short integration times, the Gamma distribution often provides a better fit. The Gamma-type distribution is given by:

$$N(D) = N_0 D^\mu \exp(-\Lambda D) \tag{2.4}$$

and Λ is given by:

$$\Lambda = \frac{3.67 + \mu}{D_0}, \tag{2.5}$$

where D_0 is the mean diameter.

The value of μ, the order of the Gamma distribution, varies from -1 to 10. Figure 2.2 illustrates a range of Gamma DSDs. From the equation (2.3), when μ is zero the distribution is a Marshall-Palmer type exponential distribution. For positive μ, the concentration of smaller drops goes to zero as the drop diameter goes to zero. The values of μ can be correlated to a particular type of rain event. For the convective rain the order is in the range $0 \leq \mu \leq 1$, for the stratiform rain type $\mu > 2$ and for orographic $\mu < 0$ (Usman, 2005).
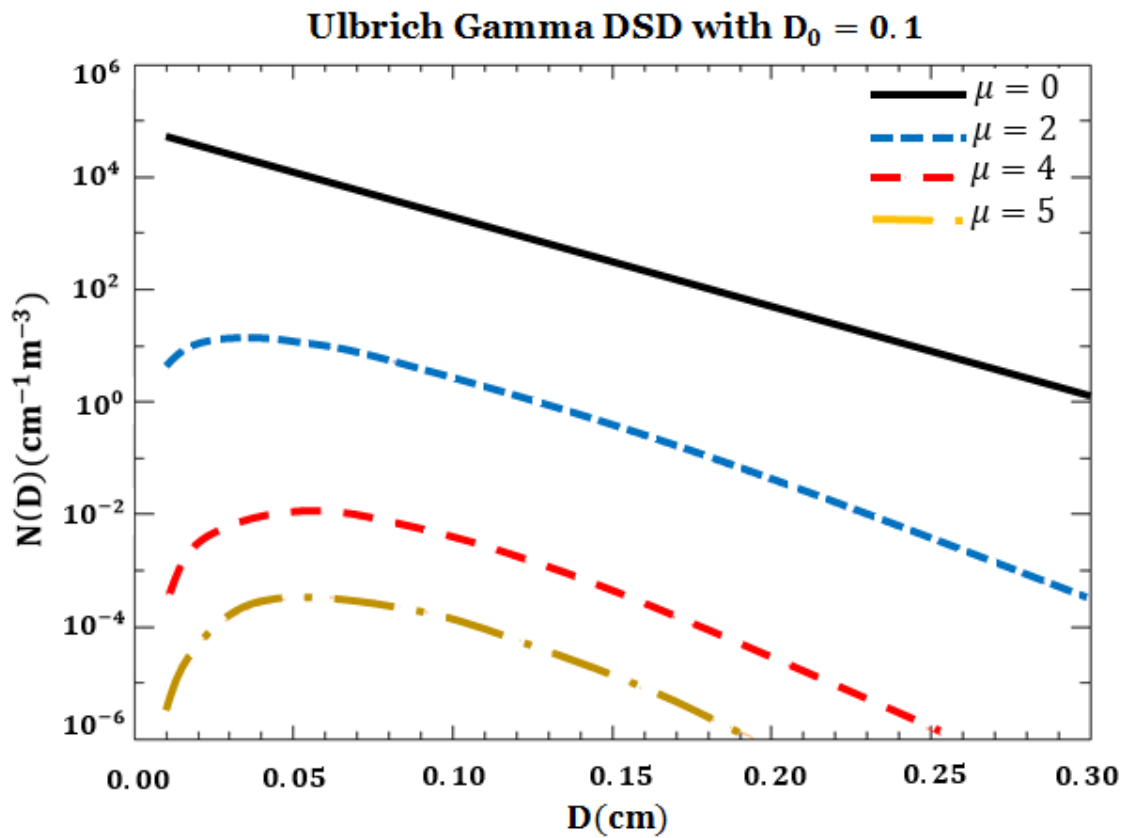
Figure 2.2: Ulbrich Gamma DSD model with variation of μ. D_0 assumed to be 0.1 cm and N_0 is 8000 cm^{-1}m^{-3} (Usman, 2005)

For the same rainfall rate, variation in the DSD can leads to variation in the predicted specific attenuation by a factor of two more or less than the average value. At higher EHF's this uncertainty grows due to the increasing importance of the

smaller rain drops. At millimetre wave frequencies, the uncertainty is large due to variation in the number of large rain drops. Nevertheless the uncertainty in link fade due to this variation is expected to be reduced by integration of specific attenuation along the link path. Using the specific attenuation predicted by Rec. ITU-R P.838-3 (ITU:Rec.P.838-3, 2005) it is expected to be sufficient for the prediction of average annual distributions.

2.3 Rain Attenuation

Rain attenuation (measured in dB) can be defined as the reduction of power in the received signal due to rain, compared to received signal power under clear weather (also known as "clear sky") conditions. The specific attenuation of atmosphere containing rain is a function of many time-varying parameters such as the number of raindrops, raindrop water temperature, raindrop shape and the drop size distribution, the spatial variation of rain parameters and other parameters such as wind velocity, the incidence of up or down drafts and other effects (Lin, 1973).

The total attenuation A along a short path of L experiencing rain can be calculated as the sum of contributions due to each individual drop and it can be derived from;

$$A = 4.34L \int_0^\infty C_{ext}\ N(D)d(D) \tag{2.6}$$

where C_{ext} is the total extinction cross section of the particle and is given by:

$$C_{ext} = \lambda^2/\pi Re[S(\theta)] \tag{2.7}$$

where S(θ) is a dimensionless function of the scattering angle θ and $S(\theta)$ is the forward scatter cross-section (Hulst, 1981). The attenuation in the dB per unit length of propagation path in known as the specific attenuation and is given by;

$$\gamma = \lim_{L \to 0} 10 \log(A)/L \qquad \text{dB/k} \qquad (2.8)$$

The total attenuation experienced by a certain propagation path may be approximated by the path integral of the specific attenuation along the path:

$$A = \int_0^L \Upsilon(\ell)\, d\ell \qquad \text{dB} \qquad (2.9)$$

This approximation does not take multiple paths into account and so is most accurate for narrow beam-widths and high frequencies with thin Fresnel zones.

Rather than explicitly accounting for the spatial variation of rain rate by integrating specific attenuation along paths, ITU-R models use an approximation to estimate average annual fade exceedances:

$$A_{x\%} = \gamma_{x\%} L r \qquad (2.10)$$

In this expression, the link attenuation exceeded $x\%$ of the time is proportional to the point specific attenuation exceeded $x\%$ of time and the link length. If rain rate, and hence rain specific attenuation, were spatially homogeneous then this expression would be adequate. However, as heavier rain tends to be more localised, it is likely that only a proportion of long links will be experiencing the high specific attenuation. To account for this spatial inhomogeneity, a path reduction factor r is introduced. The path reduction factor depends on path length and the rain rate, or equivalently the exceeded time percentage. Many expressions yielding path reduction factors have been proposed. The steps of predicting rain

attenuation exceeded for 0.01% of an average year using Rec. ITU-R P.530-15 (ITU:Rec.P.530-15, 2013) are summarised in chapter 3.

2.4 The Specific Attenuation of Rain

The internationally accepted and recognized model linking rain rate R with specific attenuation γ, is provided by the frequency dependant $\gamma - R$ power law model in Rec. ITU-R P.838-3 (ITU:Rec.P.838-3, 2005). Specific attenuation γ_R (dB/km) is obtained from the rain rate R (mm/h) using the relationship;

$$\gamma_R = kR^\alpha \tag{2.11}$$

where k and α are frequency and polarisation dependent coefficients. They are determined by the equation given below. The coefficients a_i, b_i, c_i and the similar j coefficients, along with c_α, m_α, c_k and m_k are given by the Rec. ITU-R P. 838-3 (ITU:Rec.P.838-3, 2005);

$$\log_{10}k = \sum_{j=1}^{4} a_j \exp\left[-\left(\frac{\log_{10}f - b_j}{c_j}\right)^2\right] + m_k\log_{10}f + c_k \tag{2.12}$$

$$\alpha = \sum_{j=1}^{5} a_j \exp\left[-\left(\frac{\log_{10}f - b_j}{c_j}\right)^2\right] + m_\alpha\log_{10}f + c_\alpha \tag{2.13}$$

where f is the frequency in the range 1 to 1000 GHz.

2.5 The Number and Duration of Rain Fade Events

The rain and fade duration distributions can be described as the number (or proportion) of events in an average year, where rainfall rate or rain fade exceed a certain threshold, in mm/h or dB correspondingly, for a certain duration τ or longer i.e. the rain duration distribution $N(R,\tau)$ is the number of times in an average year when the point rainfall rate exceeded R for a period of at least τ. The relation between rain and rain fade duration distributions is complex and depends upon the specific attenuation – rain rate relationship, the spatial-temporal statistics of rain fields and link geometry. If $T(A)$ is the total time for which an attenuation of A dB is exceeded and $D_m(A)$ is the mean duration for the fades contributing to the total time then number of fade can be given by; $D_m(A) = T(A)/N_\tau(A)$ where, $N_\tau(A)$ is the number of fade. A larger number of different forms have been suggested as good fits to empirically measured rain rate and rain fade duration curves; for example power-laws Rec. ITU-R 838-3 (ITU:Rec.P.838-3, 2005) and log-Normal (Lin, 1973, Easterbrook and Turner, 1967, Turner and Turner, 1970, Paulson and Gibbins, 2000)

2.6 Rain Rate Distribution

Link rain attenuation distributions are generally predicted from point rain statistics provided by rapid response rain gauges. For historical reasons, ITU-R models of rain and rain fade are based on one-minute integration times. It is widely believed that 5 to 10 years of point rain rate data is required to estimate the regional rain rate exceeded for 0.01% of an average year.   Rain rates with lower exceedance probabilities need much longer observation times. The parameter $R_{0.01}$ is the notational point rain rate averaged over a period of 1 min and exceeded for 0.01% of an average year in the link region. Rec. ITU-R P.837-6 (ITU:Rec.P.837-6, 2012) provides yearly statistics for the entire globe, as a function of latitude and longitude, derived from the numerical weather prediction reanalysis data (ERA40). Rec. ITU-R P.837 (ITU:Rec.P.837-6, 2012) is briefly summarised in Chapter 4. The rain rate distribution may be determined experimentally using field measurements and recordings made over long periods of time. If these are not available, as is genearlly the case, globally accepted models such as Rec. ITU-R P.837-6 (ITU:Rec.P.837-6, 2012) and Crane Global model (Crane, 1980) may be used. Both of these models have been derived using NWP (Numerical Weather Prediction) data. Crane's Global Model is presented in Chapter 3. Both the ITU-R and Crane models have their detractors. Noteworthy differences exist between field measurement results and prognostic models. Ambiguity stems from year-to-year and location-to-location variability (Myers, 1999), from methodical errors in numerical weather models and from variation at scales below the model resolution. Comparisons of predicted and measured, long term fade distributions are further complicated by the mix of physical processes

present in the experimental data i.e. multipath is strongly dependent upon the path terrain and this can change dramatically over measurement periods in urban environments.

2.7 Chapter Summary

Microwave links operating above 5 GHz suffer fade due to a range of mechanisms, such as absorption by atmospheric gasses and scattering by solid and liquid hydrometeors. For many high-capacity terrestrial and Earth-space microwave links, hydrometeor fade limits the availability. The ITU-R maintains a set of models, in the P Recommendations, which allow engineers to predict the performance of radio systems globally. Hydrometeors are very complex and highly variable in both space and time. ITU-R models for rain rate distribution and rain specific attenuation, are averages. Specific events or periods can have distributions or specific attenuations that are very different from those provided by ITU-R models. The estimation of these averages requires data often acquired over long periods, often more than a decade, and so inherently assume that the climate is stationary.

CHAPTER 3

Rain Models for Fade Prediction

3.1   Rain Fade Models

To design SHF and EHF radio communication systems, rain attenuation statistics are needed. Historically, annual distribution data derived from rain gauges has been available from selected regions around the world, but mainly in North America and Europe.   Often, point measurements were extrapolated to large geographic regions. The ITU-R maintains a large database DBSG3 (ITU-R Study Group 3 Database) of propagation measurements (ITU-R:StudyGroup3). Typically, these are annual attenuations and/or rain rates exceeded at a small number of prescribed proportions of a year, observed on experimental links. Over the years, several models have been introduced based on these measured distribution statistics and the fundamental physics of rain attenuation, to automate the forecasting process for a location of interest. To predict rain attenuation, rainfall rate statistics are required. These statistics apply to the climate over the path of interest (Crane, 2003). Rain attenuation models fall into two different categories: where the first derives rain fade from measured or modelled rain fields, while the second are empirically derived from fade measurements on many links at several locations. Empirical procedures are most commonly used but both approaches are strictly limited by lack of data.   In microwave system design there are two empirical rain fade models, which are

widely used. Rec. ITU-R P.530-15 (ITU:Rec.P.530-15, 2013) is the internationally recognised model for predicting path attenuation on terrestrial line-of-sight links. Important input parameters come from the $R_{0.01\%}$ climate maps provided by Rec. ITU-R P.837-6 (ITU:Rec.P.837-6, 2012) (or local measurements if available) and the Rec. ITU-R P.838-3 (ITU:Rec.P.838-3, 2005) parameters for the specific attenuation. The second empirical model is the Crane's attenuation predication model (Crane, 1980), which is based on the Crane's global rain rate climate regions and rain rate climate regions within United States.

Rain Rate Climate Regions

Polar:	Temperate:	Sub Tropical:	Tropical:
A Tundra (Dry)	C Maritime	E Wet	G Moderate
B Taiga (Moderate)	D Continental	F Arid	H Wet
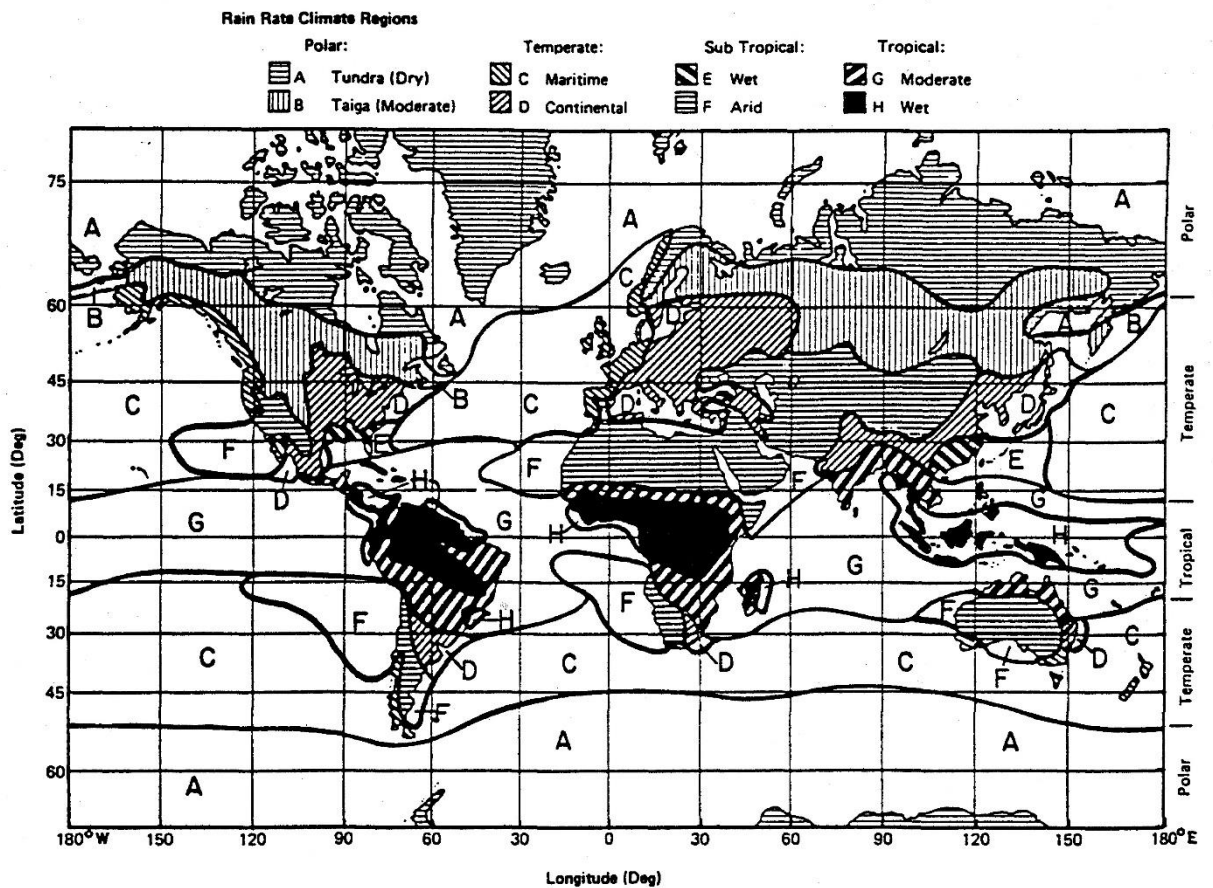
Figure 3.1: Crane's Rain Rate Climate Regions (Crane, 1980)

For terrestrial systems, the ITU has recommended a calculation method specified in Rec. ITU-R P.530-15 (ITU:Rec.P.530-15, 2013), and for Earth-space links Rec. ITU-R P.618-11 (ITU:Rec.P.618-11, 2013) can be used. In these models path-length reduction factors are introduced to account for the spatial variation of rain. The Crane models have been used for both Earth-space and terrestrial links. There are three different versions of Crane models; Global Crane model developed in 1980 (Crane, 1980), Two-Component model developed in 1982 (Crane, 1982) and the Revised Two-Component model developed in 1989 (Crane and Shieh, 1989). Myers (Myers, 1999) states that in most occasions Crane models predict higher rain attenuation than the ITU-R models relevant at the time.

3.1.1 Crane's Global Model

Crane's global model was constructed using empirical data acquired by Bell Laboratories in United States. The rain fade for a range of links with path lengths of 5 km, 10 km and 22.5 km were modelled using data from dual-polarized weather radar. The global model is based on the vertical variation of atmospheric temperature, geophysical surveillance of rainfall rate and rain structure. The path mean model provides the link between the rainfall rate at a given point and the rainfall rate averaged over a straight path of various lengths. A statistical model for the profile of rainfall rate along the path is needed, which then can be used to construct the desired attenuation (Mandeep, 2009). The Crane model has two components: the specific attenuation of rain is given by a power law involving the constants α and β, and a multiplying factor that combines the path length and expected spatial extent of the rain event.

$$A(R_P, D) = \alpha R_P^\beta \left[\frac{e^{u\beta d} - 1}{u\beta} - \frac{b^\beta e^{c\beta d}}{c\beta} + \frac{b^\beta e^{c\beta D}}{c\beta} \right] ; d \leq D \leq 22.5 \text{ km} \qquad (3.1)$$

$$A(R_P, D) = \alpha R_P^\beta \left[\frac{e^{u\beta D} - 1}{u\beta} \right] ; \qquad 0 \leq D \leq d$$

where;

A is in dB And R_P = Rain Rate mm/h, the specific attenuation in dB/km is related to point rain rate by αR^β, and the remaining coefficients are empirical constants of the piecewise exponential model;

$$u = ln \left[\frac{b e^{cd}}{d} \right]; \qquad\qquad d \text{ in km} \qquad\qquad (3.2)$$

$$b = 2.3 R_P^{-0.17}; \qquad\qquad R_P \text{ in mm/h} \qquad\qquad (3.3)$$

$$c = 0.026 - 0.03 \ln(R_P) \qquad\qquad (3.4)$$

$$d = 3.8 - 0.6 \ln(R_p) \qquad\qquad (3.5)$$

(Crane, 1980)

3.1.2   Recommendation ITU-R P.618-11

The propagation effects that are relevant when designing an Earth-Space telecommunication system are rather different from those applicable to the terrestrial line-of-sight communication systems. Specifically, multipath propagation produced by atmospheric layers can be ignored except for paths at low elevation angles less than 4°. However the effects of rain are similar to those on terrestrial line-of-sight radio links with the exception of, in earth-space links the effective path length through the rain is limited by the maximum rain height and its vertical and horizontal distributions compared to the length of the link and the horizontal distribution of the rain along the path in terrestrial line-of-sight radio links.

If rain attenuation statistics are derived from long-term measurements carried out in the locality of the site and on a path at the same or comparable angle of elevation are available, then it is recommended that the essential attenuation statistics are acquired by scaling these data to the appropriate frequency. Nonetheless, if reasonable measured data are unavailable, Rec. ITU-R P.618-11 (ITU:Rec.P.618-11, 2013) provides a method for predicting the statistics of rain attenuation for an average year from the statistics of point rainfall. Figure 3.1 illustrates the path geometry used in Rec. ITU-R P.618-11 (ITU:Rec.P.618-11, 2013) propagation model.
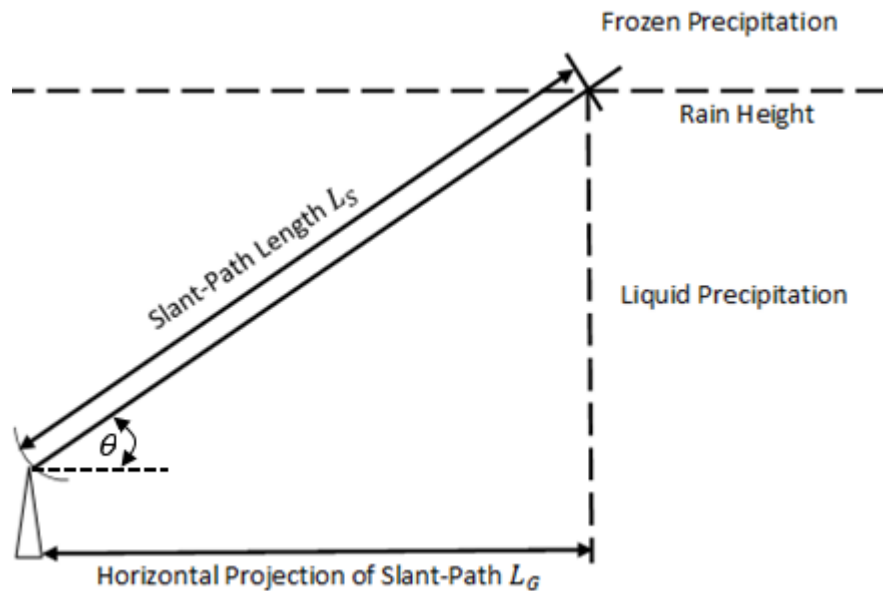
Figure 3.2: Schematic presentation of an Earth-Space path given in ITU-R Rec. P.618-11 propagation model (ITU:Rec.P.618-11, 2013)

It is assumed that the rain extends from the ground to a rain ceiling. The slant-path length below the rain ceiling L_S is calculated;

I. for a path elevation angle (θ) less than 5° taking to consideration of earth curvature and atmospheric refraction

II. for a path elevation angle (θ) higher than or equal to 5°using a simpler flat earth refraction and earth curvature

In each of the above scenarios the projected length along the surface of the slant-path L_G is calculated. This length then can be used to determine the horizontal and vertical reduction factors. The specific rain attenuation corresponding to a precipitation rate is equal to that exceeded for 0.01% of an average year $(R_{0.01\%})$, which then can be used with the effective path length to calculate attenuation exceeded for 0.01% of an average year. The attenuation exceeded for other

percentages ranging from 0.001% to 5% can be determine from 0.01% attenuation value.

Rainfall statistics are strongly dependent upon integration time and to determine the value of $R_{0.01\%}$ using Rec. ITU-R P.618-11 (ITU:Rec.P.618-11, 2013), an integration time of one minute should be used. At the given time, if a value for $R_{0.01\%}$ is unavailable from long-term locally measured data then an estimate could be obtained from maps of precipitation rate given in Rec. ITU-R P.837-6 (ITU:Rec.P.837-6, 2012).

3.1.3 Recommendation ITU-R P.530-15

The ITU-R Rec. P.530-15 provides propagation data for the planning and design of terrestrial line-of-sight communication systems that typically operate in frequencies between 1 GHz to 100 GHz. The recommendation predicts the rain attenuation exceeded for 0.01% of an average year from $R_{0.01\%}$ and link parameters using the following steps;

1. Estimate $R_{0.01}$ using locally measured data or ITU-R Rec. P. 837-6 (ITU:Rec.P.837-6, 2012)

2. Determine the associated specific attenuation γ_R exceeded for 0.01% of the time using ITU-R Rec. P.838-3 (ITU:Rec.P.838-3, 2005)

3. Determine the effective path length $d_{eff} = r \times d$ using the following equation given in ITU-R Rec. P.530-15 (ITU:Rec.P.530-15, 2013);

$$r = \frac{1}{1 + d/d_0} \tag{3.6}$$

where d is the actual length of the communication link and the r is the path reduction factor. For rain rate less than or equal to 100 mm/h;

$$d_0 = 35e^{-0.015R_{0.01\%}} \tag{3.7}$$

For rain rate greater than 100 mm/h, the $R_{0.01\%}$ value is 100 mm/hr

4. Finally, the effective path length is multiplied with specific attenuation to estimate the rain attenuation at 0.01% exceeded level $A_{0.01}$

$$A_{0.01} = \gamma_R \, d_{eff} = \gamma_R \, dr \tag{3.8}$$

The Recommendation also provides a method to extrapolate from this attenuation to those exceeded at a wide range of time percentages.

3.2 The Stationary Climate Assumption

The recent Fifth Assessment Report of the IPCC (Field et al., 2014) concluded that; *"In recent decades changes in climate have caused impacts on natural and human systems on all continents and across the oceans."* Furthermore, it states that *"Observed impacts of climate change are widespread and substantial"*. Indications of climate change impacts are most dramatic and extensive for natural systems. In several regions, changes in precipitation or melting snow and ice are changing hydrological systems, which affects the water resources in terms of quality and quantity. Glaciers are shrinking in the northern hemisphere due to climatic changes, affecting runoff and water resources downstream (Field et al., 2014).

Early rain attenuation models used the idea of a rain climate zone covering a particular region of the globe, where annual rain rate statistics average should be similar. Crane's Global model was developed using rain statistics gathered from a temperate climatic region, where the incidence of heavy precipitation is low and assumes climatic parameters to be stationary i.e. having a distribution that does not change in time. In 2009 Mandeep (Mandeep, 2009) concluded that ITU-R Rec.p.618-11 model (ITU:Rec.P.618-11, 2013) *"agrees reasonabally well with the measured attenuation values and tends to devidate at higher rain rates"*. He further states that the *"major drawback affecting the emiprical models is the lack of information that exists in propagation-measurement databases required to allow complete modelling of rain attenuation for different climate regions. Therefore, the lack of rain-measurement data from equatorial and tropical*

regions for verification causes predictions obtained from existing models to deviate from direct measurements".

Stationary means that the underlying statistics do not change over multi-year periods. For periods shorter than a year, weather is not stationary due to seasonality. Nevertheless, stationary is often understood to mean that the underlying annual distributions of significant climatic parameters are not changing. Mandeep further states that rainfall attenuation statistics for different climatic regions should be embedded into propagation measurement databases.

The assumption of climate stationary is built into ITU-R models in two different ways; firstly Rec. ITU-R P.530 and P.618 provide models of rain fade distributions that are independent of time. Similarly, the Rec. ITU-R P.837 rain rate distributions and Rec. ITU-R P.839 median rain heights, are time invariant. Secondly, when combining empirical measurements of rain or rain fade, it is clear that no account is taken of when measurements were made; for example, when using of DBSG3 to verify models.

In the past, yearly mean rain parameters have been estimated using averages over rain gauges, which are assumed to experience the same climate. If these parameters have significant temporal tendencies then these trends need to be integrated into the models, which are used to estimate climatic parameters from various databases. Moreover, estimation of these parameters needs to be based on best estimates given by historical data, surveyed tendencies, climate scenarios and climate simulations (Paulson, 2011b). Paulson and Al-Mreri (Paulson and Al-Mreri, 2011b) state that the existing ITU−R models of rain height presume a static yearly mean level and annual variation relative to the median, described by a specific Normal distribution. It also assumes that the rainfall rate exceed 0.01% of

the time to be constant. Furthermore, Paulson and Al-Mreri states that these assumptions may be insufficient for the design of satellite communication systems (Paulson and Al-Mreri, 2011b), as fade distributions could change significantly over the typical 30-year life cycle of a satellite system.

In 2010, Paulson (Paulson, 2010) analysed rain gauge data spanning 20 years from 30 different sites in southern United Kingdom. The study revealed increasing trends over this analysis period, in the occurrence of rainfall rates associated with outage on fixed terrestrial links. Notably, these identified trends are consistent with the increasing trends of general precipitation at hydrological scales that are predicted by all UKCIP (United Kingdom Climate Impacts Programme) climate change scenarios and partly consistent with known trends in North Atlantic Oscillation (NAO). Paulson further states that the expected effect of the increasing trend in the occurrence of rain rates at outage levels on fixed microwave links are a doubling or tripling of the outage rate over the decade of 1997 to 2007. It is likely that these trends will continue for the next few decades. Considering this, regulators and operators of microwave networks need to integrate these trends into regulation and operation of link networks. If not, either link availability will continue to decline or expensive fade mitigation techniques, such as interference cancellation, will need to be introduced.

3.3 Consequences of Systematic Errors in Existing Models

When designing microwave telecommunication systems, several scenarios need to be considered, which are consistent with best existing knowledge. Present best knowledge is that several climatic parameters, with direct effect on fading, are exhibiting multi-decade trends. Therefore, networks will have to adapt over time to preserve the system availability, otherwise network operators will have to accept deteriorating system performance. Significant effort is required globally in order to identify trends in fading experienced by Earth-Space and Terrestrial links. Furthermore climate change scenarios need to be embedded into existing ITU-R recommendations models, so that the existing and future telecommunication systems can be engineered to optimise spectrum efficiency and cost benefit performance (Paulson, 2011b).

Several studies have shown significant increasing temporal trends in the 0.01% exceeded rain rate $R_{0.01\%}$ in the UK. However, there is no evidence of similar trends in rain fade. This may be due to the lack of data i.e. these measurements require long-term (decades) of data from stable links. It is possible that no fade trends exist. For example, if rain events are becoming more intense but also have smaller foot-prints, then the increase in specific attenuation could be compensated by the reduction in path length through the rain. In either case, the ITU-R recommendations face problems. As the $R_{0.01\%}$ parameter is changing, Rec. ITU-R P.837-6 (ITU:Rec.P.837-6, 2012) will need constant updating to reflect this change. A better approach would be to introduce temporal trends into ITU-R Rec. P.837, as this would allow extrapolation a few decades into the future. If fade is

not increasing then the fade models will become increasingly inaccurate without similar updating reflecting changes in path reduction factors.

3.4 Chapter Summary

When designing microwave telecommunication systems it is important to obtain rain attenuation statistics. Over that past few decades, numerous fade models have been introduced based on the measured distribution statistics. There are two different rain fade model categories; where the first derives rain fade from measured or modelled rain fields while the second type of models are empirically derived from fade measurements on many links at several locations. In microwave system design there are two types of empirical fade models; firstly, ITU-R models that are commonly and widely used, ITU-R Rec. 618-11 for Earth-Space communications links and ITU-R Rec. P. 530-15 for terrestrial line-of-site links. The second empirical model is the Crane's attenuation prediction model (Crane, 1980). It is indisputable that the global climate has been changing rapidly over that past 3 decades, and will almost certainly continue change in coming decades. These climate change trends need to be integrated into current globally accepted fade models. Subsequent chapters of this thesis will investigate non-stationary climate parameters that effect telecommunications systems. The introduction of these parameter changes into ITU-R models will be explored.

CHAPTER 4

Meteorological Measurements and Global Precipitation Datasets

4.1 Rainfall Measurement Techniques

This chapter evaluates the meteorological data available for estimating trends in atmospheric fading globally. Estimating or forecasting temporal and spatial distributions of rain events remains an important challenge for meteorological services. An array of different rainfall measuring instruments are in use, such as rain gauges, weather radars (both Earth and space based), and aircraft. Rain gauges provide direct measurement of rainfall rates but lack spatial coverage due to the small collection area for each rain gauge and low gauge densities. In particular, rain gauges are usually unavailable over the sea and analysts are often rely on weather radars or satellites to forecast rainfall rates. Usually rain gauges are used as "ground truth" in order to compare, calibrate and verify other remote measurement instruments such as radars, or Numerical Weather Products (NWP). The meteorological radars employ an echo-sounding system to estimate hydrometeor parameters. Polar or cross-polar radar reflectivity can be related to parameters of the drop-size-distribution and derived hydrometeor parameters such as rain rate. These meteorological radars are capable of providing extensive spatial coverage and high spatial and temporal resolution. Nevertheless, the ground-based radars only cover parts of the globe such as Western Europe, Japan and North America. There are many effects such as ground clutter, variation of

raindrop size distribution and bright band reflections which could lead to imprecise rain parameter estimation.

Measuring weather parameters, including rainfall rate, from sensors on board satellites is becoming increasingly significant as it can yield global coverage relatively economically. Satellite observations suffer fundamental limitations as they observe weather from above. Surface parameters, such as rain rate, generally need to be estimated from measurements of cloud top parameters. These estimates can have large uncertainties and some have low temporal and spatial resolutions. Meteorological satellites are typically fitted with radiometers that can measure emissions from the Earth's surface and cloud tops. Many weather satellites have been equipped with rainfall radars, i.e. the Tropical Rainfall Measuring Mission (TRMM) and some satellites such as the National Oceanic and Atmospheric Administration (NOAA)'s Geostationary Operational Environmental Satellite (GOES) measure the infrared (IR) visible radiation emission from Earth to estimate the rainfall rate (Scofield and Kuigowski, 2003).

4.1.1 Rain Gauges

To estimate the amount of rainfall at a point, over a certain period of time, hydrologists or meteorologists use a device called rain gauge. The history of rain gauge goes back to ancient Greece and the Egyptian Nilometer which provided a time series of the size of Nile inundations spanning 5000 years (WaterHistory.Org). In 1441, King Seiong and his son Prince Munjong invented the first standardized rain gauge. These Seiong gauges were sent throughout the United Kingdom as an official tool to assess land taxes based upon a farmer's potential harvest. However, in 1662 Sir Christopher Wren invented the

mechanical self-emptying tipping bucket rain gauge, which is the type of rain gauge used today for rainfall measurement in most Environment Agency and Meteorological Office weather stations. Many hydrologists and meteorologists depend upon rain gauges to get accurate estimates of rainfall intensity. Gauge measurements are often assumed to represent point measurements. To calculate the rainfall rate using a standard rain gauge, the volume of water collected by a funnel is divided by the area of water catchment area (funnel) and the collection period. Several other methods are currently being used to automatically measure the volume of collected water such as weighing and drop counting mechanisms. Furthermore, a wide range of optical devices have become more popular over the past decade.

Tipping bucket rain gauges have several different peripherals which allow an accurate rainfall measurement. When rain falls in the gauge funnel it travels down into a small bucket which is balanced on a pivot. The bucket is held in place using a magnet until it fills to the calibrated amount. When the water level reaches the calibrated amount the magnet releases its hold, which causes the bucket to tip and triggers a switch to send an electric signal back to the weather station. The water in the bucket tips out and empties through a drain. Either the bucket raises back to its collection position underneath the funnel, or a rocking mechanism is used so two buckets are filled and emptied alternately.

The drop counting rain gauge forms the collected water into drops. The rainfall is collected in a sump, which overflows producing equal sized drops and these drops are detected optically. As the tipping bucket and drop counting rain gauges physically measure the collected rainfall in small quantities, it can lead to errors in extreme precipitation rates, where drops coalesce into a steam or buckets over-fill before emptying. They both experience the same funnel collection efficiency

problems as the conventional rain gauges. They also fail when non-liquid hydrometeors collect in the funnel. Ice can be melted using a heated funnel, but this leads to increased evaporation from the funnel and poor measurement of light rain. Weighing rain gauges operate by measuring the weight of collected water. The mass is independent of hydrometeor phase and so weighing gauges are useful where sleet, snow and hail contribute significantly to rain accumulation. Furthermore they can provide an accurate measurement of intense rain events, compared to tipping bucket or drop counting rain gauges.

Rain gauges require regular maintenance and have many limitations. Gauge funnels effect the wind field around the gauge and this can change the apparent rain rate, especially for light rain and high wind speeds. Snow is often blown in the wind and it is hard to distinguish windblown snow from fresh-fall, making snow accumulation difficult to measure by gauge. During cold periods funnels can become blocked by ice particles or frozen collected water. This often leads to false measurement of heavy events when the blockage clears upon thawing. Even though heating the funnel decreases this issue, it causes evaporation in the funnel and largely reduces the accuracy of light rain measurements. Birds often sit on the funnel edge and defecate into the funnel causing blockages. Spiders and insects can build nests in the funnel or block the funnel with their bodies. Dust, pollen and windborne soil can also lead to blockages. It is also very difficult to find appropriate sites for rain gauges, specifically in urban areas. The rain gauge site has to be secured from human and animal interference. They also need to be in an open area where the microclimate is not affected by surroundings such as buildings and trees. Rain gauges provide direct rainfall measurements, compared weather radars, but a single rain gauge has poor spatial coverage and only indicates precipitation intensity in a small local area.

For all the reasons above, rain gauge data needs to be treated with some scepticism. Many authors treat gauge data as the gold standard as measurements are based on actual rain water collection. However, gauges require considerable maintenance, often daily, and are very expensive to operate. Even when maintained, very few gauges are sited to meet WMO (World Meteorological Organization) standards. Gauge measurements need to be treated with caution in moderate to high winds or if non-liquid hydrometers may be present.

Smith et al (Smith et al., 1994, Smith et al., 1996) have shown that a rain radar can perform better than a network of rain gauges in terms of illustrating the intensity and spatial extent of heavy precipitation. Weather radars do not suffer the limitations associated with extreme winds, and several other mechanical limitations, of rain gauges during convective precipitation events (Groisman and Legates, 1994) and (Peck, 1997). Radars usually rely upon a simple power-law to convert radar reflectivity into rain rate, and this leads to uncertainties associated with variation in drop size distributions (DSD). Multi-frequency or polarisation radars can perform better at rain rate estimation by providing more information on the DSD. However, all radar derived rain rates assume the drops are falling. The fall speed does not affect the radar reflectivity and strong up-drafts are often present in convective rain events. This can lead to large errors in radar estimated rain rates, particularly those measured at altitudes high above the surface. To some extent, radar reflectivity is more closely related to microwave specific attenuation than rain rate, as neither depend upon fall speed of drops.

4.1.2 Weather Radar

Radio Detection and Ranging (RADAR) was developed by British meteorologist Robert Watson-Watt in 1935. Initially it was designed to detect aircraft echoes and not for precipitation or weather purposes. During this period weather echoes were treated as unwanted signals or noise. Figure 4.1 exemplifies the operation of a Radar, where it transmits and receives the echoes;
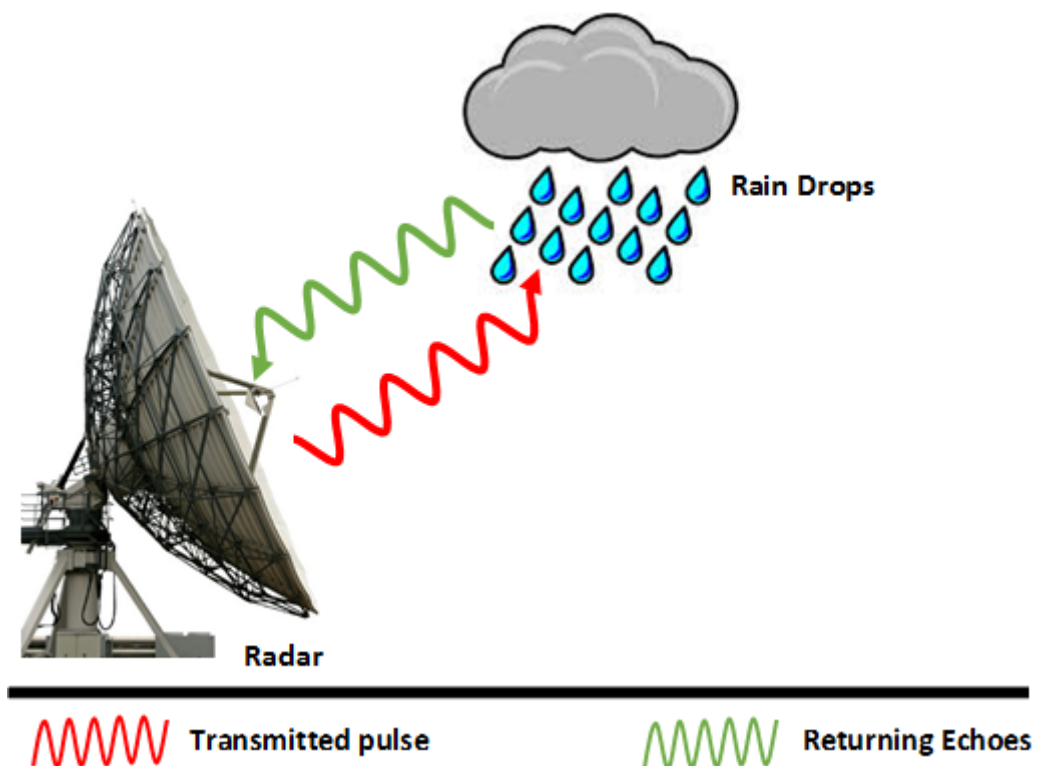
Figure 4.1: Basic diagram of an echo-sounding radar system

The radar transmits electromagnetic wave pulses through a narrow beam for a very short period of time i.e. Chibolton's CAMRa (Chibolton Advanced Meteorological Radar) weather radar operates with a pulse length of 0.5 microseconds. Some of these transmitted pulses are reflected back to the radar when the transmitted beam collides with rain drops. The radar continuously gathers the reflected energy

until reflections are too small to measure before transmitting a new pulse. The listening time for the reflected energy is approximately 3300 microseconds for the radars that operate under UK Meteorological Office. Typically, the beam width of a modern radar is around 1º. The distance between the radar and the precipitation can be derived from the time taken for the pulse to travel back and forth between radar and the targeted precipitation particles. The reflected energy collected by the radar is considerably weaker than the transmitted pluses due to free-space loss in both directions, and absorption and scattering due to atmospheric components.

The single polarisation radar is the most traditional weather radar. They transmit and receive pulses using either horizontal or vertical polarisation. More advanced weather radar systems such as Dual and Doppler radars can extract several other different measurement parameters. Doppler radars are generally used to acquire information on the direction and the speed of atmospheric particles. The Dual polarisation radars can be used to measure the horizontal and vertical polarised components of reflected radio waves. Larger raindrops tend to flatten and be wider than they are tall. Therefore, radar reflectivity of horizontally polarised waves tends to be higher than vertically polarised waves. This difference in polarisation reflectivity permits the radar to estimate the proportions of large and small raindrops.

Many of the limitations associated with rain gauges, can be overcome with weather radars. Furthermore, weather radar provides real time rainfall information whereas it often takes time to collect precipitation data from rain gauges. Nevertheless, conversion of radar measured reflectivity into precipitation rate is known to be challenging and yields estimation errors due to many factors, such as reflection from non-liquid hydrometeors, variation in DSD, variation in fall speed of drops due to updrafts; and non-meteorological aspects like beam blockage,

ground clutter and false echoes. Calibration variation between weather radars are also known to lead to estimation errors where a difference of 1 dB can lead to 17% variance in precipitation rate (Hunter, 1996). Radar beams need to be angled above the horizon to minimise reflections from surface structures. By necessity, measurements at long range are at significant altitudes above the surface. At long ranges, the radar beam could be above rainfall which may evaporate at lower levels below the radar beam, therefore precipitation is undervalued or frequently undetected (Kitchen and Jackson, 1993, Hunter, 1996, Smith et al., 1996).

4.1.3 Meteorological Satellites

Weather satellites can be equipped with active and passive sensors to probe and detect emission of radiation from the earth surface and atmosphere. Meteorological satellites typically orbit over the poles in a low earth orbit (LEO) e.g. NOAA, RESURS and FY; or over the equator in geostationary orbit e.g. GOES, MTSAT and METEOSAT. These satellites are used to measure or estimate a range of meteorological structures such as clouds and precipitation events. Rainfall estimation using a weather satellite can be separated into two different categories based on the EM frequencies used: infrared (IR) and microwave based precipitation estimates. The IR-based satellites such as GOES, operated by the National Oceanic and Atmospheric Administration (NOAA), estimate the precipitation rate by measuring the radiance or brightness temperatures from cloud-top infrared (IR) imagery. This is related to cloud-top height for optically thick clouds below the tropopause. This correlation assumes that the cloud height is related to cloud thickness and colder clouds are more likely to produce rain than

the warmer clouds. This technique could only work for convective rain events where cloud-top parameters are more closely associated with surface rainfall, however this method will be problematic for warm top stratiform clouds and for non-precipitation cirrus clouds since they have low brightness temperature (Scofield and Kuigowski, 2003). Use of microwave-based satellite measurements to estimate rainfall rates is a more straightforward method compared to IR-based satellite systems. It estimates the precipitation rate by measuring the absorption of microwave radiation by liquidized precipitation or on the scattering by ice particles within the microwave spectra (Scofield and Kuigowski, 2003). Nevertheless microwave-based satellites have a poorer spatial resolution than IR-based satellites. The resolution is typically inadequate to determine small scale rainfall events. Moreover, the long revisit times of the LEO satellites that carry these instruments lead to a substantial sampling errors for accumulated rainfall estimation (Ebert and Manton, 1998).

Rainfall rate estimation using satellites offers significant advantages over weather radars and rain gauges. It provides critical rainfall information in areas such as over the sea, where weather radars and rain gauges are not usually available. Furthermore, satellites yield fewer spatial inconsistencies than ground based radars, where radar beam height and width vary with range, and different radars require different calibration factors. Nonetheless, the relationship between satellite-measured radiance and surface precipitation rates are less vigorous than the relationship between ground-based weather radar reflectivity surface rainfall rates. Therefore, estimation of rainfall using satellites must not be considered as a replacement for radars and rain gauges but as a complement (Scofield and Kuigowski, 2003). The IR radars and microwave-based satellites can be combined (known as 'blending') to expand their applications and to increase the accuracy.

Multi-sensor Precipitation Estimate (MPE) is an example algorithm of this combination and MPE frequently uses rain gauges or radars for validation purposes. Modern weather satellite systems, such as the Tropical Rainfall Measuring Mission (TRMM), are equipped with precipitation radar, (Scofield and Kuigowski, 2003, Usman, 2005). The PR (Precipitation Radar) provides three dimensional maps of storm structure. The measurements produce the information on the intensity and the distribution of rain on a particular rain type, depth of the storm and the height which snow melts into rain. Systems like TRMM are relatively new alternatives for IR and microwave-based satellite precipitation estimation.

TRMM is a joint project between NASA (National Aeronautics and Space Administration) and JAXA (Japan Aerospace Exploration Agency) and it is known to be the first weather satellite utilising precipitation radar to estimate rainfall in the tropics. TRMM satellite is equipped with several sensors and instruments such as TRMM Microwave Imager (TMI), precipitation radar, visible and infrared sensors and lightning detector. TRMM satellite is capable of providing vertical profiles of rain and snow from the surface up to 12 miles in height and offers average rainfall over $5^o \times 5^o$ (for lower resolution) and $0.5^o \times 0.5^o$ (for higher resolution) regions with a monthly precipitation rate. The TRMM venture is exceedingly ambitious as it offers rainfall estimation over a large coverage area. Nevertheless, even high resolution rain data are not adequate for radio propagation simulation (Usman, 2005) due to low temporal resolution. Pixels 0.5^o in diameter are still large compared to coastal irregularities and vast compared to Fresnel zones of radio systems. Figure 5.2 illustrates wide variety of weather satellites operated under different space agencies and in different orbits.
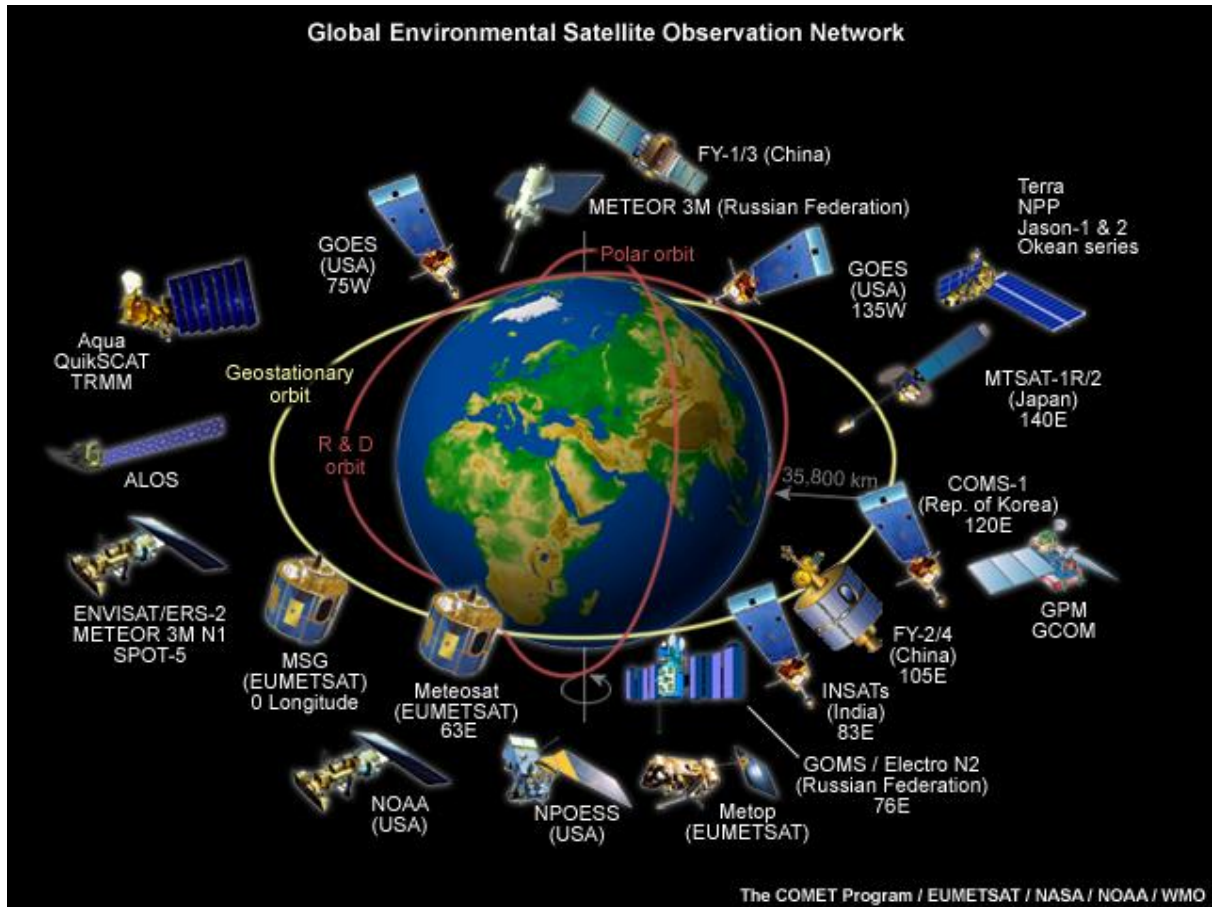
Figure 4.2: Weather satellites operates under various countries and space agencies. (Source:http://stream2.cma.gov.cn/pub/comet/SatelliteMeteorology/GOESRBenefitsofNex tGenerationEnvironmentalMonitoring/comet/goes_r/envmon/print.htm)

4.2 Global Precipitation Datasets

Precipitation plays a significant part in the global energy and water cycle. Knowing the precise rainfall amount reaching the land surface is of special importance for fresh water assessment and management related to land use, agriculture and hydrology. There is a significant interest in the analysis of long-term precipitation records to evaluate climate change and its impacts at all spatial scales. Therefore, national and international organizations have initiated and supported several research and monitoring schemes (Schneider et al., 2011). Despite the growing demands for high quality precipitation datasets from meteorologists and hydrologists, there is a lack of reliable (or any) datasets over fine-scales in both spatial and temporal dimensions. A significant research problem exists to determine the algorithms to combine precipitation measurements made over different spatial-temporal integration volumes, by different instruments with different systematic and random errors, to yield the best estimate of the underlying rain fields. This is mainly due to large spatial and temporal variability in precipitation data, which includes rain gauge observations, satellite observations and outputs from several other numerical models, where each of these methods has their own advantages as well as deficiencies (Xie and Arkin, 1997).

4.2.1   ITU-R Study Group 3 Dataset (DBSG3)

In the process of revising or modifying ITU recommendations for channel modelling in telecommunication systems, standardised datasets are required for verification (Belen et al., 2010). The ITU-R Study Group 3 database DBSG3 for Terrestrial and Earth-Space, contains experimentally measured propagation data from many locations globally. It includes 743 experimental CCDF rain and fade statistics acquired from over 139 locations. This includes average annual rain rate distributions gathered over one or more years, and average annual attenuation statistics for various links operating at different frequencies and elevation angles, at many places on Earth (Kourogiorga et al., 2010). The database for the terrestrial links contains 89 experimental sets, from 16 different counties and link path ranges from 0.5 to 58 km and around 550 records are included for Earth-space links. Both of these are restricted to links operating over 10 GHz (Luini and Capsoni, 2010).

DBSG3 data have been acquired since the early 1960s. Over the 50 years since radio systems and applications have changed dramatically. In particular, the frequencies employed have increased consistently over this period. Also, early data were acquired from temperate regions such as Europe and North America whereas more recent data are predominantly from South America and tropical regions such as Asia and Latin America.

There is a possibility that these strong trends in the DBSG3 data could lead to problems, when these data are used to verify ITU-R Recommendations, particularly when climate change is also happening over this period. Revisions to ITU-R P Recommendations are tested against the DBSG3 database. Predictions are compared to modern Asian data, but the majority of European and North

American data were collected before global temperatures increased significantly. Even in a stationary climate, the location and frequency trends in DBSG3 could lead to compensating errors. In testing, the high frequency performance is more strongly weighted in temperate zones than the high frequency in the tropics. For another example, fade predictions depend upon both the specific attenuation-rain rate model and the path reduction factor. Single path reduction factor equations are used globally, whereas it would be expected that regions with more convective rain, such as the tropics, would require smaller path reduction factors. However, this would be masked by a specific attenuation-rain rate model that under-estimated specific attenuation at higher rain rates. These observations question the validity of the current ITU-R method of model validation. Other questions are raised later when the quality and quantity of data in DBSG3 is examined.

4.2.2 ECMWF ERA-15/40 and ERA-Interim Reanalysis Datasets

In 1979 European Centre for Medium-Range Weather Forecast (ECWMF) started its operational activates and since then its archive of analysis and estimations has become a significant data source in meteorological research. These data are widely used by scientists around globe in a wide variety of studies and applications. Distinctive research applications includes studies of predictability, monitoring system performance, atmospheric low-frequency variability and the global hydrological and energy cycle, (Gibson et al., 1999).

4.2.2.1   ECMWF ERA-15

ECWMF's first Re-Analysis dataset (ERA) assimilated 15 years of validated precipitation data for the period between 1979 to 1993 (ERA-15). In the early stages of the Re-Analysis project, acquisition and construction of the observations and forcing fields were required. A significant experimentation programme, co-ordinated with ECMWF Research and Operational activities, was also completed. This entire process empowered the scientific mechanisms of the entire re-analysis project. The end product was initiated in 1994 followed by a series of validations throughout 1995 and early 1996.   The ERA-15 contains observational data obtained in real time from the World Meteorological Organization's Global Telecommunication Systems (GTS) since 1979 and from several other additional data sources (Gibson et al., 1999).

4.2.2.2   ECMWF ERA-40

ERA-40 is a re-analysis of metrological observations from September 1957 to August 2002 made by the ECMWF in collaboration with several other establishments. The data available for assimilation changes significantly over this re-analysis period, with data provided by a succession of satellite-borne instruments since 1970's, and increasing numbers of observations from ocean-going craft, ocean-buoys and alternative surface platforms, but with a declining amount of radiosonde ascents since the late 1980's. The observations utilized in ERA-40 were accumulated from several different sources. ERA-40 built on

knowledge developed during ERA-15 and benefits from several modifications recently made to the operational system. The ERA-40 re-analyses provides greater horizontal and vertical resolution in the terrestrial boundary layer and stratosphere than ERA-15 re-analyses. Furthermore it provides a significant second source of re-analyses data for the periods of 1957-1978, which was only covered previously by original NCEP/NCAR re-analyses. Spectral T159 model resolution is used in ERA-40 and it is higher than T106 (Lat: 160 x Lon: 320) used in ERA-15 and T62 (Lat: 94 x Lon: 192) resolution used in NCEP/NCAR. The ERA-40 data integration system was primarily designed to produce analyses of surface variables such as atmospheric temperature, humidity and horizontal winds and several other variables (UPPALA et al., 2005).

4.2.2.3 ECMWF – Interim

The latest global atmospheric reanalysis dataset produced by ECMWF is known as ERA-Interim. The goal of the ERA-interim reanalyses was to replace the ERA-40 re-analyses, which extends back to early parts of the twentieth century. The principle motivation for producing the ERA-Interim was to address the numerous data integration difficulties that occurred during the construction of ERA-40. These issues are mainly associated with representation of the hydrological cycle, the superiority of the stratospheric circulation and the consistency in time of reanalysed geographical fields. The second major goal was to advance on numerous technical aspects of reanalysis such as data selection, quality control, performance monitoring and bias correction, as each of these could have a large influence on the quality of the reanalysis products. The ERA-Interim reanalysis is

produced with a successive data integration scheme, progressing forward using a 12-hourly analysis cycle. In each of these cycles, the observations that are available are combined with previous information from a forecast model to estimate the evolving state of the global atmosphere and its underlying surface. In ERA-Interim, partial resolution of the outer loop is T255 (approximately 79 km) and two sequential inner loops at resolutions T95 (approximately 210 km) and T159 (approximately 125 km) are used (Deea et al., 2011).

4.2.3   NCEP-NCAR Reanalysis Dataset

The principle idea of reanalysis is to run a numerical weather simulation constrained by the assimilation of historical weather observations. The simulation algorithms are fixed over the simulation period and so any variation in the simulation parameters is either due to changes in assimilated data or changes in the climate captured by the simulation. Reanalyses are particularly suitable for the recognition of long-term changes or variations in the atmosphere and are used extensively in climate change research.

The observational data available for assimilation has changed significantly during the second half of the twentieth century. Upper-atmosphere observations were generally acquired using radio soundings after 1957 until early 1970's. Later, satellite observations became increasingly significant and widely used (Hertzog et al., 2006). Consequently data for assimilation significantly increased in both quality and quantity from the late 70's with the use of satellite observation over the both hemispheres (Mo et al., 1995, Jenne, 1999, Kistler et al., 2001, Simmons and Gibson, 2000).

The primary motivation of NCEP-NCAR (National Centres for Environmental Prediction-National Centre for Atmospheric Research) Reanalysis venture is to use a frozen state-of-the-art analysis or forecast system and to accomplish data integration using past data from 1957 to present. The NCEP-NCAR 40 year's reanalysis is a research quality dataset suitable for several uses such as weather and short term climate research. The development of NCEP-NCAR dataset was supported by NOAA's (National Oceanic and Atmospheric Administration) Office of Global Programs (Kalnay et al., 1996). The NCEP-NCAR Reanalysis dataset is a global model with triangular 62 wave truncated ("T62") horizontal resolution (roughly around 2º Latitude x 2º Longitude) with 28 vertical levels. The integration system runs with new preliminary data every 6-hours (0000 UTC, 0600 UTC, 1200 UTC and 1800 UTC). The reanalysis precipitation output data resides on a Gaussian grid with 192 longitudes and 94 latitudes (192 x 94). Precipitation accumulation is categorised into convective and total. For this project, the 6-hourly accumulated precipitation data are summed to produce daily totals of convective and total precipitation. From these data, mean annual convective and total accumulation can be calculated. The annual proportion of 6-hourly intervals during which precipitation was detected can also be calculated. These parameters are used in the Rec. ITU-R P.837 rain rate distribution model. For this project NOAA NCAP/NCAR Reanalysis data are selected instead of ECMWF ER-40. This is mainly due to the high resolution NOAA NCEP/NCAR data over 1.824º integration region are freely available up to 2010 compared to freely available low resolution (2.5º) ECMWF ER-40 data which is only available until 2002.

4.2.4   JRA – 25 Reanalysis

Japanese 25-year Reanalysis (JRA-25) is a long-term atmospheric reanalysis dataset created using the JMA (Japan Metrological Agency) numerical integration and forecast system. This is known to be the first reanalysis undertaken in the Asian continent and it covers the periods from 1976 to 2004. One of the many motivations behind the JRA-25 was to perform analysis to a superior quality in the Asian region. In JRA-25 dataset, six-hourly data integration cycles are performed, which produces the 6-hourly atmospheric analysis and forecast fields of numerous physical variables. The JRA-25 reanalysis has a spectral resolution of T106 which equivalent to a horizontal grid size of approximately 120 km and 40 vertical layers. The observational data used in JRA-25 reanalysis were provided by NCEP/NCAR, ECMWF ERA-40, and National Climate Data Centre (NCDC) and several other numerical prediction centres (Onogi et al., 2007). The key strengths of JRA-25 are that it offers a much improved radiation scheme and the length of record is comparable with NCEP – NCAR Reanalysis 1. Furthermore it's known to be the best among other second generation reanalyses for long-term series of the global precipitation (NCAR/UCAR, 2014).

4.2.5 GPCP Dataset

In 1986 the World Climate Research Program (WCRP) initiated and established the Global Precipitation Climatology Project (GPCP) to produce global analyses of precipitation for the use in climate research. To attain a widespread spatial coverage, the GPCP uses simple precipitation estimates derived from IR and microware satellite observations (Arkin and Xie, 1994). The principle aim of the GPCP is to provide monthly mean rainfall data on a global 2.5°x 2.5° latitude-longitude grid. The initial GPCP combined precipitation dataset, also known as version 1, covered the period of July 1987 through to December 1995. This was later extended to cover the periods of 1986-2000 (Huffman et al., 1997) and the latest version, which is GPCP version 2.2, covers the data period up through to November 2012 (Huffman and Bolvin, 2013). Furthermore, the principal product in the GPCP dataset is a combined analysis incorporating rainfall estimates from LEO satellite microwave data, geosynchronous-orbit-satellite infrared data and rain gauge observational data. In the GPCP combined dataset, microwave estimates are built upon Special Sensor Microwave/Imager (SMM/I) data acquired from Defence Meteorological Satellite Program (DMSP, United States) which occupies sun-synchronous low-earth orbits. The infrared (IR) precipitation estimates are acquired mainly from geostationary satellites operated by Europe, Japan and United States and also from polar-orbiting satellites. Rain gauge rainfall data are accumulated and evaluated by the Global Precipitation Climatology Centre of the Deutscher Wetterdienst. The GPCP combination method is designed to use the strengths of each input dataset empirically to produce compound global monthly precipitation fields which are superior to any of the distinct datasets. This combined method is an improvement of the satellite-gauge-model (SGM)

technique defined in (Huffman et al., 1995). Figure 4.7 outlies the merged technique (Huffman et al., 1997).
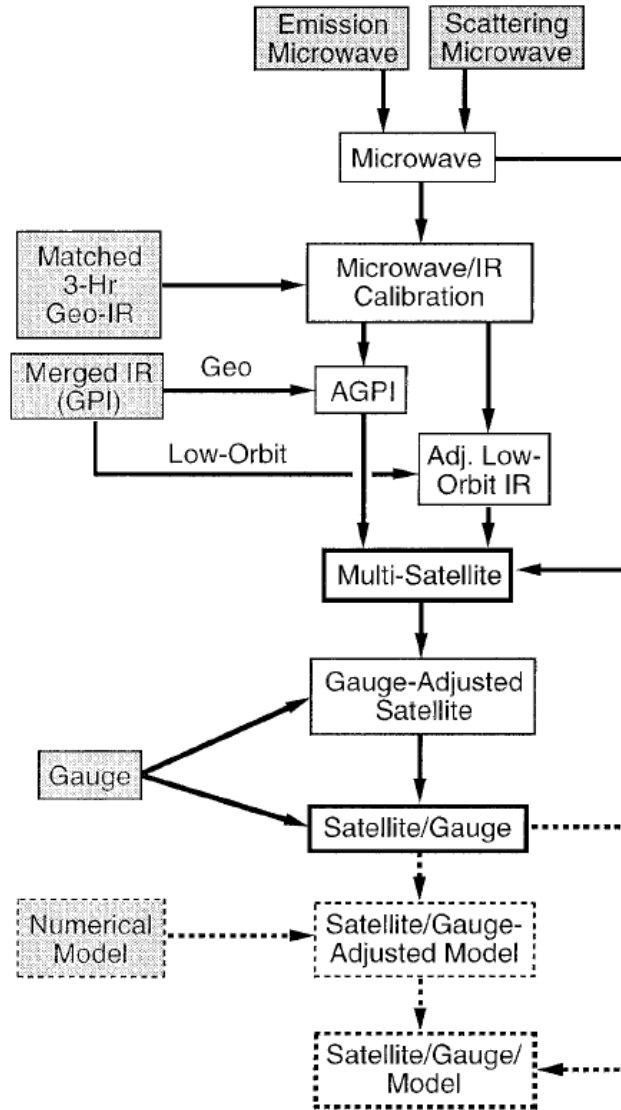

Figure. 4.3: Flow chart of the satellite-gauge-model precipitation combined technique (Huffman et al., 1997)

Where;

GPI - Global Precipitation Index

AGPI – Adjusted Global Precipitation Index

4.2.6 GPCC VASClimO Dataset

Due to a request from the World Meteorological Organization (WMO) in 1989, the Global Precipitation Climatology Centre (GPCC) was established. GPCC is governed by Deutscher Wetterdienst (DWD – National Meteorological Service of Germany) which is the German collaborator to the WCRP (World Climate Research Programme). GPCC provides monthly global analysis of precipitation on Earth's land surface, which are based on *in situ* rain gauge data. GPCC products include gauge-based gridded monthly precipitation data for the global land surface and are presented with 1.0º x 1.0º and 2.5º x 2.5º (Latitude x Longitude) spatial resolutions (Schneider et al., 2011). Providing gridded time-series of monthly rainfall rates for the land surfaces for climate variations and trend analysis is based upon the data selected with respect to a complete temporal data coverage and homogeneity of the time series. The GPCC VASClimO (Variability Analysis of Surface Climate Observations) 50 year dataset version 1.1 is based on time-series of over 9,300 stations covering more than 90% of the periods between 1951-2000. The VASClimO dataset supplies monthly precipitation data which has spatial resolutions of 0.5º x 0.5º, 1.0º x 1.0º and 2.5º x 2.5º (Becker, 2012, Beck et al., 2004, Parker et al., 2011). The GPCC full reanalysis product covers the best spatial coverage for each distinct month and VASClimO is enhanced for completeness and homogeneity for the 50-year (1951-2000) period. GPCC VASClimO is the only known product that has been designed to support observation of long-term precipitation variability and trend analysis (Schneider et al., 2011). The VASClimO dataset the preferred choice for analysis of temporal climate variations, specifically the spatial distribution of climate change with respect to precipitation (Rudolf and

Fuchs, 2006). Moreover VASClimO also contributes to the IPCC Assessment Reports.

4.3 Chapter Summary

Rain gauges are often used as "ground truth" since they measure rainfall rate directly but with poor spatial coverage. Rain gauges are also used for verification purposes or calibration of indirect precipitation estimates. Satellite rainfall estimation offers wider spatial coverage than the ground based weather radars but the rainfall measurements are considered to be less reliable and requires further developments before they can fully replace ground based radars.

There are a range of global meteorological precipitation datasets currently available, which are derived from ground based and space instruments. Numerical Weather Prediction data sets such as NCEP-NCAR Reanalysis, ECMWF ER-15/40 Reanalysis and JRA-25 Reanalysis are widely used in weather and climate research. On the other hand, datasets like VASClimO offers high resolution 50-years of rain gauge data over land with more than 90% availability. Due to the unreliability of NWP precipitation estimates, data needs to be calibrated against rain gauge data. Datasets engineered for areal consistency, such as VASClimO, are ideally suited for this purpose.

CHAPTER 5

The estimation of one-minute, rain rate parameters from NWP data

5.1 Salonen-Poiares Baptista Method

The Salonen–Poiares Baptista (SPB) Method is a transformation of the long term average (many years) of three NWP reanalysis outputs to the average annual distribution of one-minute rain rates. The transformation is assumed to be valid for all climates and is integral to Rec. ITU-R P.837-6 (ITU:Rec.P.837-6, 2012). This chapter will test the transformation using a network of high resolution rain gauges. In particular, two questions will be explored: how much information do distributions of six-hourly accumulations provide on the incidence of one-minute rain rates at outage levels and how many years of data are required for any link between theses parameters to be used. If a region experiences climate change, then the SPB method should be applicable to intervals both before and after the change, as long as the climates stay within the very wide global range, from desert to rain forest, over which the model has been verified. Quantifying this approach is limited by unanswered questions as to the rate of convergence of distributions of measured rain rates to average annual distributions, and the rate of convergence of averages of reanalysis parameters to long term averages. Both these questions are further complicated by natural climate cycles of various periods and the possibility of anthropogenic climate change.

The SPB distribution of one-minute rain rates and the method described in (Poiares Baptista and Salonen, 1998, Salonen and Poiares Baptista, 1997) and (ITU-R:StudyGroup3, 2012) provides a method for estimating the distribution parameters from reanalysis data. The average annual one-minute rain rate complementary cumulative distribution function (CCDF) is assumed to have a distribution well described by the expression:

$$P(R) = P_0\, e^{-aR\frac{1+bR}{1+cR}}\ .\tag{5.1}$$

$P(R)$ is the probability of experiencing a rain rate greater than R and P_0 is the probability of a one-minute interval experiencing rain. The four parameters P_0, a, b, c; control the shape of the distribution and match the distribution to the local climate. At low rain rates, as $R \to 0$, (5.1) is exponential with an exponent of $-aR$. For large rain rates it is exponential with an exponent $-(ab/c)R$. Typically, the rain rate exponent is larger for high rain rates than for low, and so $0 < c < b$. The parameters b and c control both the final exponent and where the transition occurs. A major disadvantage of (5.1) is that it cannot be analytically integrated to yield rain accumulations. It can be differentiated to yield a complex probability density function. The distribution has four parameters and this is likely to be the minimum required to adequately describe the variety of distributions that exist globally.

Rec. ITU-R P.837-6 (ITU:Rec.P.837-6, 2012) provides a method to calculate these distribution parameters from three, long-integration temporal rain parameters. These parameters are:

M_S = the mean annual stratiform rain accumulation (mm),

M_C = the mean annual convective rain accumulation (mm),

P_{r6} = the probability of rainy 6-hours periods (%).

The Rec. ITU-R P.837-6 (ITU:Rec.P.837-6, 2012) model estimates the distribution parameters from these input parameters using:

$$
P_0 = P_{r6} \cdot \left(1 - e^{-\alpha_1 \frac{M_S}{P_{r6}}} \right) \tag{5.2}
$$

$$
b = \frac{M_C + M_S}{\alpha_2 \times P_0} = \frac{M_T}{\alpha_2 \times P_0}
$$

$$
c = \alpha_3 . b
$$

$$
a = \alpha_4
$$

The constants have changed with revisions of Rec. ITU-R P.837-6 (ITU:Rec.P.837-6, 2012) and the current values are: $\{\alpha_1, \alpha_2, \alpha_3, \alpha_4\} = \{0.0079, 21797, 26.02, 1.09\}$. The four SPB distribution parameters are estimated from three NWP parameters and this necessitates the fixing of one parameter.

The SPB method defines a complex relationship between the average annual values of three regional rain parameters and the distribution of average annual

one-minute rain rates. The global availability of NWP data, combined with this transformation, yields a globally applicable method to estimate the one-minute rain rate distribution, in particular R0.01%, and hence the rain fade distribution. NWP data provides coarse-scale parameters, typically averaged over six-hour periods and over regions with linear dimensions of one or two hundred kilometres. It is not clear from published sources, how the SPB model was developed. However, it is consistent with several reasonable heuristics i.e. regions that experience rain more often will experience more low rain fade, and higher mean rain rates are associated with more extreme fades.

It has been proposed that the SPB transformation will have application in the study of climate change effects on telecommunications. As developed, the SPB method links average annual NWP parameters and one-minute rain distributions. Nevertheless, the method must be applicable to parameters derived from sufficiently long multi-year intervals, as parameters approach average annual values as the number of year's increases. Given this, time-series of NWP parameters, as provided by reanalysis data, should provide guidance globally on trends in rain fade experienced by both terrestrial and Earth-space links. For these results to be accepted, it is important that the SPB transformation be tested.

This thesis chapter explores the link between annual accumulations and one-minute rain rates, using a network of high resolution rain gauges. This gauge network allows an accurate calculation of both one-minute distributions and annual accumulations, at a point and at NWP scales. Initially, the individual gauges-years are considered i.e. essentially point measurements for particular years. Large variation can be expected in these data due to year-to-year and point-to-point variation. If correlations between coarse and fine-scale parameters can

be found at the individual gauge-year scale then it is likely that methods, similar to SPB, will be able to reproduce year-to-year variation at the regional NWP scale. To test this hypothesis, similar tests are applied to rain rate distributions averaged over gauges within regions.

5.2   UK Environment Agency (EA) Rain Gauge Data

The UK Environment Agency (EA) runs a network of 1350 high resolution rain gauges across the UK. Each tipping-bucket rain gauge records the time of each tip, corresponding to an accumulation of 0.2 mm, to a range of temporal resolutions ranging from one minute to one second. In this study, data from three EA regions: Midlands East, Midlands Central and Midlands West are used. The data used is a subset of that used by Paulson (Paulson, 2010) in studies of temporal trends in the UK rain parameters effecting telecommunications, and by Bacon (Bacon, 2012) in a similar study performed for the UK spectrum regulator Ofcom. Data from 38 gauges has been selected based on the quality and temporal span of the data. Only data with a tip-time resolution of one second is used to avoid bias in the one-minute rain rate distribution due to changes in the data acquisition temporal resolution. Each gauge-year, starting on a month boundary, with data covering at least 360 days i.e. 98.6% of the year, was used. This yielded 8418 overlapping gauge-years of data spanning 1985 to 2010.

5.3 Individual Gauge-Year One – Minute Distributions

The SPB method depends upon a strong link between the total annual rain accumulation, M_T, and the one-minute rain rate distribution. The most simplifying, albeit unrealistic, assumption to make is that the distribution of rain rate while raining, $f_R(R)$, is constant; and that only the proportion of time it rains each year P_R, accounts for all year-to-year variability.

The annual rain rate distribution is then;

$$f(R) = (1 - P_R)\delta(R) + P_R f_R(R) \tag{5.3}$$

where $\delta(R)$ is the Dirac delta function and the rain rate complementary cumulative probability function is directly proportional to the probability of rain:

$$f(R) = P_R F_R(R) \tag{5.4}$$

Note that P_R scales with the total rain accumulation:

$$P_R = \frac{M_T}{\bar{R}T_{year}} \tag{5.5}$$

where $\bar{R}$ is the mean rain rate when raining and T_{year} is a normalisation factor depending upon the time units used to measure rain rate. Using this model, the effect of M_T is a vertical translation of the log-exceedance versus rain rate curve leading to near-linear variation of the rain rate for a given exceedance, with larger gradients for smaller exceedances.

Figure 5.1 compares the annual accumulation M_T, with the 0.1% and 0.01% exceeded one-minute rain rates, $R_{0.1\%}$ and $R_{0.01\%}$ respectively, for individual gauge years. Near linear variation can be observed between M_T and $R_{0.1\%}$, consistent with the simplest constant distribution model. However, variation of M_T and $R_{0.01\%}$ exhibits far more scatter, implying far more year-to-year variation in the distribution of heavier rain. This is to be expected as rain rates at these low exceedances are determined by a relatively small number of heavy events each year.
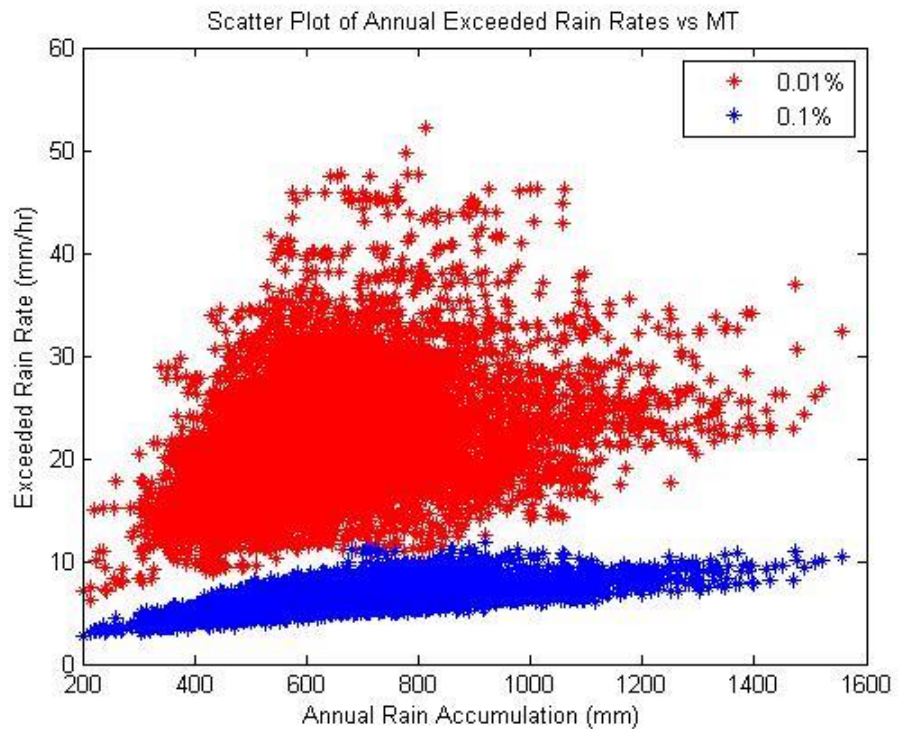

Figure 5.1: Scatter Plot of Annual Exceeded Rain Rates vs M_T

Figure 5.2 examines the same data but plots the exceeded rain rates against the annual rain accumulation due to rain rates above 20 mm/hr, M_{20}. This is an attempt to approximate the SPB parameter M_C, the annual accumulation due to convective rain. It is not possible to discriminate between convective and stratiform rain from rain gauge records. However, convective rain tends to be heavier and the rate of 20 mm/hr was chosen as an arbitrary but reasonable threshold.
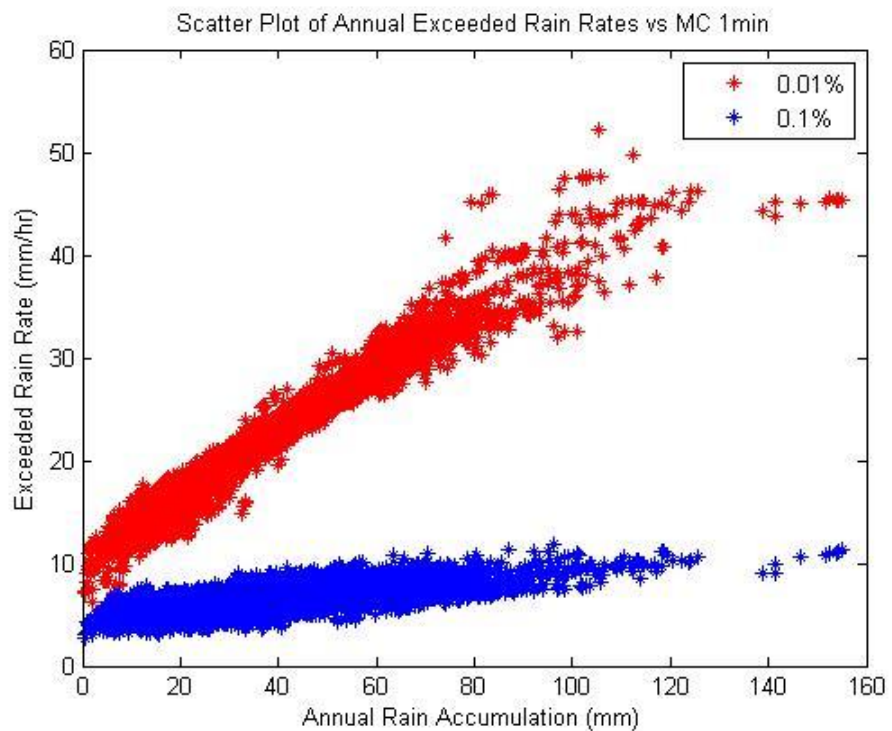
Figure 5.2: Scatter Plot of Annual Exceeded Rain Rates vs M_C

The linear relationship between M_{20} and $R_{0.1\%}$ is less strong than that in Figure 5.1, illustrating separate annual variation in the proportions of light and heavy rain. However, there is a strong correlation between M_{20} and $R_{0.01\%}$ with a correlation coefficient of $\rho = 0.977$. This is not surprising as the accumulation due to rain rates above 20 mm/hr is closely related to the period of time for which these rain rates occur.

Table 5.1, lists the correlation between $R_{0.01\%}$ and annual accumulation due to rain rates above given values. It can be seen that the correlation is not particularly sensitive to the choice of threshold; any rain rate between 15 mm/hr and 35 mm/hr yields high correlation. In particular, values in the range of typical UK 0.01% exceeded rain rates: 20 to 30 mm/hr, all yield very high correlation.

Rain Rate mm/hr	0	10	15	20	25	30	40
Correlation	0.34	0.92	0.97	0.98	0.97	0.95	0.88

Table 5.1: Correlation between $R_{0.01\%}$ and one-minute M_R for a range of values for R.

These results demonstrate strong correlations between average annual accumulations due to rain rate above different intensities and rain rates at exceedances associated with outage. However, the calculation of these accumulations requires one-minute rain rates. Typical NWP integration periods of 6 hours can, and often do, include shorter intervals of both convective and stratiform rain. It is possible that the NWP parameter M_C is closely approximated by M_{20}, and in this case these results support a link between M_T and M_{20}, and the radio parameters $R_{0.1\%}$ and $R_{0.01\%}$ respectively. However, in the next section we explore correlations between $R_{0.1\%}$ and $R_{0.01\%}$, and accumulations calculated using six-hour integration time data.

5.4 Individual Gauge-Year One–Minute and Six-Hour Distributions

This section investigates correlations between $R_{0.1\%}$ and $R_{0.01\%}$, and accumulations calculated using six-hour integration time data. NWP systems often yield six-hour integration time rain data. The same Environment Agency rain gauge data used in Section 5.2 are used in this analysis. The tip-time data have been accumulated yield to six-hourly rain rates and these have been formed into distributions. This allows comparison between the one-minute rain rates of interest and parameters derived from the six-hour distributions. Of particular interest are the annual accumulations due to six-hour intervals with higher average rain rates. These analyses are still for individual gauges sites. However, if correlations can be found for individual sites then the same should hold for regions. Similar to the analysis in Section 4.3, scatter plots have been produced of annual one-minute $R_{0.1\%}$ and $R_{0.01\%}$ and annual accumulation due to six-hourly rain rates greater than specific values. Due to the much longer integration period, the six-hourly rain rates are much smaller than one-minute rain rates. Figure 5.3 illustrates the scatter plot for rain accumulations due to six-hourly rain rates greater than 2.5 mm/hr. It is clear that the correlation is much weaker than with the 1-minute rain rate accumulations.
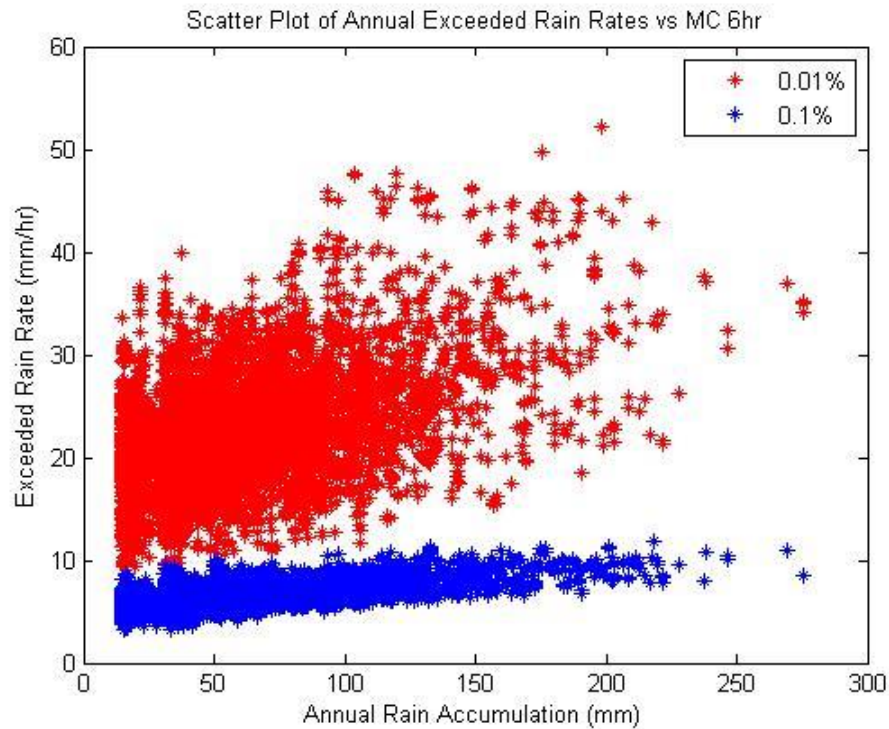
Figure 5.3: Scatter plot of the 0.1% and 0.01% exceeded rain rates against annual accumulation due to six-hour rain rates above 2.5 mm/hr.

The six-hour periods with high accumulations will contain a mixture of heavy, light and no-rain intervals. These intervals include accumulations that NWP systems would divide into convective and stratiform components, which is not possible with gauge data. Table 5.2 shows the correlation between $R_{0.01\%}$ and six hourly M_R for a range of values for R. These results show that the annual distribution of six-hourly accumulations are poor predictors of annual $R_{0.01\%}$. For a given distribution of six-hourly rain rates, considerable variation in $R_{0.01\%}$ is possible. This variation is expected to reduce as multi-year periods are considered as the mixture of stratiform and convective rain converge to average annual values. This is considered in Section 5.6. Similar convergence is expected from spatial averaging over a region and this is considered in the next section.

Rain Rate mm/hr	0	1.0	1.5	2.0	2.5	3.0
Correlation	0.34	0.40	0.45	0.49	0.49	0.44

Table 5.2: Correlation between $R_{0.01\%}$ and six hourly M_R for a range of values for R.

5.5 Regional Annual One-minute and Six-Hour Distributions

This section extends the results of the previous section to cover averages over the combined Midlands regions. Distributions of one-minute and six-hour rain rates from all the 38 gauge-sites in the three EA regions, are combined and the correlations identified in the previous section are tested. The regional average six-hour accumulation is close to the NWP total accumulation M_T but, as in the previous Section, there is no possibility to distinguish between stratiform and convective accumulations.

Figure 5.4 shows the scatter plot of the 0.1% and 0.01% regional exceeded rain rates against regional annual accumulation due to six-hour rain rates above 2.5 mm/hr. There are far fewer points in the scatter plot as all 38 gauges are used to produce a single average accumulation. The correlation between the accumulation due to regional average 6-hour rain rates greater than 2.5 mm/hr and regional 0.1% and 0.01% rain rates are 0.73 and 0.63 respectively. This is higher than for individual gauge-years as averaging over location reduces variation in the number of events with rain above the 0.01% exceeded rain rate.
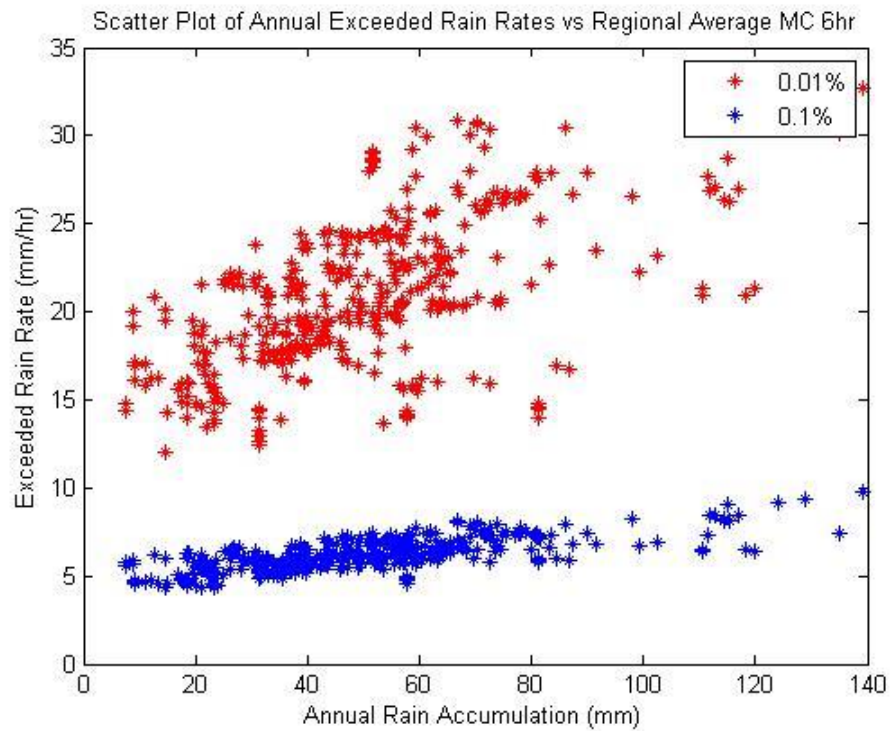
Figure 5.4: Scatter plot of the 0.1% and 0.01% regional exceeded rain rates against regional annual accumulation due to six-hour rain rates above 2.5 mm/hr

Convective rain cells are typically 5 to 10 km in diameter. Gauges more than a few kilometres apart experience a different selection of heavy rain events during the same period. A true regional accumulation, rather than one based on averaging over a small number of rain gauges, is likely to provide a slightly higher correlation. Convective cells are often associated with much larger weather systems and there is large year-to-year variation in the number of such systems a region will experience. However, some scatter will remain due to the year-to-year variation in the number of such systems experienced by the region.

5.6 Regional Averages over Multiple Years

Much of the scatter in Figure 5.4 was due to year-to-year variation. However, the SPB method was designed to be applied to long-term statistics. The meaning of long term depends upon the exceedance probability of interest, and increases with decreasing exceedance probability. Figures 5.5 compares regional accumulations due to six-hour rain rates above 2.5 mm/hr with $R_{0.1\%}$ and $R_{0.01\%}$, all derived from multi-year periods i.e. 2, 5, 10 and 20 years. The associated correlations are given in the Table 5.3.

Figure 5.5a: 2 years
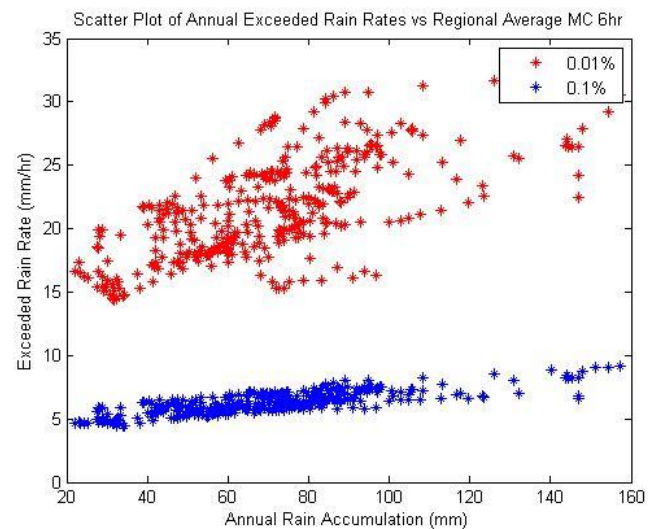
Figure 5.5b: 5 years

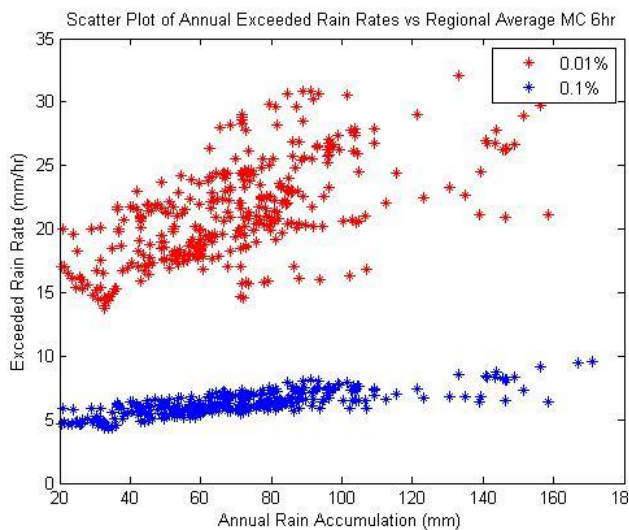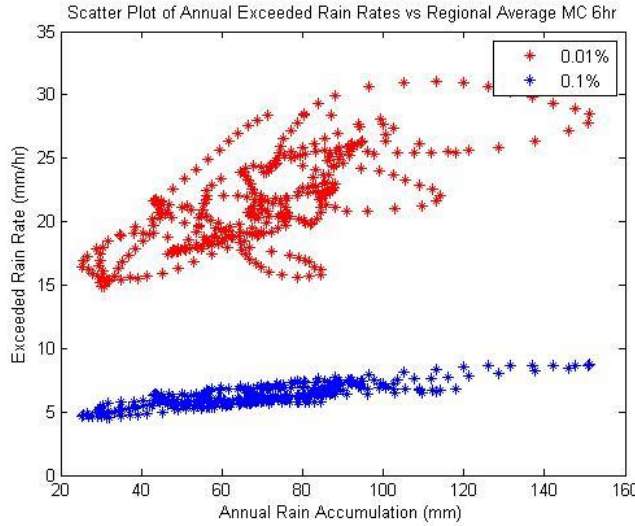Figure 5.5c 10 years
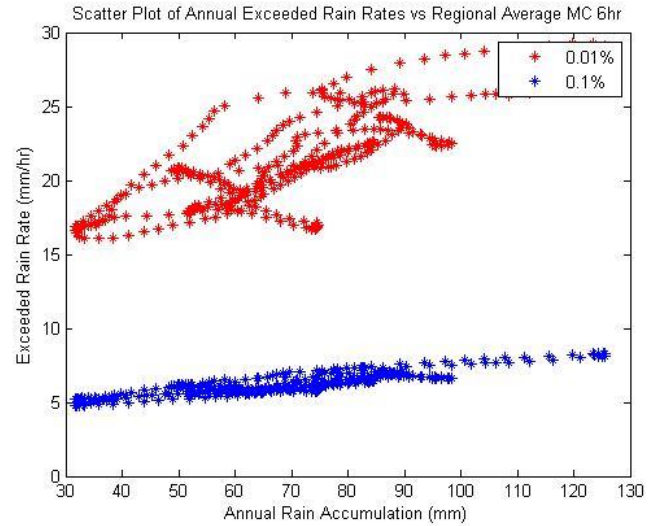
Figure 5.5d 20 years

Figure 5.5: Scatter plot of regional multi-year 0.1% and 0.01% exceeded one-minute rain rates against multi-year average accumulation due to six hour rain rates above 2.5 mm/hr for the periods of; a) 2 years, b) 5 years, c) 10 years and d) 20 years.

Years	1	2	5	10	20
Correlation 0.01%	0.63	0.63	0.66	0.71	0.80
Correlation 0.1%	0.73	0.78	0.80	0.84	0.89

Table 5.3: Correlation between multi-year $R_{0.01\%}$ and six hourly M_R multi-year averages

Correlation grows steadily when accumulation and rain distributions are averaged over increasing number of years, as expected. However, to some extent this may be due to the short total observation time i.e. 1985-2010 is a period of 25 years, only 5 years longer than the longest integration time considered. It is difficult to say whether this trend would be so strong, or would continue, if a longer dataset was available.

5.7 Discussion

The results have revealed that six-hourly accumulations are inherently poor estimators of the incidence of one-minute rain rates; as a wide range of events can yield the same six hourly accumulation i.e. a long period of light rain or a short period of intense rain. If the mix of rain events was the same for six hourly intervals with the same accumulation, then the correlation would be high. For periods of one or two years, this mix can vary by a large factor, mainly due to the incidence of extreme events, even over regions several hundreds of kilometres across. As the region gets larger and the averaging period becomes longer, then the mix becomes more stable and, for a specific climate, the six hourly accumulations become a better predictor of the one-minute distribution. However, the link between six-hourly and one-minute distributions will strongly depend upon climate and so relationships derived in this document will not necessary be translatable to other regions.

The Salonen-Poaires Baptista method uses the total annual rain accumulations due to all rain and just convective rain. It is not possible to distinguish convective rain from other forms, from rain gauge records. In this document, convective rain has been associated with high rain rates. At one minute integration times this association is a reasonable approximation. However, with six hour accumulations it is far from accurate. From this work it is impossible to tell if the six hour accumulations due to convective rain, as provided by Reanalysis datasets, is a useful parameter or not. The strongest statement that can be made is that increasing annual rain accumulation is positively correlated to one minute rain rates exceeded at outage levels. This is a useful result as regions with increasing trends in total annual accumulation can expect to see similar increases in one

minute rain rates, and probably with rain fade and outages. Total rain accumulation is a commonly estimated parameter and will be useful in identifying areas that may be experiencing increasing trends in rain at outage levels. The link between the incidence of rain at outage levels and outage is not definite and is still an open research question. Link fade depends upon rain rate along a link path, and so if events become smaller in diameter then rain rates at outage exceedances could increase while rain fade and outage rates could decrease.

5.8 Chapter Summary

The SPB model and method has been tested using a network of rain gauges. The underlying heuristics have proven to be reasonable. In particular, the link between M_T and the incidence of one-minute rain rates suggests a method to estimate trends on these rain rates globally from NWP reanalysis data. The development of the SPB method is opaque and it is likely that better transformations exist. It is likely that the convective accumulation M_C could play a stronger part in defining the incidence of heavy rain. This depends on the reliability of NWP M_C estimates, which is defined by the ability of the NWP models to characterise rain structures much smaller than the simulation integration regions. NWP reanalysis data will be reviewed in the next chapter.

CHAPTER 6

A Method to Estimate Trends in Distributions of One-Minute Rain Rates Globally

Dynamic fading due to rain and wet snow tends to be larger and longer lasting than that due to other mechanisms, on terrestrial and Earth-space links at frequencies above approximately 5 GHz. The International Telecommunication Union (ITU-R) maintains a set of models for predicting average annual distributions of rain fade, with a one-minute integration time, on individual links. An important parameter in these models of rain fade is the one-minute rain rate exceeded for 0.01% of an average year (R0.01%). This chapter will describe a method for predicting the evolution of one-minute rain rate distributions over land areas, globally.

High resolution rain gauge data is available in only a very small proportion of the globe. By contrast, numerical weather models, particularly reanalysis data, spans the globe and assimilates large amounts of measured data, including rain data from gauges and rain radar networks. The major drawback is that rain data is averaged over very large areas, typically hundreds of kilometres across, and accumulated over long times, usually six hours or daily. A relationship needs to be found between these low resolution rain parameters and the one-minute averaged, point rain rates required for radio regulation, spectral efficiency and performance optimization. To some extent this link has already been developed. Before 1999, Rec. ITU-R P.837-1 provided R0.01% globally by dividing the world into rain zones, over which all regions were assumed to experience the same one-minute rain rate distributions. This was replaced by a new model, Rec. ITU-R P.837-2,

where rain distributions were assumed to follow the Salonen-Poiares Baptista (SPB) double exponential model and associated method (Poiares Baptista and Salonen, 1998, Salonen and Poiares Baptista, 1997) and (ITU-R:StudyGroup3, 2012). The parameters of this distribution were linked to outputs from ERA15 reanalysis data, produced by the ECMWF and the parameters for later versions of this Recommendation were extracted from the ERA40 database. The Rec. ITU-R P.837-6 (ITU:Rec.P.837-6, 2012) model parameters are provided on global maps with a grid spacing of 1.125°.

6.1 Reanalysis and Gauge Data

The original work by SPB, as discussed in chapter 4, used parameters derived from ERA15 and later ERA40 reanalysis data provided by the ECMWF. ERA-40 data spans the interval 1957 to 2001, (Simmons and Gibson, 2000). Similar data is also provided by NOAA NCEP/NCAR: reanalysis 1 spanning 1958 to 2011. Although the NWP (Numerical Weather Predictions) algorithm does not change over the reanalysis period, the data available for assimilation does. For ERA-40 between 1973 and 1988, the amount of satellite data that were assimilated increases dramatically with time. After 1988 the amount of satellite data is large and the system can be considered stable, (Poiares Baptista and Salonen, 1998). Precipitation data from reanalysis products require calibration to surface measurements. For instance, ERA-40 has known problems with the humidity scheme of the ECMWF assimilation system, (Poiares Baptista and Salonen, 1998). The rain parameters over land-areas, used in Rec. ITU-R P.837-6, are based on calibration factors derived from the GPCC rain gauge dataset maintained by the Global Precipitation Climatology Centre of the Germany's National Weather

Service. Rain parameters over sea use a calibration factor derived from the Satellite-Gauge Precipitation Product produced by the Global Precipitation Climatology Project of the NASA Goddard Space Flight Centre (USA). In this thesis, the VASClimO dataset version 1.1 is used, (Schneider et al., 2011). Furthermore, reference are made to UK rain rate trends derived from rain gauge data acquired by the UK Environment Agency, (Paulson, 2011b, Paulson and Al-Mreri, 2011a, Bacon, 2012). Each tipping bucket gauge records the time of each 0.2 mm accumulation to the nearest second. Most gauges started recording to this resolution in the mid 1990's although the earliest data started in 1990.

6.2 Time Series of Precipitation Parameters

Although the original work by Poiares Baptista and Salonen that leads to the current global ITU-R rain models was based on ERA-40 data; the NCEP/NCAR reanalysis data was chosen for use due to the temporal span of data up to 2011. For statistically significant trend identification, the length of interval is important. Furthermore, as underlying climate trends appear to be accelerating i.e. surface temperatures (Solomon et al., 2007), it is important to include the most recent data. Two precipitation parameters have been extracted from the NOAA NCEP/NCAR reanalysis databases: total precipitation and convective precipitation, over 1.875° integration regions, over 6 hour periods. The three parameters M_T, M_C and P_{r6}; are estimated over each integration region and for each 365-day interval starting at midnight UTC. M_T and M_C are calculated as running sums of 4×365 consecutive values while P_{r6} is the percentage of 4×365 consecutive values for which the total precipitation is greater than 0.1 mm/6hr.

Three NOAA grid regions have been explored in detail. Each has a diameter of 1.875º and centred on the points listed in Table 6.1;

Name	Latitude	Longitude
North	54.6º	-0.9º
Midlands	52.8º	-0.9º
South	51.0º	-0.9º

Table 6.1: Centres of NOAA grid regions spanning the UK.

The accumulations need to be calibrated to VASClimO surface rain gauge measurements. Figure 6.1 provides a scatter plot of M_T derived from NOAA NCEP/NCAR and VASClimO, for the NOAA grid region covering the southern UK. The corresponding VASClimO estimates are produced by forming weighted sums of the smaller 1º VASClimO regions where the weights are proportional to the region overlap areas.
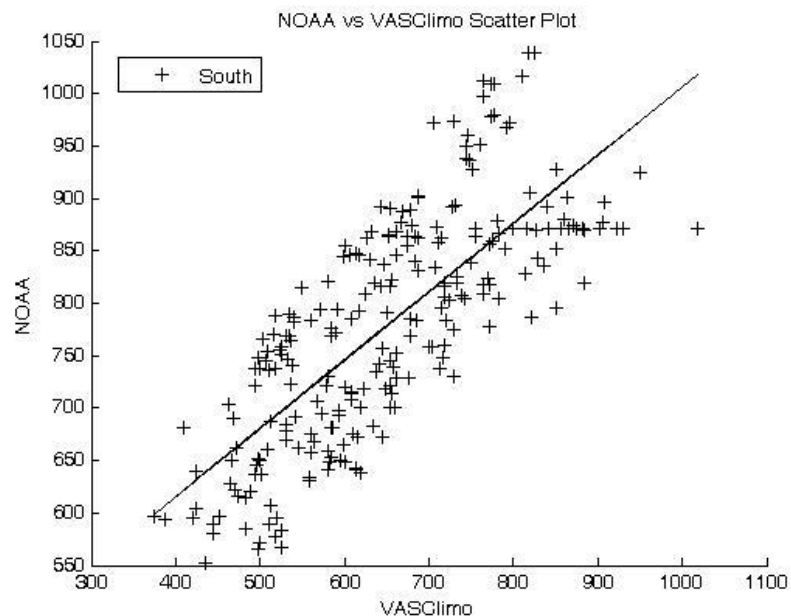

Figure 6.1: Scatter plot of Annual Total Precipitation Accumulation in mm (M_T) derived from NOAA NCEP/NCAR and from VASClimO for the Southern UK.

These plots show high correlation between the accumulation estimates, with regressions lines, with slope very close to one, but a significant offset as large as 30% of the annual accumulation. This result is in marked contrast with that of (Poiares Baptista and Salonen, 1998) where a multiplicative calibration factor was required to match ERA-40 accumulations with GPCC data. Table 6.2 lists the slope a, intercept b and Pearson correlation coefficient ρ; for the three UK NOAA regions.

Name	a	b (mm)	ρ
North	1.02	250	0.92
Centre	1.03	300	0.94
South	1.04	200	0.93

Table 6.2: regression slope, intercept and correlation coefficient for three NOAA grid regions spanning the UK.

Constant linear calibrations, such as those listed in Table 6.2, have been applied to all average annual NOAA accumulations, to make them consistent with the VASClimO database of gauge measurements. Assuming that the NOAA convective fraction:

$$(6.1)$$

$$\beta = \frac{\text{annual convective accumulation}}{\text{total annual accumulation}}$$

remains unchanged, then the same linear calibration can be applied to the annual convective accumulation, M_C and the assumption is made that calibration does not change over time. Figures 6.2a & 6.2b illustrates the time series of the three parameters M_T, M_C and P_{r6}; for the three UK NOAA grid cells. All parameters exhibit increasing temporal trends.
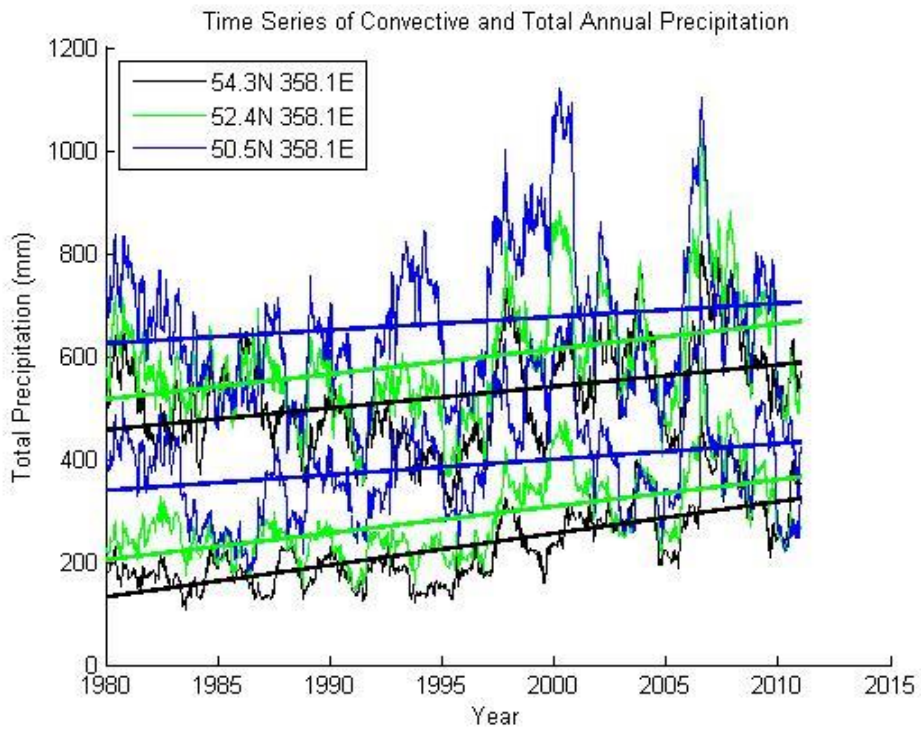
Figure 6.2a: Time Series of Annual Convective (lower) and Total (upper) precipitation accumulation for three NOAA grid areas covering the UK.
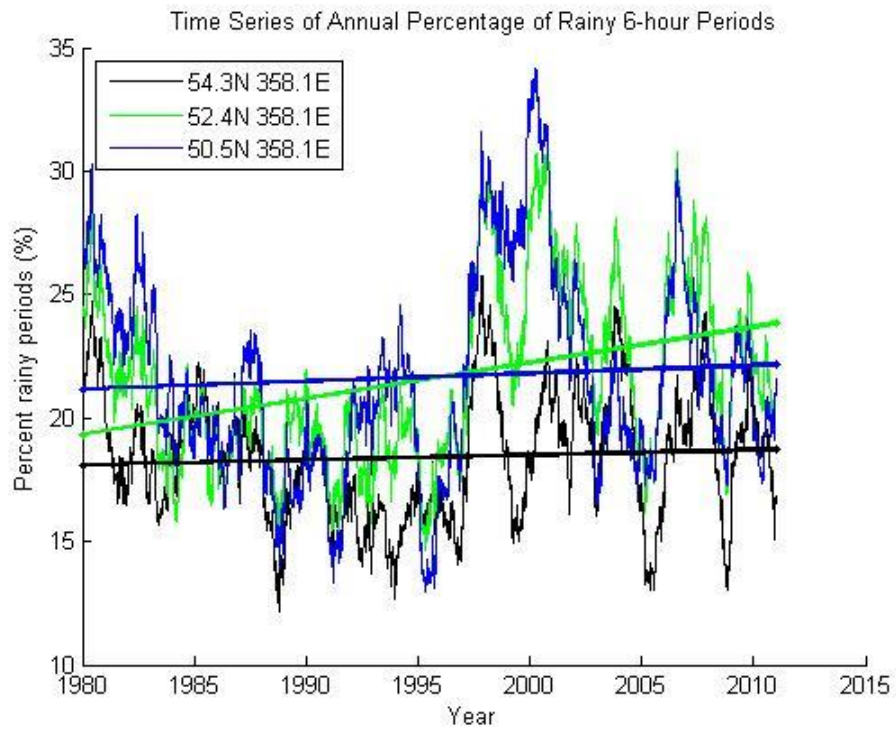

Figure 6.2b: Time Series of the Percentage of Annual 6-hour periods that experience rain for three grid areas covering the UK.

The percentage of annual 6-hour rainy periods is a function of integration area, therefore different NWP systems yield different results. Also, the majority of NWP systems will not return a rain accumulation of zero. This is almost certainly due to noise and round-off in the NWP calculations. Thus, Pr6 is often actually the percentage of 6-hour periods where the rain accumulation is larger than a certain threshold, which is chosen to be above the accumulation noise. The threshold chosen is subjective as the tail of the noise will overlap with real accumulations. It is likely that a better choice of parameter for models like SPB would be the percentage of 6-hour periods, where the rain accumulation is larger than some small but reliably measurable value (or values), such as 0.1 mm or 1 mm depending upon integration area.

6.3   Estimation of The Rain Rate Distribution

SPB proposed a link between the three parameters M_T, M_C and P_{r6}; and the average annual distribution of one-minute rain rates. As described in chapter 4, the four distribution parameters P_0 ,a, b, c; from (5.1), need to be determined from the three meteorological parameters; as in (5.2). The transformation defined by (5.2) is specific to ERA-40 1⁰ reanalysis data, due to the accumulation areas. The form of the transformation is expected to remain but the constants with numerical values in (5.2) are likely to be different when using NOAA NCEP/NCAR 1.824⁰ data.   When optimising the fit to the DBSG3 database, the data can be used in different ways. SPB assumed stationarity and so used values of meteorological parameters, averaged over all ERA-40 data from 1957 to 2001. In this thesis, non-stationary trends in precipitation are investigated and an alternative use of the

DBSG3 data is used. The meteorological parameters from the experimental time interval (one year experiments have been selected) over which the exceeded rain rates were measured are used. It is expected that this may yield a better fit as wet years, with a larger M_T are likely to be correlated with a higher R0.01%.

A number of cases are defined, using combinations of average annual (assuming stationarity) and specific annual reanalysis parameters. The four constants α_j in the SPB method (5.2) are allowed to vary to optimise the fit between DBSG3 measured R0.01% values, and the prediction using equations (5.2) with inputs being either average or specific annual meteorological parameters. Two sets of annual accumulation data are available: calibrated NOAA NCEP/NCAR reanalysis and VASClimO. Either VASClimO calibrated NOAA NCEP/NCAR data, or VASClimO data directly, may be used. The data in the DBSG3 database are not from sites evenly distributed around the world. To partially address this bias, site data is assigned a weight which is inversely proportional to the number of sites in a specific country.

The four cases considered are:

Case 1: Specific annual M_T, M_C and P_{r6}; from VASClimO calibrated NOAA NCEP/NCAR reanalysis data;

Case 2: Average annual M_T, M_C and P_{r6}; from VASClimO calibrated NOAA NCEP/NCAR reanalysis data;

Case 3: Specific annual VASClimO M_T, and specific annual M_C and P_{r6} from NOAA NCEP/NCAR reanalysis data;

Case 4: Average annual VASClimO M_T, and average annual M_C and P_{r6} from NOAA NCEP/NCAR reanalysis data.

The error functional is defined in a way analogous to the definition in Rec. ITU-R P.311-14 (ITU-R P.311-14), but with a weighted sum to compensate for the distribution of sites:

$$Error = \frac{1}{nCountry} \sum_{i=1}^{415} W_i \left| \log \left(\frac{R_i^{DBSG3}}{R_i^{S-B}} \right) \right| \tag{6.2}$$

In (6.2), W_i is the weight for the ith site, and R_i^{DBSG3} and R_i^{S-B} are respectively the exceeded rain rates from DBSG3 and from the model using the test parameters for the case being tested. In this method, only the 0.01% exceeded rain rate was used, as this is the input parameter to ITU-R fade models. The normalising constant $nCountry$ is the number of countries with sites used in the DBSG3 database, and its use allows the functional value to be interpreted as the average relative error. This functional has been minimized using the Nelder-Meade simplex method, starting from the current Rec. P.837-6 values. Numerical experiments showed that doubling or halving any initial parameter yielded the same minimum.

	Optimal Solution				Error
	α_1	α_2	α_3	α_4	
Case 1	48.15	0.635	0.838	0.4603	0.2976
Case 2	19.50	0.609	1.391	0.7791	0.2418
Case 3	8.79	0.921	1.151	0.5866	0.3167
Case 4	10.47	0.961	1.078	0.5392	0.2789

Table 6.3: Experiment results with optimal values and the minimum errors.

The experimental results show that the case 2, which uses the stationary parameters, yields the minimum error value of 0.2418. Although an average 24% error appears large, it can be compared with the Castanet *et al* study (Castanet et al., 2007) which yielded average relative errors around 0.3.   It must be remembered that DBSG3 provides specific annual measurements which are being compared with an average annual distribution, and so a large spread of 0.01% exceeded rain rates is to be expected.

Figures 6.3 illustrates the DBSG3 R0.01% values for the 415 DBSG3 site-years with annual data, and the best fit predicted R0.01% values using the optimal parameters from cases 1, 2 and 4. The data are in temporal experiment order and the increasing trend in the rain rates is due to the increasing amounts of data from Asia and South America in recent decades. The best fit follows gross trends well but there is still considerable deviation for specific site-years. For case 2, the 0.01% exceeded rain rate yields values around 20-40 mm/h for temperate regions such as Europe and Northern America and it is clear that the predicted 0.01% rain rate over estimates in temperate regions, while its underestimates in the tropics. This suggests that stronger dependence on the convective fraction β may yield an improvement to the SPB method.
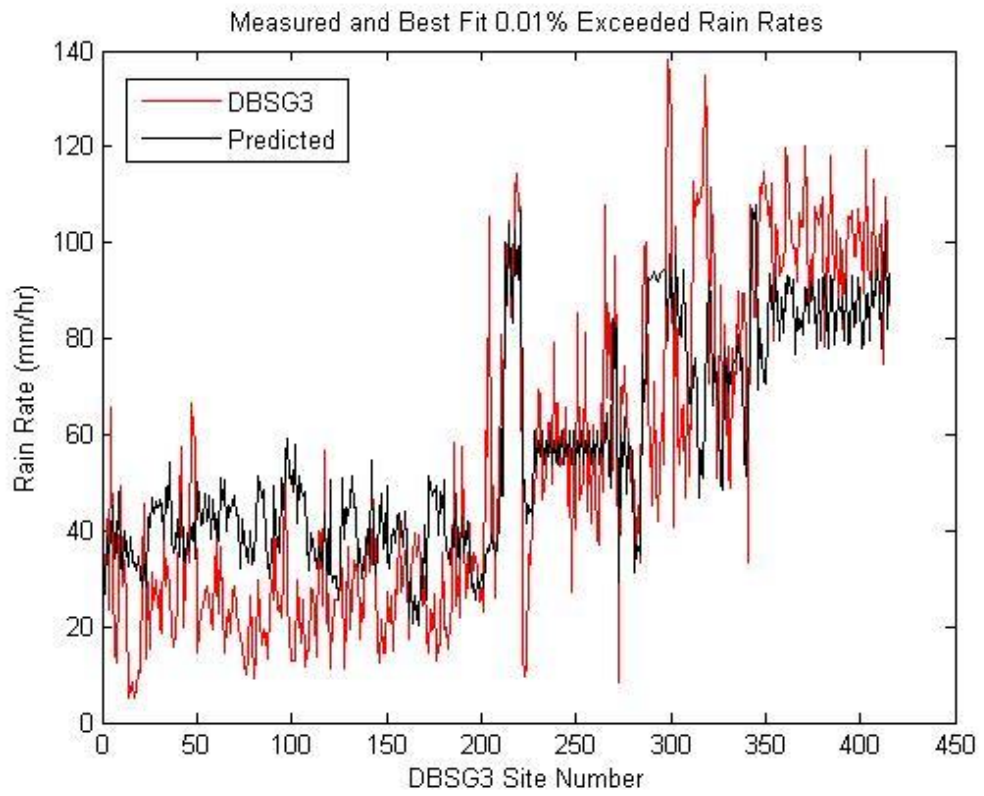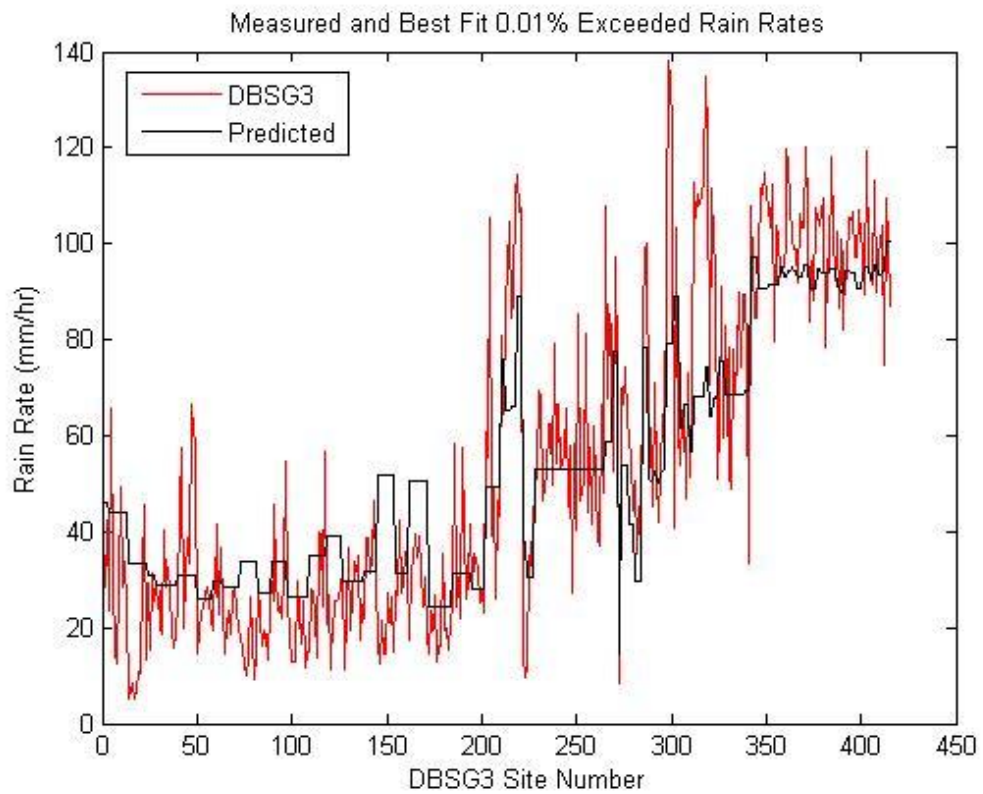
Figure 6.3a: Case 1.

Figure 6.3b: Case 2
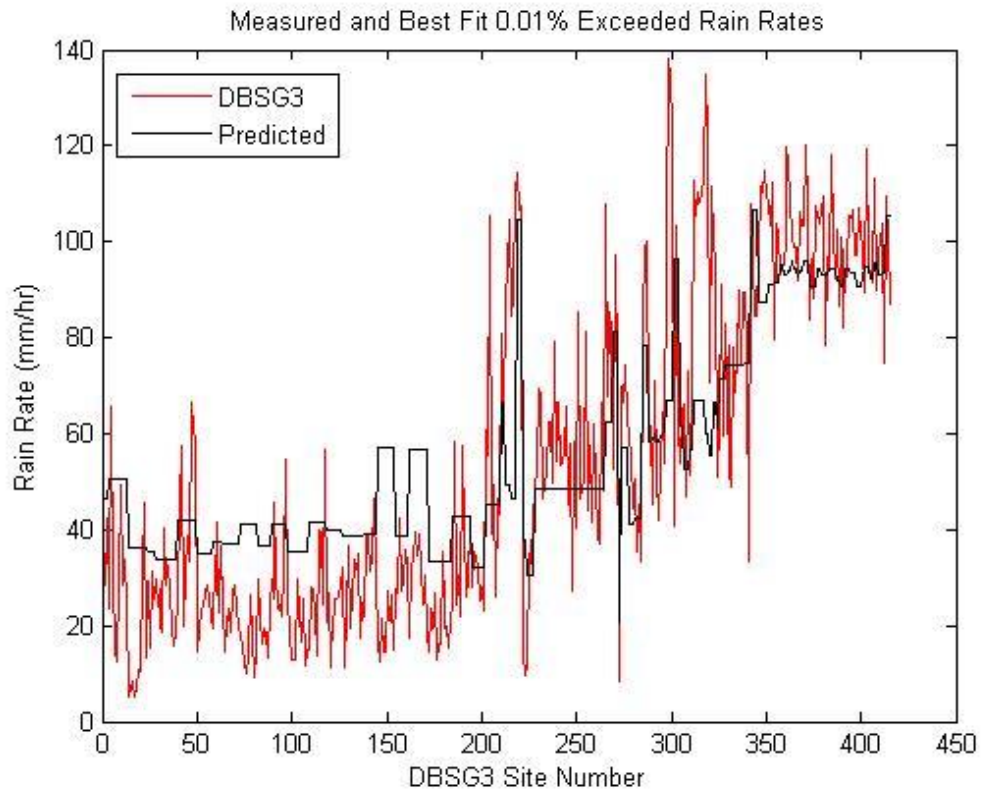
Figure 6.3c: Case 4

Figure 6.3: Time Series of Measured Annual 0.01% exceeded rain rates compared to the best fit prediction using: a) Case 1, b) Case 2 and c) Case 4.

6.4 The Time Series of Predicted Rain Rates

The calibrated NOAA NCEP/NCAR data illustrated in Figs 6.1 and 6.2, allow the calculation of time series of 0.01% exceeded rain rates using the distribution (5.1) and the transformation (5.2) using Case 2 optimised constants. This is speculative as the input and output parameters to the SPB distribution and transformation are average annual values, as discussed in the introduction. However, even if the method is a poor predictor of individual yearly rain rate distributions, it is possible that long term trends will be reproduced. Figure 6.4 illustrates these 0.01% exceeded rain rate time-series, calculated using the refined SPB method, for the

87

three NOAA grid regions spanning the UK. All three time-series show large year-to-year variation, but also exhibit increasing trends of approximately 0.4, 1.0 and 0.1 mm/hr/year for the regions South, Midlands and North respectively.
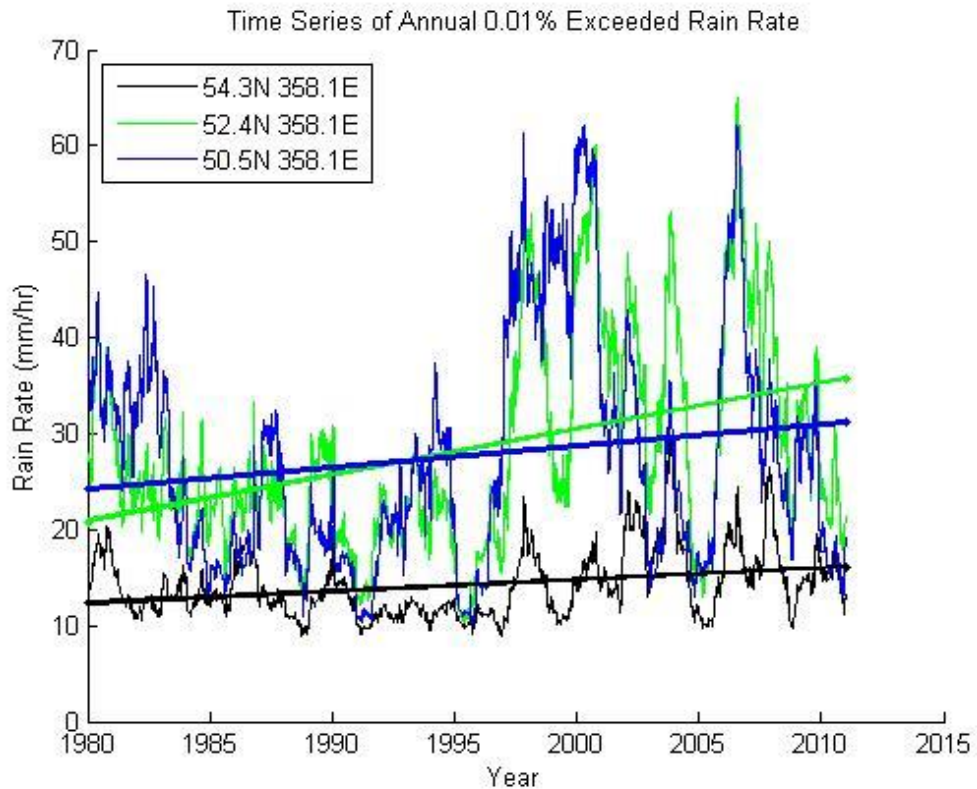
Figure 6.4: Time Series of 0.01% exceeded rain rates derived from NOAA NCEP/NCAR Reanalysis data using distribution (5.1) and the transformation (5.2).

Figure 6.5 shows the rain rates exceeded at annual time percentages of 0.005%, 0.05%, 0.03%, 0.01%, and 0.1%, for the eighty rain gauges in Southern England, (Paulson, 2011b). Error bars indicate the mean, upper and lower quartiles for the best fit Weibull distribution to all the available exceeded rain rates for each annual period. The gradient of the Maximum Likelihood (MLE) line fitted to the 0.01% exceedance data has a slope on 0.44 mm/hr/year.
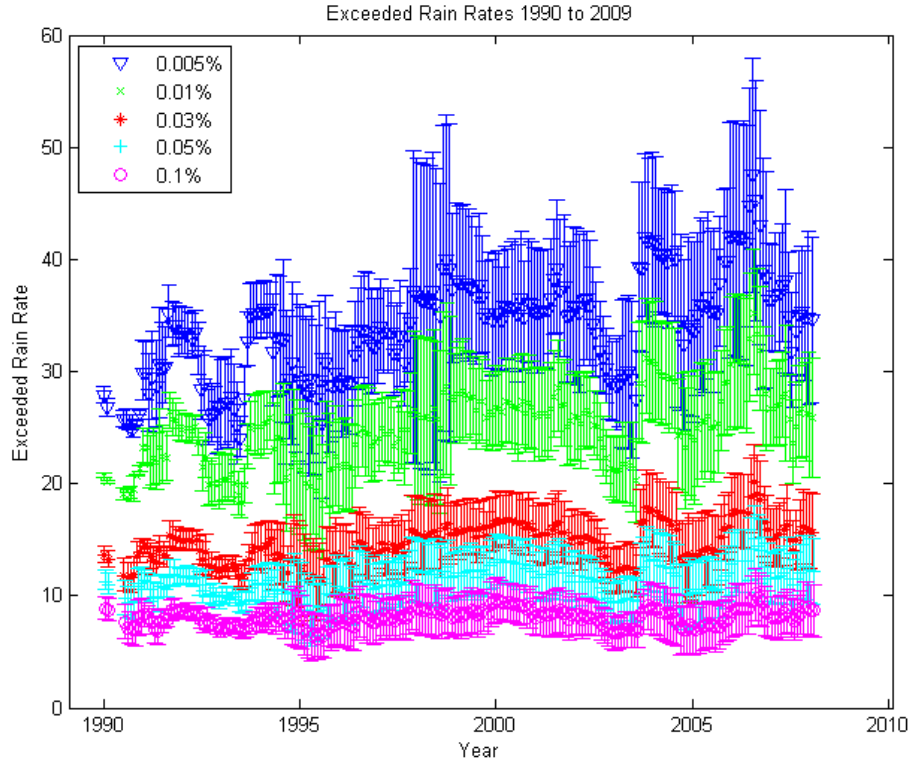
Figure 6.5: Time Series of exceeded annual rain rates from 80 gauges in the Southern UK.

The slope of the 0.01% exceeded rain rate can also be compared to that found in the Ofcom study, based on 1350 high resolution rain gauges across the UK, (Bacon, 2012). This found increasing trends in 0.01% exceeded rain rates around 0.4 mm/hr/year in the North and 0.8 mm/hr/year in the South.

A simpler method is considered where the transformation from rain parameters to 0.01% exceeded rain rate is linearised i.e.

$$\frac{dR_{0.01\%}}{dt} = \frac{dR_{0.01\%}}{dM_T}\frac{dM_T}{dt} + \frac{dR_{0.01\%}}{dM_C}\frac{dM_C}{dt} + \frac{dR_{0.01\%}}{dP_{r6h}}\frac{dP_{r6h}}{dt} \qquad (6.3)$$

The derivatives of M_T, M_C and P_{r6}; were estimated by fitting linear regression lines to 21 year time-series, 1980 to 2001, of calibrated NOAA parameters. The derivatives of the transformation between rain parameters and the 0.01% exceeded rain rate were evaluated numerically around the 21 year average parameter value. From the chain rule (6.3), trend slopes in the 0.01% rain rate was estimated for the three regions spanning the UK and results are shown in table 6.4. Given the different time periods considered and the standard errors in the slopes, these results are consistent.

Region	This Work Slope	Ofcom Study Slope
North	0.6 mm/h/year	0.4 mm/h/year
Midlands	0.8 mm/h/year	0.6 mm/h/year
South	1 mm/h/year	0.8 mm/h/year

Table 6.4: Trend slopes of 0.01% exceeded rain rates over 3 UK regions.

6.5 Global Trends in 0.01% Rain Rates

The time-series method, used to estimate the 0.01% rain rate trends over the UK, can be applied to the rest of the world. The VASClimO calibration data is only available for land areas and so the predictions are similarly constrained. From the calibrated NOAA NCEP/NCAR and GPCC meteorological parameters, the time-series of 0.01% exceeded rain rates can then be calculated for each NOAA grid region. From the time-series, the slope of the trend line for each grid cell can be calculated. Figure 6.6 illustrates this trend slope.
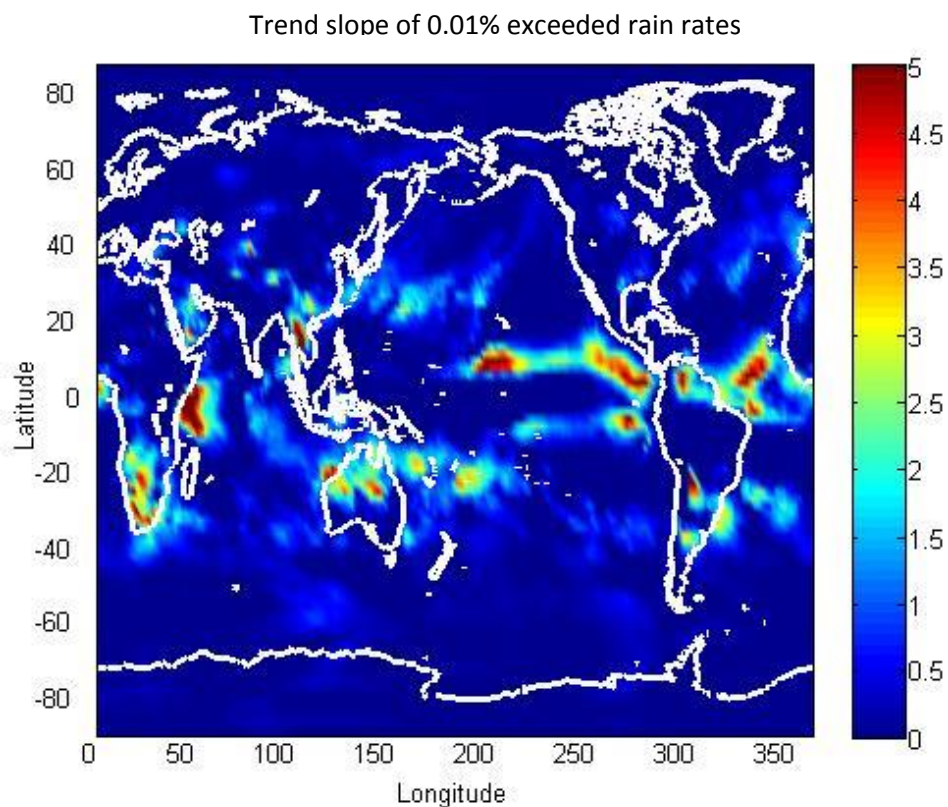
Figure 6.6: Trend slope of 0.01% exceeded rain rates, in mm/hr/year, derived using the SPB distribution and transformation from NOAA/GPCC time series of precipitation parameters.

This approach is speculative as it has only been tested in the UK. However, it is better to have some estimate of 0.01% rain rate trends than none at all. For some regions the trend slopes are not reliable due to the low incidence of rain, particularly Saharan Africa and mountainous regions such as the Himalayas, Andes and Rockies. Of all the NOAA grid cells, 90% yielded trends that are statistically significant with a probability of occurring by chance of less than 1%. Of the trend slopes greater than 0.2 mm/hr/year, 40% are statistically significant. The results presented in Fig. 6.6 suggest many parts of the world are experiencing rapid increases in 0.01% rain rate; particularly tropical areas within 30° of the equator.

6.6 Maps of Mean Annual Total Precipitation (M_T) and Mean Total Convective Precipitation (M_C) derived from NCEP/NCAR, VASClimO and ITU-R P. 837-6

Figure 6.7, 6.8 and 6.9 compares the Mt derived from VASClimO data with mean annual total precipitation derived from NCEP/NCAR reanalysis data and ITU-R Rec. P. 837-6.

Figure 6.7: Mean annual total precipitation from VASClimO dataset

Figure 6.8: Mean annual total precipitation from NOAA NCEP-NCAR
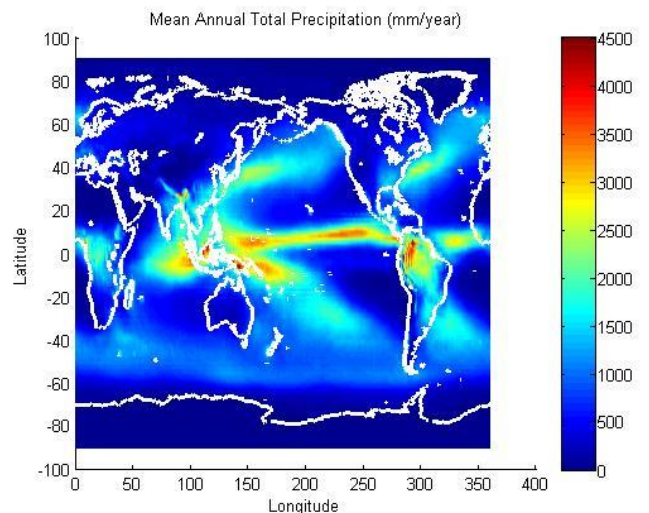
Figure 6.9: Mean annual total precipitation from ITU-R. P. 837-6

The VASClimO dataset only provides daily precipitation accumulation over the land areas. Therefore VASClimO data has been extrapolated over the sea using NOAA NCEP/NCAR pixels. Figure 6.10, 6.11 and 6.12 compares the extrapolated VASClimO Mt with mean annual total precipitation derived from NCEP/NCAR reanalysis data and ITU-R Rec. P. 837-6.

Figure 6.10: Mean annual total precipitation extrapolated over sea from VASClimO Dataset

Figure 6.11: Mean annual total precipitation NOAA NCEP-NCAR

Figure 6.12: Mean annual total from precipitation from ITU-R. P. 837-6

Figure 6.13, 6.14 and 6.15 compares the Mc derived from VASClimO data with mean annual convective precipitation derived from NCEP/NCAR reanalysis data and ITU-R Rec. P. 837-6.
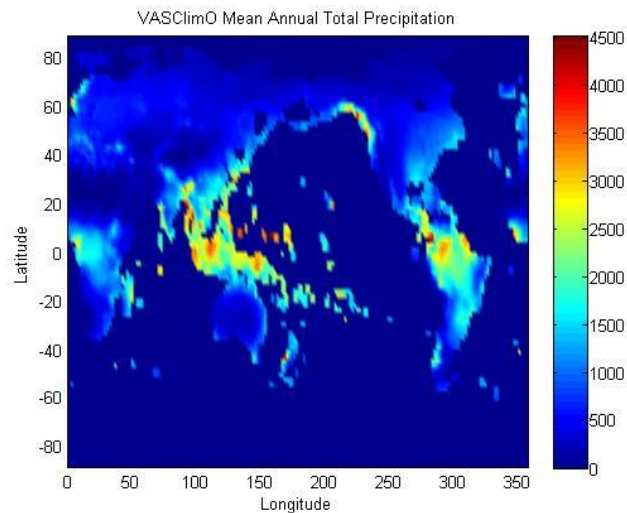

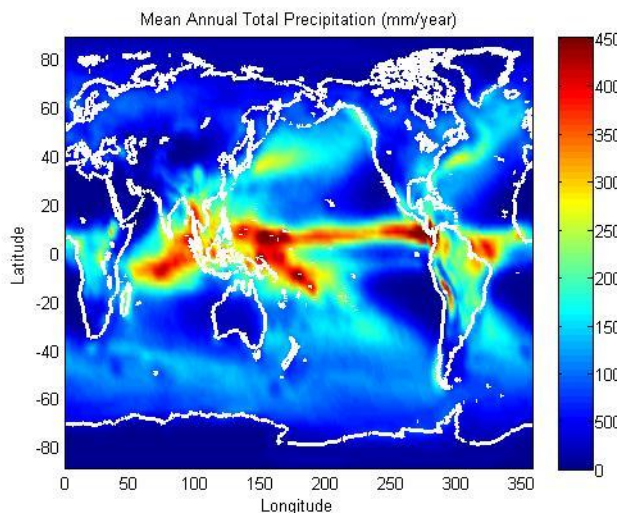Figure 6.13: Mean annual convective precipitation from VASClimO dataset

Figure 6.14: Mean annual convective precipitation from NOAA NCEP-NCAR
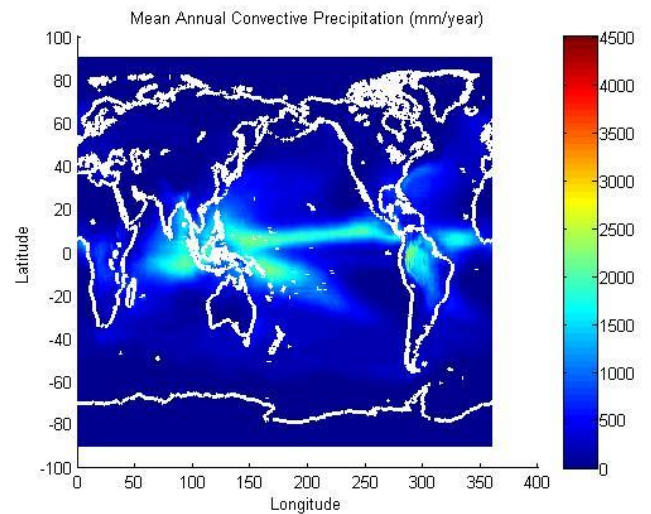
Figure 6.15: Mean annual convective precipitation from Rec. ITU-R P.837-6

Figure 6.16, 6.17 and 6.18 compares the extrapolated VASClimO Mc with mean annual convective precipitation derived from NCEP/NCAR reanalysis data and ITU-R Rec. P. 837-6.
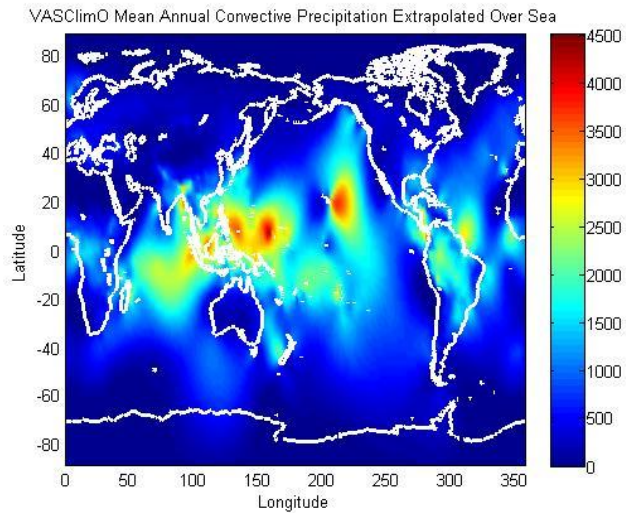
Figure 6.16: Mean annual convective precipitation extrapolated over sea from VASClimO Dataset
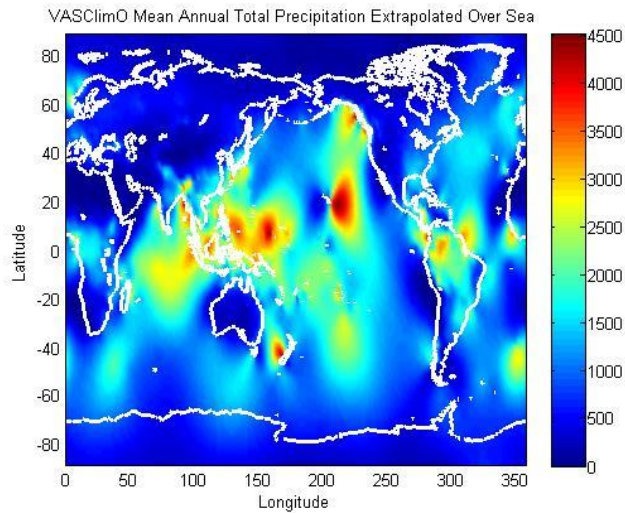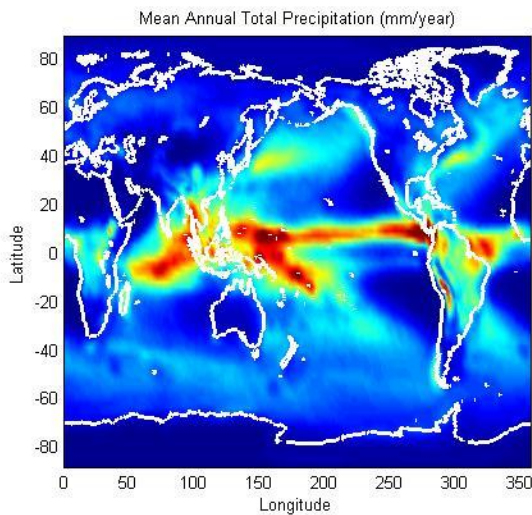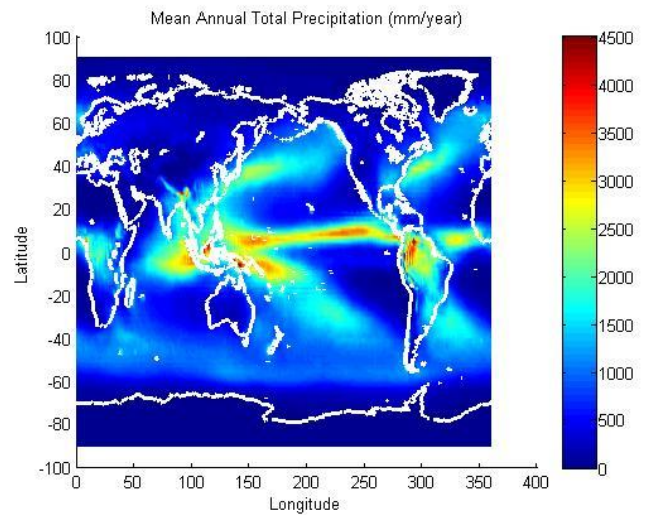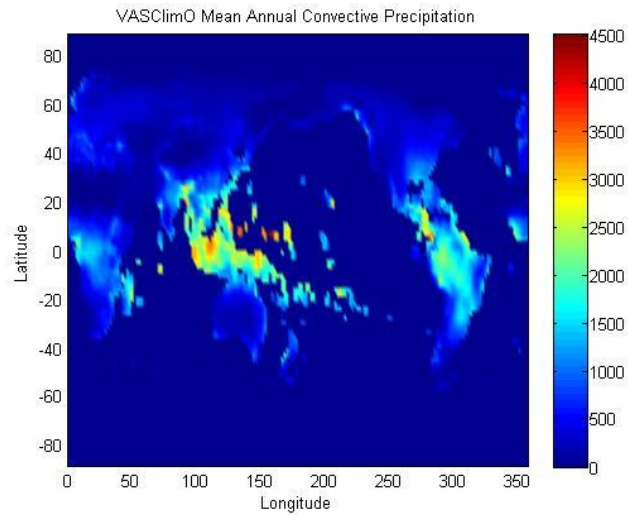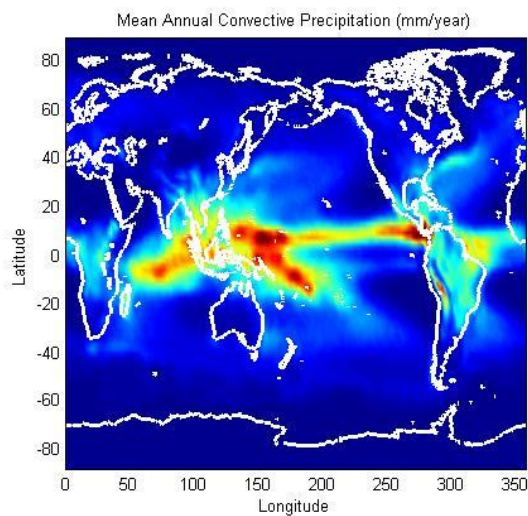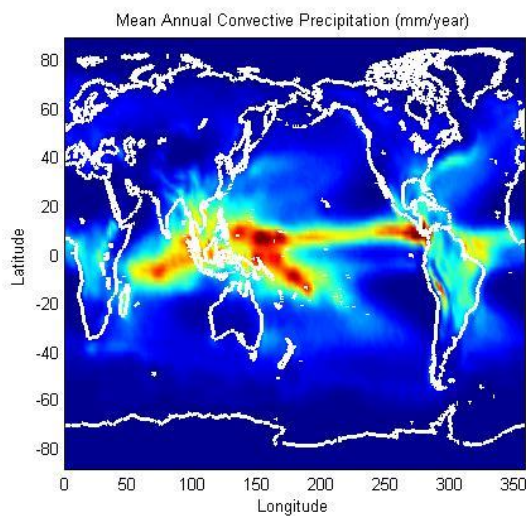

Figure 6.17: Mean annual convective precipitation from NOAA NCEP-NCAR
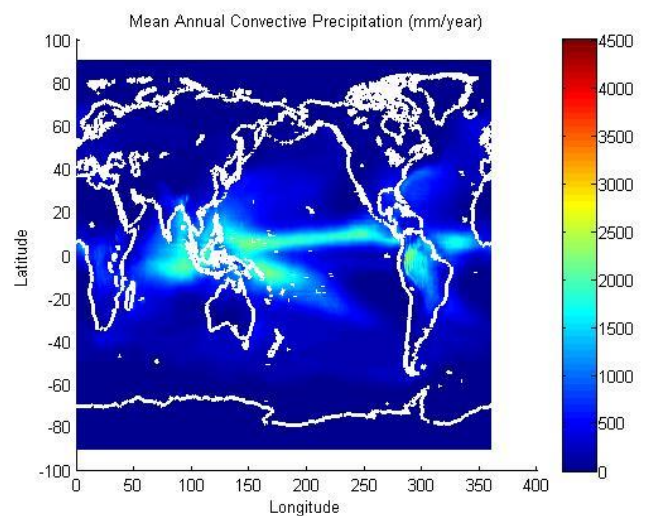
Figure 6.18: Mean annual convective precipitation from Rec. ITU-R P.837-6

6.7 Chapter Summary

A method has been developed for predicting the evolution of one-minute rain rate distributions, over land areas, globally. The method is based on the widely accepted Salonnen-Poiares-Baptista method that is integral to Rec. ITU-R P.836. An extended version of Salonnen-Poiares-Baptista method has been introduced by removing the implicit assumption of climate stationarity, and using GPCC calibrated NOAA NCEP/NCAR reanalysis data rather than the ECMWF ERA-40 data. The trend slope in 0.01% exceeded rain rates in three NOAA grid regions spanning the UK have been estimated with the new method and are consistent with results produced by two independent researchers analysing a large database of high resolution rain gauge data.

When climate trends lead to large changes in the underlying fade distributions, over the lifetime of a radio system, then these can have serious effects on system performance. Such changes can undermine the system business model or make it not fit for purpose. These considerations are particularly important for expensive space based systems where hardware adaptation is difficult or impossible. Such systems are designed with wide margins to allow for climate variability. Introducing climate trends into the margin calculation may lead to more realistic estimates of the range of climates a system will encounter over its lifetime.

The assumption of climate stationarity is deeply embedded in the ITU-R recommendations and the processes controlling their evolution. Refinements of Recommendations are tested against the DBSG3 database of measurements, collected over the last 50 years. Removing the assumption of stationarity changes the way this database is used, as described in this chapter. When predicting the

performance of systems several decades into the future, non-stationary recommendations are likely to produce more reliable results.

CHAPTER 7

Conclusions and Future Outlook

The main focus and the objective of this thesis has been to investigate the introduction of climate change into global radio propagation models. The global model of one-minute rain rate distributions, Rec. ITU-R P.837-6, provides fundamental inputs to models of both terrestrial and Earth-space links. A major outcome has been the development of a method to predict trends in rain rate distributions globally.

There exists a worldwide lack of data, both rain rate and rain fade data, and this leads to fundamental limitations on the confidence that can be placed on models of rain fade. This project has not addressed a fundamental unknown: do trends in rain rate lead directly to trends in rain fade. As rain fade is a line-integral quantity, trends in point quantities like rain rate need not lead to changes in the integrated quantity. In either case, ITU-R models need modification.

The UK is unique in having a large database of high resolution rain rate data. In most regions of the globe there is none. Due to the almost entire lack of one-minute rain data globally, estimates of trends in distributions needed to be derived from surrogate variables, assumed to be correlated with one minute rain rates. This process has already been built into the ITU-R recommendations, where a link between rain parameters from coarse-scale NWP reanalysis data and one-minute distributions, is inherent in Rec. ITU-R P.837-6. It therefore follows that trends in NWP parameters would correlate with trends in fine scale rain distributions.

The following sections summarise some of the significant conclusions reached in earlier chapters followed by potential future work.

7.1 Main Conclusions

7.1.1 Salonen – Poiares Baptista Method

The Salonen–Poiares Baptista method has been tested using Environment Agency gauge data. The double exponential distribution is a reasonable choice, but has limitations. Specifically, it cannot be integrated and so the distribution cannot be analytically linked to rain accumulation. Furthermore, the distribution parameters were not found to correlate with any measured annual accumulations. A link was found between M_T and rain rates exceeded at large time percentages e.g. 0.1% to 1%. It is likely that the convective accumulation M_C should have more influence when modelling the incidence of heavier rainfall. However this depends upon how reliable NWP derived M_C estimates are. This is constrained by the ability of the NWP systems to characterise rain structures much smaller than the simulation integration regions.

The current Rec. ITU-R P.837-6 is based on work by Salonen and Poiares-Baptista using ECMWF ERA-15/40 reanalysis data. The method developed in this thesis employs NOAA NCEP/NCAR reanalysis data, calibrated using VASClimO data. The evaluation of these data for propagation studies has identified characteristics that need to be considered when they are used. SPB found that multiplicative calibration factor was required to match ERA-40 to gauge accumulations. This

project used the VASClimO dataset of gauge based accumulations, specifically designed to reduce anomalies associated with gauge selection. To match NOAA NCEP/NACAR Reanalysis data to VASClimO required sizable additive calibration.

One of the significant reasons for using NOAA Reanalysis data was its temporal span, up to 2011. Global temperatures started to rise significantly around 1980. This is also after the period of reanalysis uncertainty where assimilation data rapidly changed to include many space based observations. The use of NOAA NCEP/NCAR data allowed trend analyses to be performed over a longer period than would have been possible with ERA-40 i.e. from 1980 to 2011 rather than to 2000. A disadvantage of NOAA NCEP/NCAR data is the lower spatial resolution compared to ERA-40.

The trends reported in this thesis are averages over 30 years. It is possible that rain rate is experiencing non-linear variation in many locations. However, the data do not support the more complex analysis required to identify these. If a region has experienced a trend over 30 years, then this is our best estimate of future variation over the next few decades. It is more difficult to make stronger statements on future variation, especially when global application is required. A future project could link the outputs of models based on recognised climate scenarios, such as those maintained by the IPCC, to trends in propagation.

7.1.2 The DBSG3

Revisions of ITU-R recommendations are tested against the DBSG3 database, composed of data acquired over past 60 years. Data in the first and second half of the 60 year period are quite different. The earlier period has mainly low frequency data from Europe and North America, while the later period contains far more high frequency data from Asia and South America. Even assuming a stationary climate, the location and frequency trends in DBSG3 could lead to compensating errors i.e. compensating errors in path reduction factors and specific attenuation-rain rate relationships.

Verification exercises have not taken the time that data was acquired into account. When the climate is experiencing significant change, then this can also lead to errors. For example, parameters effecting low frequency propagation would be fitted to historical data while higher frequency parameters are tested against more recent data.

In this project we have developed and used a verification method that does not assume climate stationarity. It is not immune to this problem, which is inherent in the data contained in DBSG3, however, it does not bias against non-stationary prognostic models. New problems are introduced, for example models with unrealistic trends may not be identified. For example, a model could include parameter trends that yield poor estimates of fade on high frequency links operated 50 years ago but good estimates of recently acquired data. This model is likely to yield poor predictions of future fade.

7.1.3 Revision of ITU-R P.837-6

Given the results of the work described in Chapter 6, the ITU-R global model of one-minute rain rate distributions could be extended. The current Rec. ITU-R P.837-6 model is the result of considerable amounts of development work and is based on the higher resolution ERA40 1° data, than the NOAA NCEP/NCARR data used in this thesis. In recent years, a lot of work has focussed on coastal regions where ERA40 integration areas span a mixture of sea and land. The biases and errors introduced in these regions effect many of the globally important population centres. For these reasons, it is not proposed to replace the current Rec. ITU-R P.837-6 model with the results developed in this project. However, the work described in this thesis has produced estimates of the trend slope in 0.01% exceeded rain rates globally. There is no trend information or guidance currently included in Rec. ITU-R P.837-6. Appendix A provides a revised version of this important ITU-R Recommendation, with a method to estimate trends in 0.01% exceeded rain rates globally. This proposed revision will be submitted to ITU-R UK Study Group 3 for consideration and possible submission to the ITU-R.

7.2 Future Work

In the course of this project, several unknowns and research questions have become apparent. In addition, there are several research results that require effort for their acceptance by the users and regulators.

7.2.1 Research Questions

A. Do trends in rain rate distributions translate to trends in rain fade distributions?

It is known that the UK is experiencing increases in the incidence of rain rates around the 0.01% exceedance level. Are rain fades similarly increasing? This question could be answered given reliable rain fade data spanning a decade or more, and of sufficient quantity to average out point-to-point and year-to-year variation. Less reliable results could be obtained from archives of rain radar data.

B. Is there are better formulation than the Salonen – Poiares Baptista model?

This project has highlighted limitations in the SPB double exponential distribution and the relationship between distribution parameters and NWP outputs. In particular, results suggest that the convective fraction should have a stronger influence on distribution shape. New models could be tested against existing DBSG3 data. More data would allow better resolution of models.

C. How well do the rain trends predictions developed as part of this project match reality in places outside the UK?

The rain rate trends need to be verified outside the UK. This requires high resolution data from places outside the UK.

D. How should revisions in ITU-R Recommendations be tested against DBSG3 data?

A method has been suggested and used in this project, but it is insensitive to some parameter trends and so could introduce errors.

7.3 Promotion of Results

A major output of this project is the revised Rec. ITU-R P.837. For this revision to be accepted by the ITU-R, considerable effort will be required to guide it through ITU-R UK Study Group 3 and ultimately on to acceptance by the ITU-R. Climate change is an intensely political subject and acceptance is far from certain.

Revisions of Recommendations usually need to be demonstrated to provide a better fit to DBSG3 data. The proposed revision to Rec. ITU-R P.837 has the advantage that it does not affect current predictions, and so as long as the standard stationary tests are used, then the results will be identical. Other work at Hull has produced a global model of rain height variation around the long term mean, based on a Skew Normal distribution. This could be formulated as an entirely new Recommendation, and referenced by revised Recommendations Rec. ITU-R P.530 and Rec. ITU-R P.618, which both currently include similar, but different, rain height distributions. This would be considerably more difficult to guide through to acceptance as it changes predicted fades for both terrestrial and Earth-space links.

The rain height work also identified significant temporal trends in rain height globally, associated with global warming. This could be incorporated into a revised Rec. ITU-R P.839, in the same way that trends have been introduced into P.837. As this revision would similarly not affect current fade predictions, it avoids one hurdle to acceptance.

ITU-R
Radiocommunication Sector of ITU

Recommendation ITU-R P.837-7

(09/2014)

Characteristics of precipitation for propagation modelling

P Series

Radiowave propagation

Foreword

The role of the Radiocommunication Sector is to ensure the rational, equitable, efficient and economical use of the radio-frequency spectrum by all radiocommunication services, including satellite services, and carry out studies without limit of frequency range on the basis of which Recommendations are adopted.

The regulatory and policy functions of the Radiocommunication Sector are performed by World and Regional Radiocommunication Conferences and Radiocommunication Assemblies supported by Study Groups.

Policy on Intellectual Property Right (IPR)

ITU-R policy on IPR is described in the Common Patent Policy for ITU-T/ITU-R/ISO/IEC referenced in Annex 1 of Resolution ITU-R 1. Forms to be used for the submission of patent statements and licensing declarations by patent holders are available from http://www.itu.int/ITU-R/go/patents/en where the Guidelines for Implementation of the Common Patent Policy for ITU-T/ITU-R/ISO/IEC and the ITU-R patent information database can also be found.

<table>
<tr><td colspan="2">Series of ITU-R Recommendations
(Also available online at http://www.itu.int/publ/R-REC/en)</td></tr>
<tr><td>Series</td><td align="center">Title</td></tr>
<tr><td>BO</td><td>Satellite delivery</td></tr>
<tr><td>BR</td><td>Recording for production, archival and play-out; film for television</td></tr>
<tr><td>BS</td><td>Broadcasting service (sound)</td></tr>
<tr><td>BT</td><td>Broadcasting service (television)</td></tr>
<tr><td>F</td><td>Fixed service</td></tr>
<tr><td>M</td><td>Mobile, radiodetermination, amateur and related satellite services</td></tr>
<tr><td>P</td><td>Radiowave propagation</td></tr>
<tr><td>RA</td><td>Radio astronomy</td></tr>
<tr><td>RS</td><td>Remote sensing systems</td></tr>
<tr><td>S</td><td>Fixed-satellite service</td></tr>
<tr><td>SA</td><td>Space applications and meteorology</td></tr>
<tr><td>SF</td><td>Frequency sharing and coordination between fixed-satellite and fixed service systems</td></tr>
<tr><td>SM</td><td>Spectrum management</td></tr>
<tr><td>SNG</td><td>Satellite news gathering</td></tr>
<tr><td>TF</td><td>Time signals and frequency standards emissions</td></tr>
<tr><td>V</td><td>Vocabulary and related subjects</td></tr>
</table>

Note: *This ITU-R Recommendation was approved in English under the procedure detailed in Resolution ITU-R*

1.

RECOMMENDATION ITU-R P.837-7

Characteristics of precipitation for propagation modelling

(Question ITU-R 201/3)

(1992-1994-1999-2001-2003-2007-2012-**2014**)

Scope

Recommendation ITU-R P.837 contains maps of meteorological parameters that have been obtained using the European Centre for Medium-Range Weather Forecast (ECMWF) ERA-40 re-analysis database, which are recommended for the prediction of rainfall rate statistics with a 1-min integration time, when local measurements are missing.

Rainfall rate statistics with a 1-min integration time are required for the prediction of rain attenuation in terrestrial and satellite links. Data of long-term measurements of rainfall rate may be available from local sources, but only with higher integration times. This Recommendation provides a method for the conversion of rainfall rate statistics with a higher integration time to rainfall rate statistics with a 1-min integration time.

In some parts of the world, 1-min rainfall rate distributions may experience significant change over the lifetime of a radio system. This Recommendation provides estimates of temporal trends in the 1-min rainfall rates exceeded for 0.01% of time.

The ITU Radiocommunication Assembly,

considering

a)   that information on the statistics of precipitation intensity is needed for the prediction of attenuation and scattering caused by precipitation;

b)   that the information is needed for all locations on the globe and a wide range of probabilities;

c)   that rainfall rate statistics with a 1-min integration time are required for the prediction of rain attenuation and scattering in terrestrial and satellite links;

d)   that long-term measurements of rainfall rate may be available from local sources with   a 1-min integration time and also, with integration times of longer than 1-min,

e)   that using a model to convert local measurements with integration times up to 1 hour has been observed to provide higher accuracy than the use of the global digital maps in Annex 1 of this Recommendation,

f)   that rainfall rate statistics with a 1-min integration time may experience long-term trends,

recommends

1   that the model in Annex 1 should be used to obtain the rainfall rate, R_p, exceeded for any given percentage of the average year, p, and for any location (with an integration time of 1 min). This model is to be applied to the data supplied in the digital files ESARAIN_xxx_v5.TXT (the data files may be obtained from that part of the ITU-R website dealing with Radiocommunication Study Group 3);

2   that, for easy reference, Figs 1 to 6 in Annex 2 should be used to select the rainfall rate exceeded for 0.01% of the average year. These figures were also derived from the model and data described in Annex 1;

3   that local long-term measurements of rainfall rate with a 1-min integration time should be used if available;

4   that long-term measurements of rainfall rate with longer integration times should be used if available and the model in Annex 3 be used to convert to rainfall rate with a 1-min integration time;

5   that local measurements, if used, are collected over a sufficient period (typically longer than 3 years), to ensure statistical stability.

6   **that FIGURE 9 in Annex 4 may be used to estimate the temporal trend in the rainfall rate exceeded for 0.01% of the average year and that this trend may be used to extrapolate this rainfall rate up to 30 years in the future.**

Annex 1

Model to derive the rainfall rate exceeded for a given probability of the average year and a given location

The data files ESARAIN_PR6_v5.TXT, ESARAIN_MT_v5.TXT and ESARAIN_BETA_v5.TXT contain respectively the numerical values for the variables P_{r6}, M_t and β while data files ESARAINLAT_v5.TXT and ESARAINLON_v5.TXT contain the latitude and longitude of each of the data entries in all other files. These data files were derived from 40 years of data from the European Centre of Medium-range Weather Forecast (ECMWF).

Step 1: Extract the variables P_{r6}, M_t and β for the four points closest in latitude (Lat) and longitude (Lon) to the geographical coordinates of the desired location. The latitude grid is from $90°$ N to $-90°$ S in 1.125° steps; the longitude grid is from $0°$ to $360°$ in $1.125°$ steps.

Step 2: From the values of P_{r6}, M_t and β at the four grid points, obtain the values $P_{r6}(Lat,Lon)$, $M_T(Lat,Lon)$ and $\beta(Lat,Lon)$ at the desired location by performing a bi-linear interpolation, as described in Recommendation ITU-R P.1144.

Step 3: Convert M_T and β to M_c and M_s as follows:

$$M_c = \beta \, M_T$$
$$M_s = (1-\beta) \, M_T$$

Step 4: Derive the percentage probability of rain in an average year, P_0, from:

$$P_0(Lat,Lon) = P_{r6}(Lat,Lon)\left(1 - e^{-0.0079\,(M_s(Lat,Lon)/P_{r6}(Lat,Lon))}\right)$$

(1)

If P_{r6} is equal to zero, the percentage probability of rain in an average year and the rainfall rate exceeded for any percentage of an average year are equal to zero. In this case, the following steps are unnecessary.

Step 5: Derive the rainfall rate, R_p, exceeded for p % of the average year, where $p \le P_0$,

from:

$$R_p(Lat,Lon) = \frac{-B + \sqrt{B^2 - 4AC}}{2A} \qquad \text{mm/h}$$

(2)

where:

$$A = a\,b \tag{2a}$$

$$B = a + c\,\ln(\,p\,/\,P_0(Lat,Lon)) \tag{2b}$$

$$C = \ln(\,p\,/\,P_0(Lat,Lon)) \tag{2c}$$

and

$$a = 1.09 \tag{2d}$$

$$b = \frac{(M_c(Lat,Lon) + M_s(Lat,Lon))}{21797 P_0} \tag{2e}$$

$$c = 26.02b \tag{2f}$$

NOTE 1 – An implementation of this model and the associated data in MATLAB is also available from the ITU-R website dealing with Radiocommunication Study Group 3.

Annex 2

FIGURE 1

Rain rate (mm/h) exceeded for 0.01% of the average year

113

FIGURE 2

Rain rate (mm/k) exceeded for 0.01% of the average year

P.0837-02

Longitude (degrees)

Latitude (degrees)

FIGURE 3

Rain rate (mm/h) exceeded for 0.01% of the average year

P.0837-03

FIGURE 4

Rain rate (mm/h) exceeded for 0.01% of the average year

P.0837-04

Longitude (degrees)

Latitude (degrees)
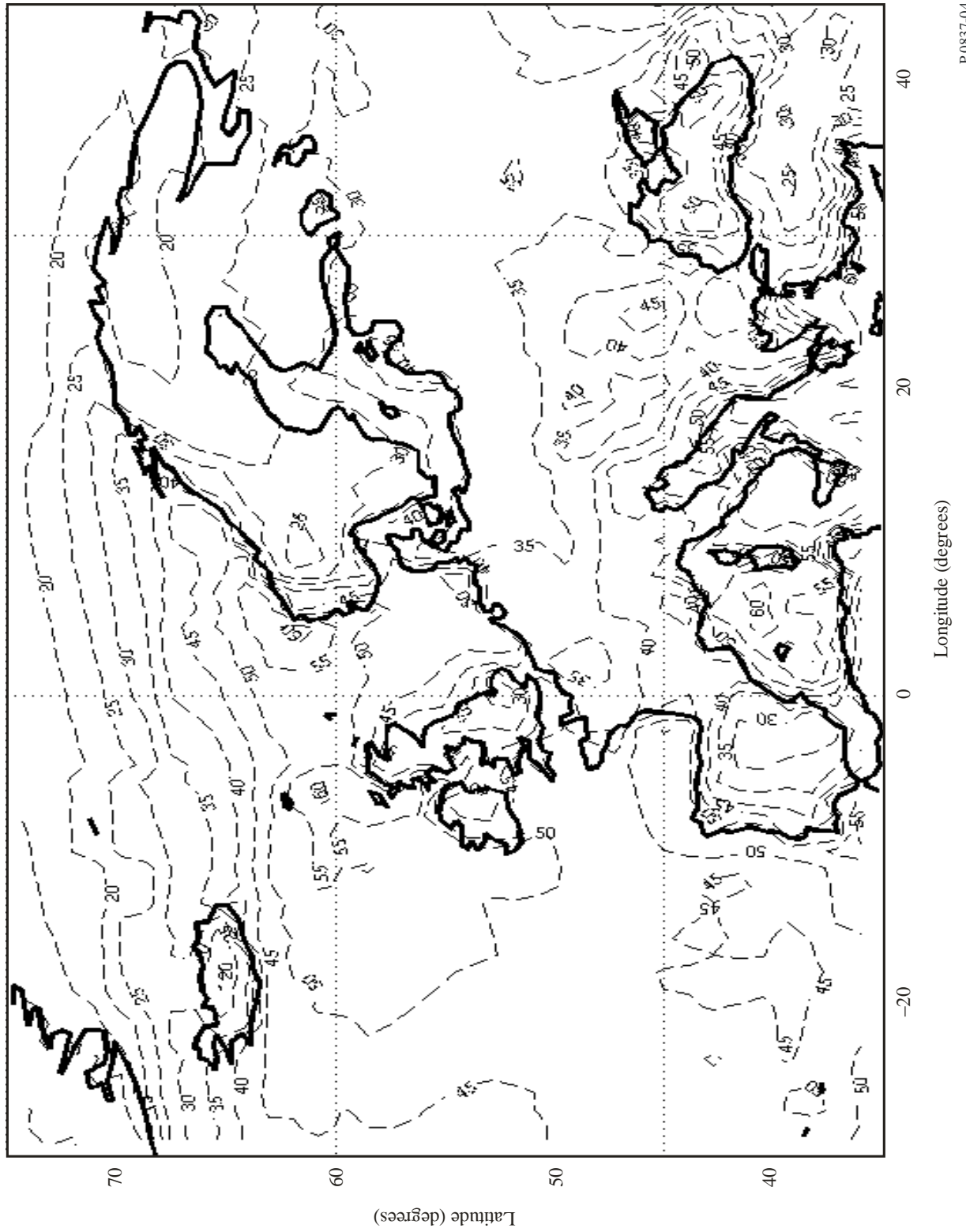
FIGURE 5

Rain rate (mm/h) exceeded for 0.01% of the average year

P.0837-05

117
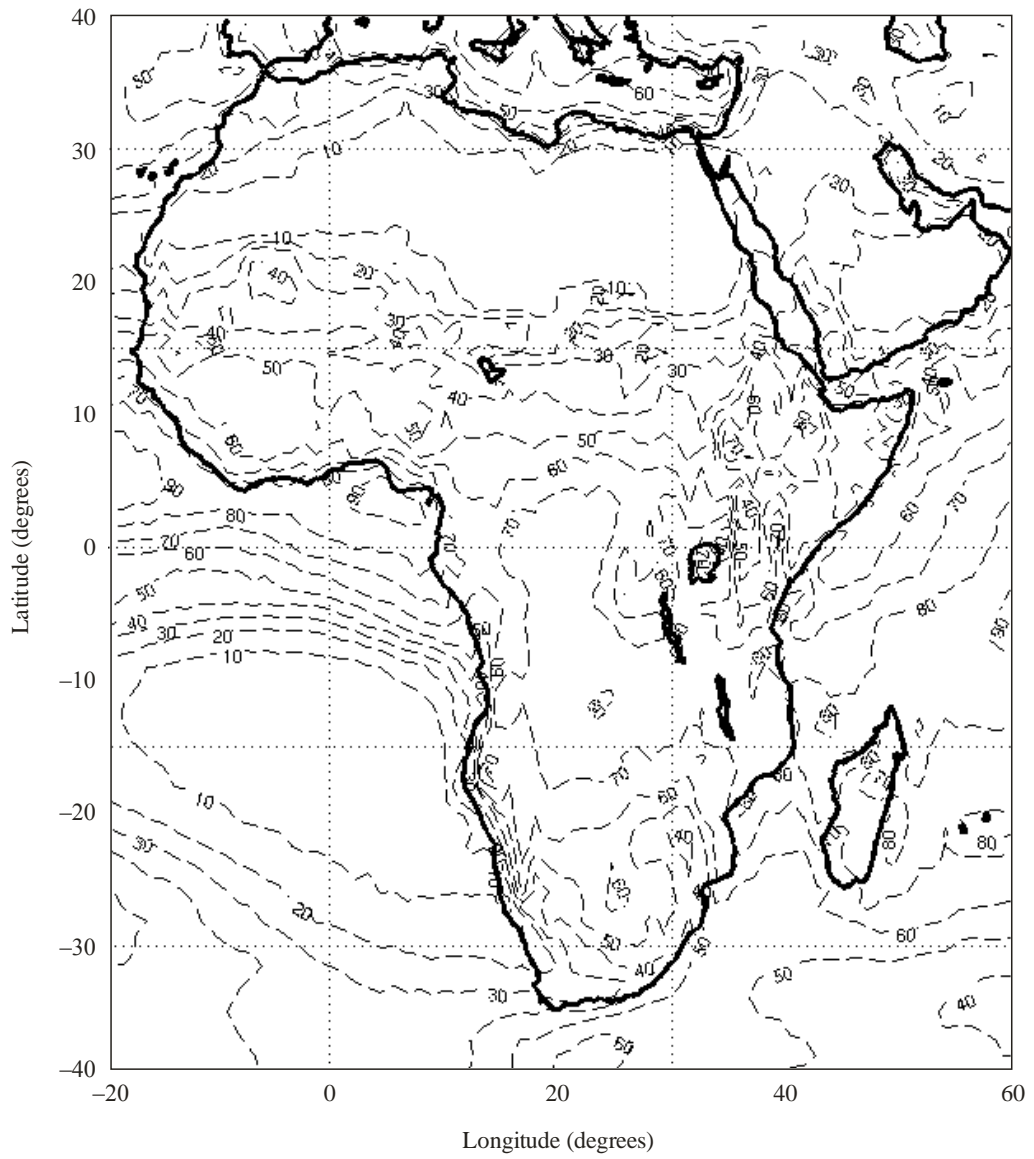
FIGURE 6

Rain rate (mm/h) exceeded for 0.01% of the average year

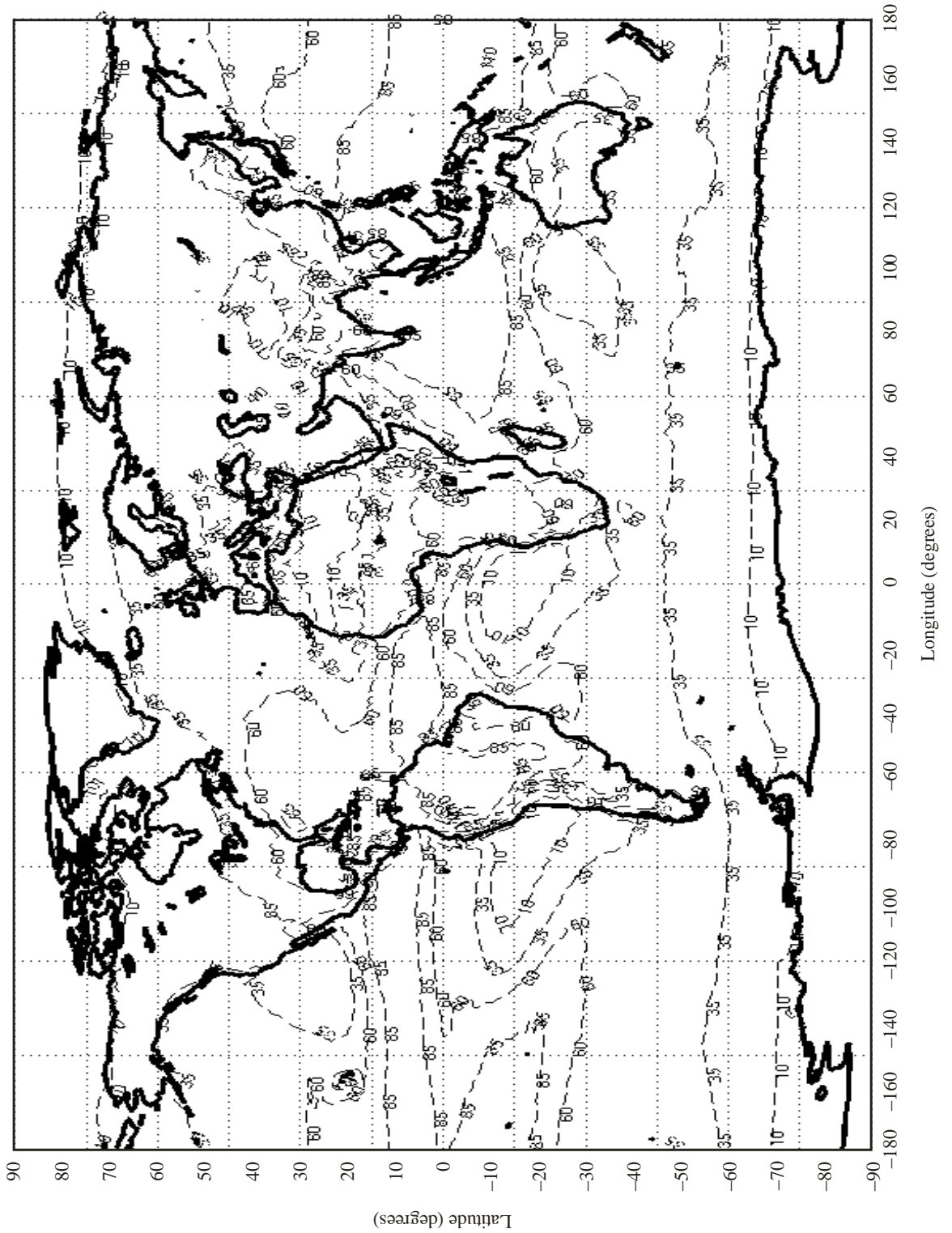

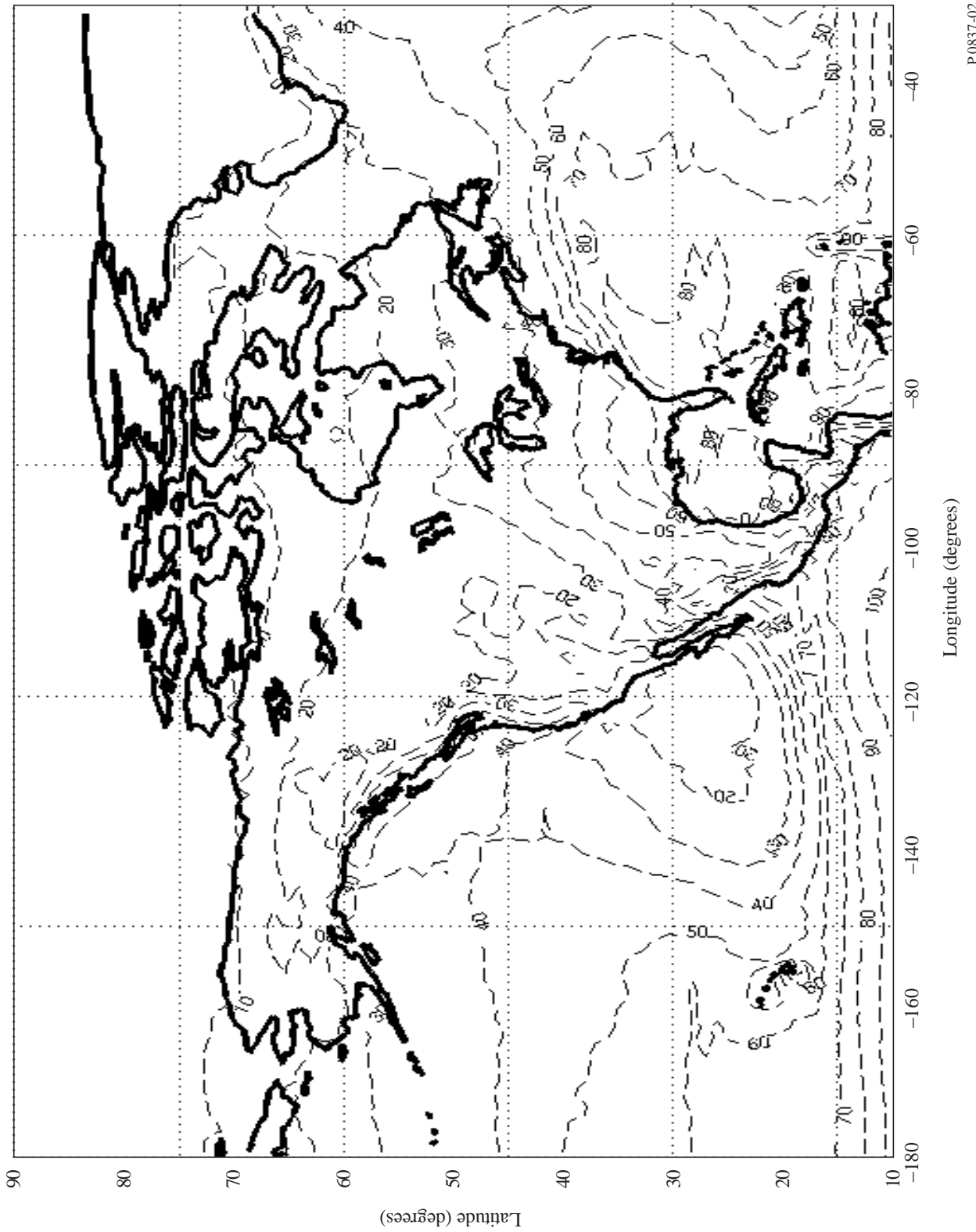P.0837-06

Longitude (degrees)

Latitude (degrees)
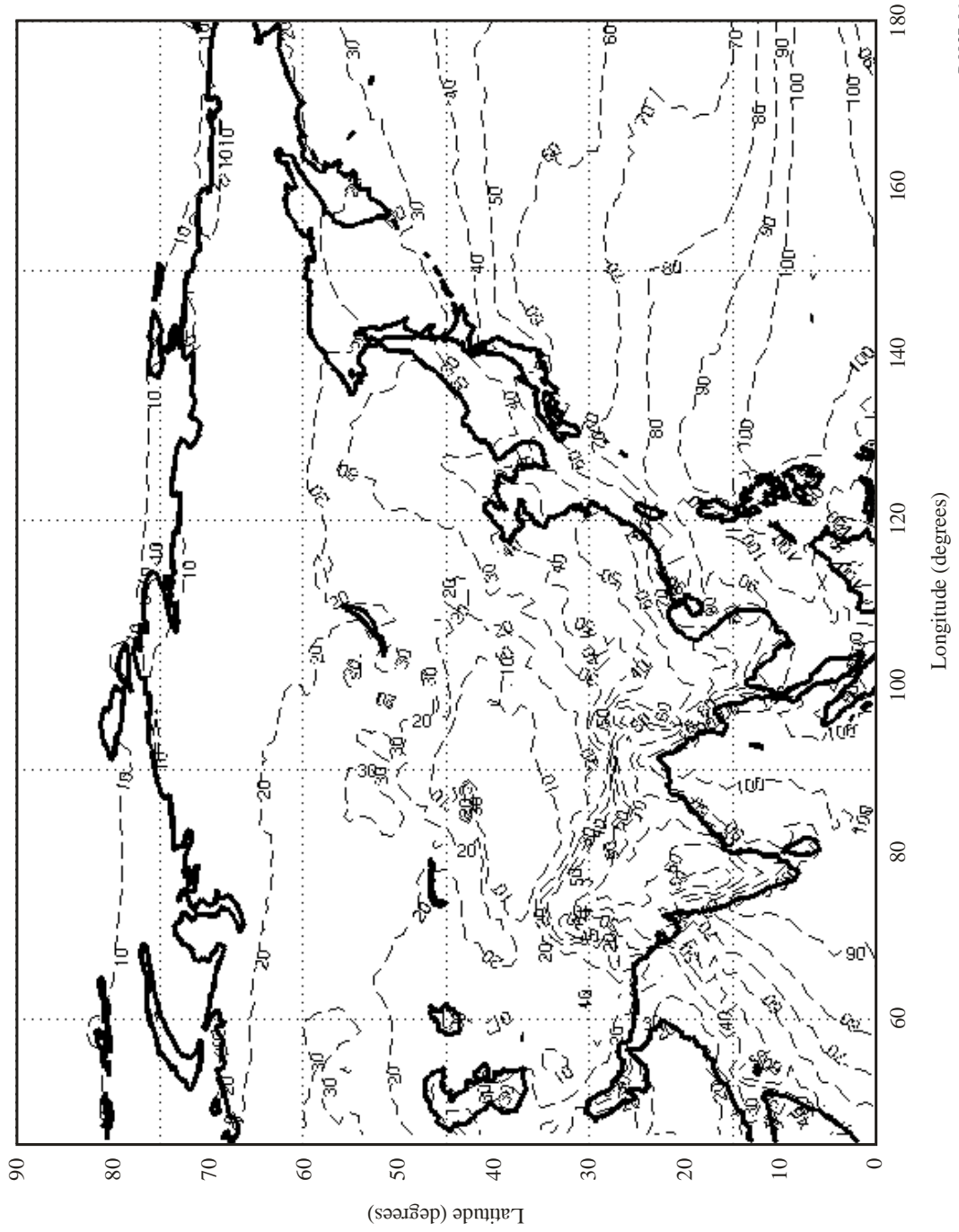
FIGURE 7

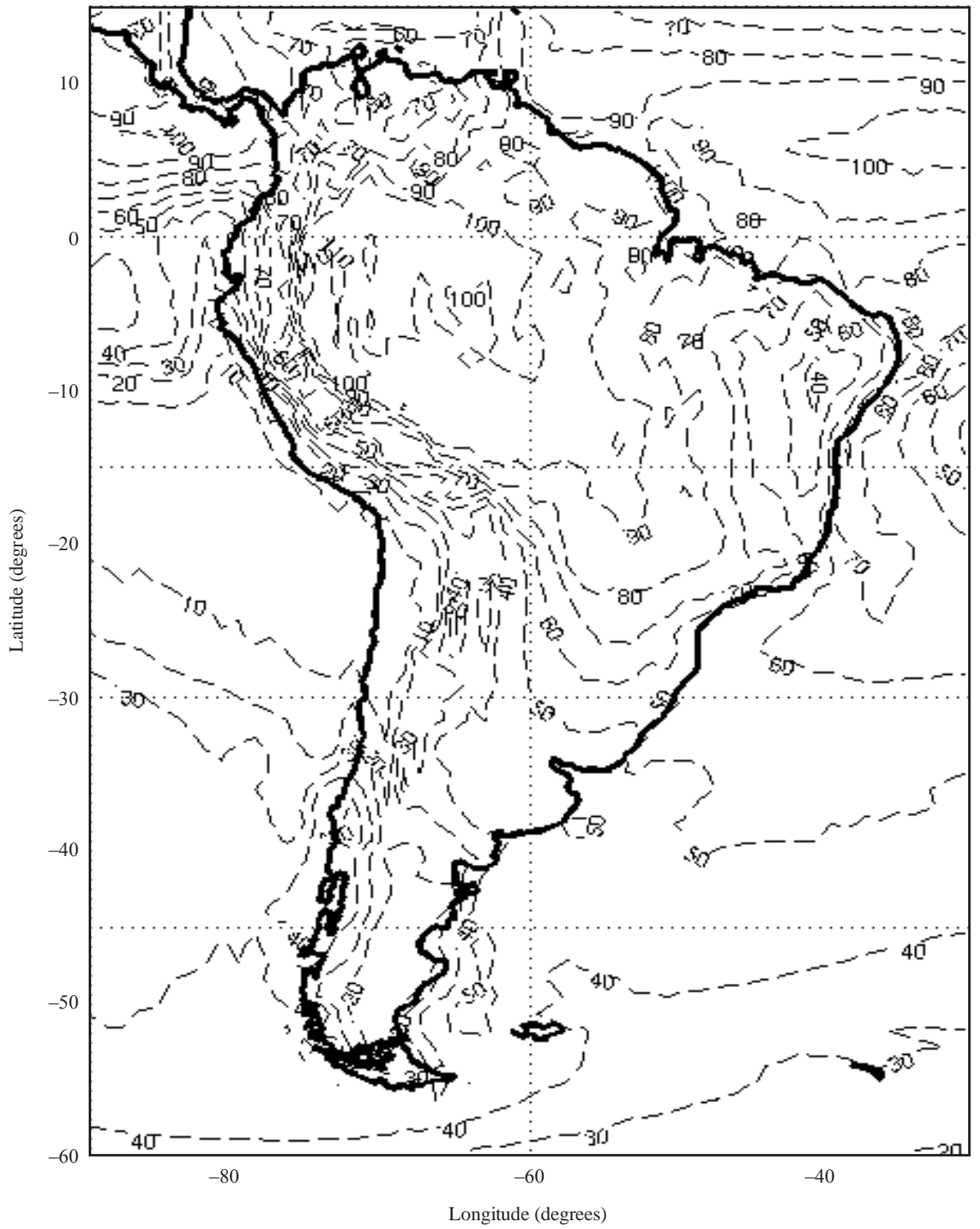**Rain rate (mm/h) exceeded for 0.01% of the average year**
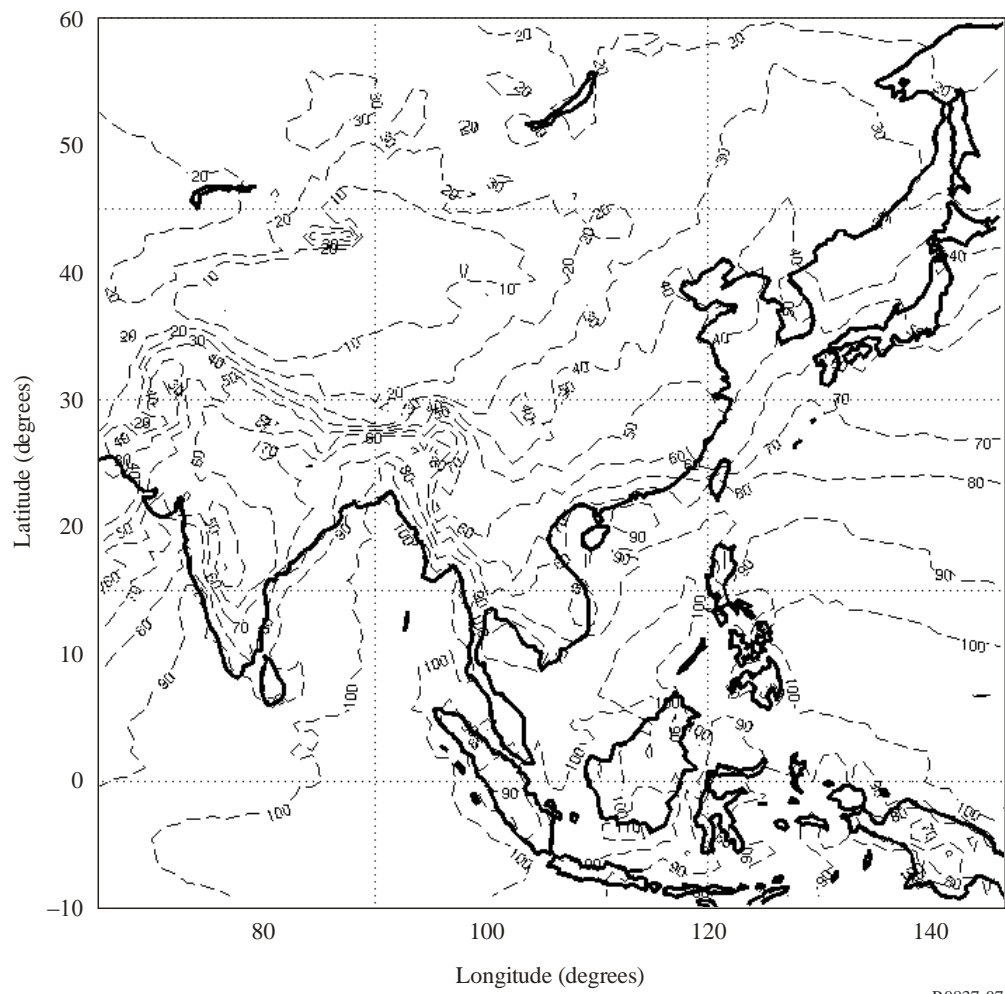
P.0837-07

FIGURE 8

Rain rate (mm/h) exceeded for 0.01% of the average year
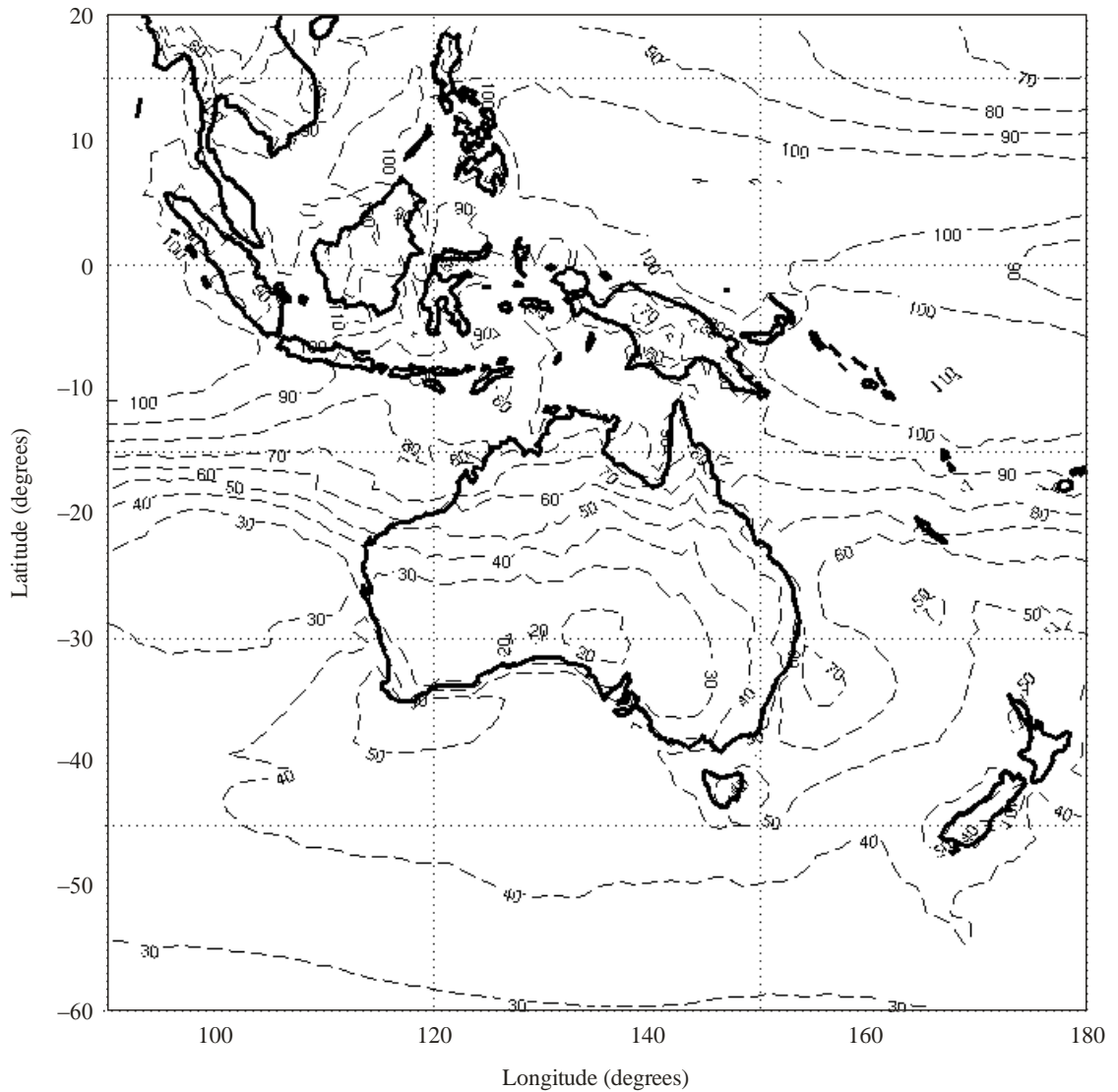
P.0837-08

Annex 3

1   The cumulative distribution of rainfall rate at 1-min integration time can be obtained by converting local cumulative distributions measured at integration times of between 5 and 60 minutes.

2   The recommended method requires as input both the cumulative distribution as well as the integration time of the source rainfall statistics and the geographical coordinates of the site of interest.

3   The method is based on the simulated movement of synthetic rain cells, whose parameters derive from the local input data and ECMWF products.

4 The recommended method is incorporated in a computer program available from the ITU-R website dealing with Radiocommunication Study Group 3. The name of the software package implementing this part of the recommendation is CONVRRSTAT_ANNEX3_P837-6.ZIP.

Annex 4

Method to estimate the temporal trend in the rainfall rate exceeded for 0.01% of the average year and a given location

The data files HULLRAIN_DR01DT_v1.TXT contains the estimated temporal trend in the rainfall rate exceeded for 0.01% of the average year at locations specified by the data files HULLRAINLAT_v1.TXT and HULLRAINLON_v1.TXT contain the latitude and longitude of each of the data entries. These data files were derived from 40 years of data from the National Oceanic and Atmospheric Administration (NOAA).

Step 1: **Extract the variable *dR01dt* for the four points closest in latitude (Lat) and longitude (Lon) to the geographical coordinates of the desired location. The latitude grid is from □90□ N to −90□ S in 1.875° steps; the longitude grid is from 0° to 360° in 1.875□ steps.**

Step 2: **From the values of *dR01dt* at the four grid points, obtain the value *dR01dt* (*Lat*,*Lon*), at the desired location by performing a bi-linear interpolation, as described in Recommendation ITU-R P.1144.**

FIGURE 9

Trend Slope of 0.01% Exceeded Rain Rate
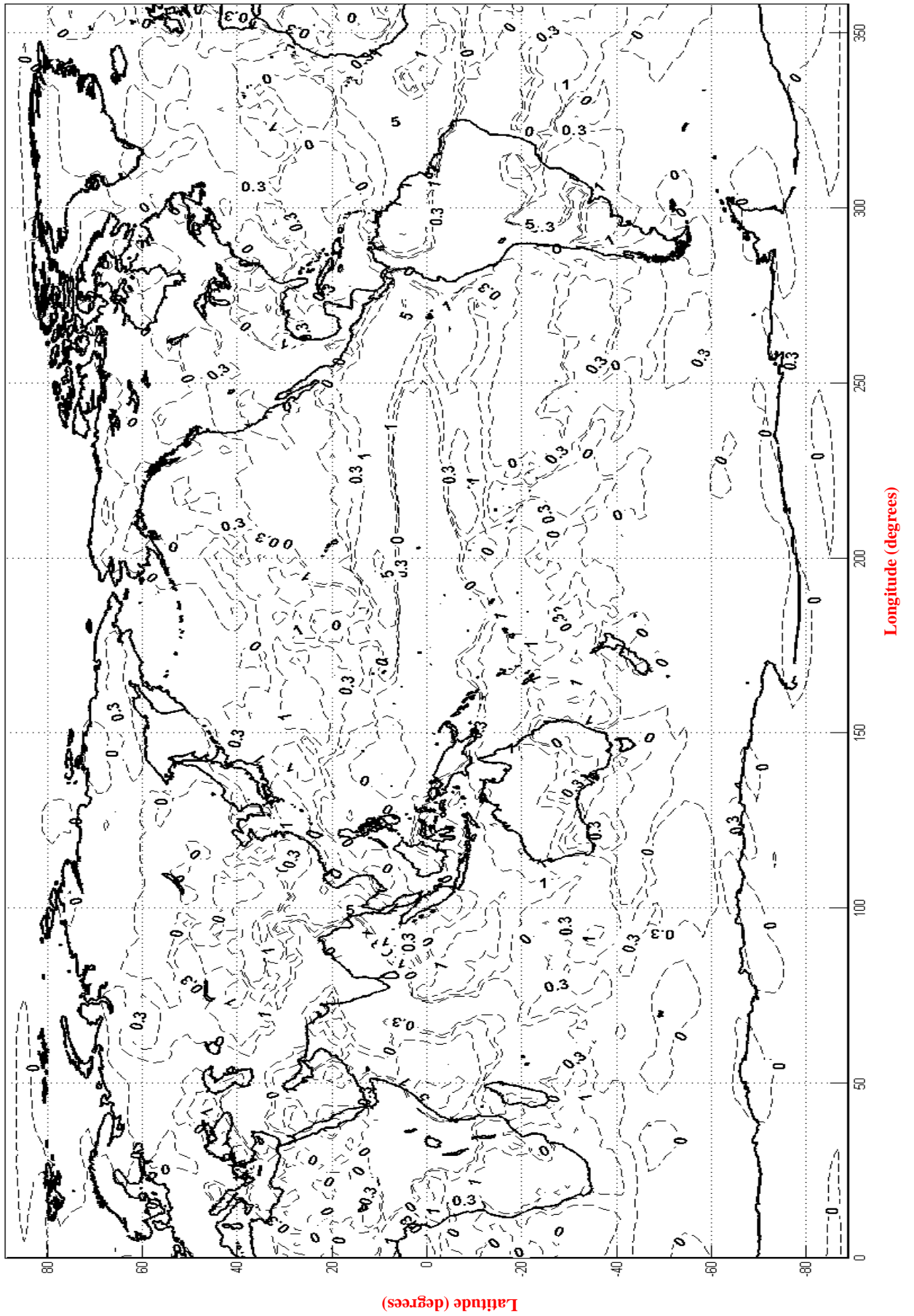
APPENDIX B

Estimation of Trends in Distributions of One-Minute Rain Rates Over the UK

Kevin S Paulson[1], Channa Ranatunga[2], Timothey Bellerby[3]

[1] (University of Hull): School of Engineering, University of Hull, Hull, United Kingdom, k.paulson@hull.ac.uk

[2] (University of Hull): School of Engineering, University of Hull, Hull, United Kingdom, c.ranatunga@hull.ac.uk

[3] (University of Hull): Dept. of Geography, University of Hull, Hull, United Kingdom, t.j.bellerby@.hull.ac.uk

Abstract— **It is known that the rain rate exceeded 0.01% of the time has experienced an increasing trend, in the UK, over the last twenty years. It is very likely that rain fade and outage experience a similar trend. This paper presents a method, applicably globally, to estimate these trends. The input data are parameters easily extracted from numerical weather prediction reanalysis data. The method is verified using rain gauge data from the UK.**

Index Terms— *rain fade, fade trends, climate change.*

I.   Introduction

Dynamic fading due to rain and wet snow tends to be larger than that due to other mechanisms on terrestrial and Earth-space links at frequencies above approximately 5 GHz. The International Telecommunication Union (ITU-R) maintains a set of models for predicting average annual distributions of rain fade, with a one-minute integration time, on individual links. An important parameter in these models of rain fade is the one-minute rain rate exceeded for 0.01% of an average year (R0.01%). Several recent reports have suggested that trends in climate parameters could be having significant effect on telecommunications systems over their lifetime. A satellite communications system has a typical life-cycle of 30 years, from initial conception to decommissioning.

The objective of this work is to develop a method to estimate trends in the R0.01% rain rate, globally, using readily accessible data. A relationship is postulated between very low resolution rain parameters from Numerical Weather Prediction (NWP) reanalysis data and the one-minute averaged, point rain rates required for radio regulation, and the optimization of network spectral efficiency and performance. Trends in these parameters can then be linked to trends in one-minute rain rates.

II.   Salonen-Baptista Method

This Section summarises the Salonen-Baptista distribution of one-minute rain rates and the method described in [1] for estimating the distribution parameters from reanalysis data. Average annual one-minute rain rate complementary cumulative distribution function (CCDF) is assumed to have a distribution well described by the expression:

$$P(R) = P_0 \cdot e^{-aR\frac{1+bR}{1+cR}} \qquad (1)$$

$P(R)$ is the probability of experiencing a rain rate greater than R and P_0 is the probability of a one-minute interval experiencing rain. The four parameters P_0, a, b, c; control the shape of the distribution and match the distribution to the local climate. Rec. ITU-R P.837-5 [2] provides a method to calculate these parameters from three,

long-integration time rain parameters. These parameters are:

M_S = mean annual stratiform rain height (mm),

M_C = mean annual convective rain height (mm),

P_{r6} = probability of rainy 6-hours periods (%).

The ITU-R model estimates the distribution parameters from these input parameters using:

$$P_0 = P_{r6h} \cdot \left(1 - e^{-0.0117\frac{M_S}{P_{r6h}}} \right) \qquad c = 31.5 \cdot b$$

$$b = \frac{M_C + M_S}{22932 \cdot P_0} = \frac{M_T}{22932 \cdot P_0} \qquad a = 1.11 \qquad (2)$$

The transformation of reanalysis parameters to one-minute rain rate CCDF parameters has been optimized to provide the best fit to the 743 experimental CCDF statistics, acquired from over the 139 locations, archived in the database of the ITU-R Study Group 3: DBSG3, [3]. Inherent in this process is the assumption that the climate is stationary. The three reanalysis parameters M_T, M_C and $Pr6$ are calculated by averaging over 44 years of ERA40 and the data collection period of DBSG3 data was ignored.

In this project we use NOAA NCEP/NCAR Reanalysis 1 data spanning 1958 to 2011. The motivation for the NOAA NCEP/NCAR Reanalysis project was to remove the apparent climate change artefacts introduced by the occasional changes made to numerical weather models, Kalnay et al [4]. The M_T and M_C data are calibrated using rain gauge measurements from the VASClimO (Variability Analysis of Surface Climate Observations) dataset version 1.1, [5]. This dataset provides daily precipitation accumulation derived from rain gauge measurements, integrated over regions of diameter 1º, over land, derived from 9,300 gauge stations.

III. Time-series of precipitation parameters

In this section we examine time-series of precipitation parameters, extracted from the calibrated NOAA data, from three regions over the UK. The three parameters M_T, M_C and P_{r6}; are estimated over each integration region and for each 365-day interval. M_T and M_C are calculated as running sums of 4×365 consecutive values while $Pr6$ is the percentage of 4×365 consecutive values for which the total precipitation is greater

than 0.1 mm/6hr. NOAA data are calibrated by comparison with VASClimO accumulations over 1º regions. Figure 1 shows a scatter plot of NOAA and VASClimO annual accumulations.
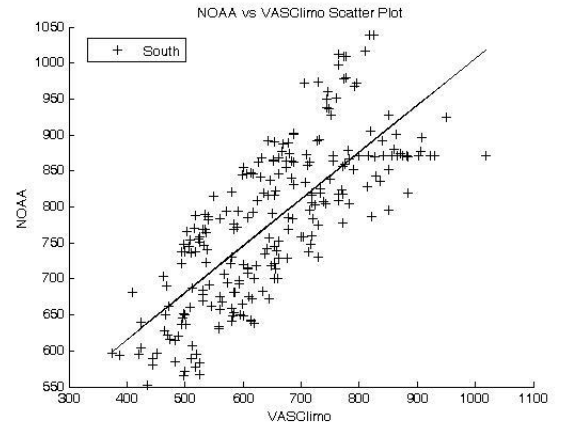
The plot shows a high correlation with regressions slope very close to unity, but with a significant offset, as large as 30% of the annual accumulation. Annual convective accumulation, M_C, is calculated from the calibrated M_T times the NOAA convective fraction.

IV. Measured time-series of exceeded rain rates

Paulson [6] calculated an increasing trend in 0.01% exceeded rain rates in the southern UK, derived from eighty rain gauges, of 0.44 mm/hr/year. The slope of the 0.01% exceeded rain rate can also be compared to that found in the Ofcom study, based on 1350 high resolution rain gauges across the UK, [7]. This found a consistent increasing trend in 0.01% exceeded rain rates around 0.4 mm/hr/year for North UK and 0.8 mm/hr/year for South UK. Given the different time periods considered and the standard errors in the slopes, these results are consistent.

V. Predicted time-series of exceeded rain rates

The three parameters M_T, M_C and P_{r6}, derived as described in Section 3, may be converted into time-series of rain distributions using the method described in Section 2. The constants in (2) need to be calculated by optimising the fit between predicted rain distributions and those in DBSG3, either with or without the assumption of stationary. Either way, the constants are different from those in [1] and [2] as the NOAA parameters are slightly different than the ERA40 parameters, particularly P_{r6}.

For this document we use a simpler method where the transformation form rain parameters to 0.01% exceeded rain rate is linearised i.e.

$$\frac{dR_{0.01\%}}{dt} = \frac{dR_{0.01\%}}{dM_T}\frac{dM_T}{dt} + \frac{dR_{0.01\%}}{dM_C}\frac{dM_C}{dt} + \frac{dR_{0.01\%}}{dP_{r6h}}\frac{dP_{r6h}}{dt}$$

(3)

The derivatives of M_T, M_C and P_{r6}; were estimated by fitting linear regression lines to 21 year time-series, 1980 to 2001, of these parameters. The derivatives of the transformation between rain parameters and the 0.01% exceeded rain rate were evaluated numerically around the 21 year average parameter value. From the chain rule (3), trend slopes in the 0.01% rain rate was estimated for the three regions spanning the UK. The trends produced are 0.6 mm/hr/year for Northern England, 0.8 mm/hr/year for the Midlands and 1 mm/hr/year in southern England. These values for the three regions spanning UK are similar to those derived from the large database of rapid response gauges [7], and exhibit the same north-south trend.

VI.   Conclusions

A method has been developed for predicting the temporal trend in one-minute rain rate distributions, and this has been tested against trends slopes measured in the UK. The method is based on the widely accepted Salonnen-Baptista method that is integral to Rec. ITU-R P.837. We have extended the Salonnen-Baptista method by removing the implicit assumption of climate stationarity, and using NOAA reanalysis data rather than the ECMWF ERA40 data. The trend slope in 0.01% exceeded rain rates in three NOAA grid regions spanning the UK have been estimated with the new method and compare favourably with results produced by independent researchers analysing a large database of high resolution rain gauge data. When climate trends lead to significant changes in the underlying fade distributions, over the lifetime of a system, then these can have detrimental effects on system performance and the system business model. These are particularly important for space based systems where hardware adaptation is difficult or impossible. Such systems are designed with wide margins to allow for climate variability. Introducing climate trends into the margin calculation may lead to more realistic estimates of the range of climates a system will encounter over its lifetime.

References

[1] Fascicle concerning the rainfall rate model given in recommendation ITU-R P.837-5, ww.itu.int/dms_pub/itu-r/oth/0A/04/R0A040000050001MSWE.doc, accessed 10/10/2013.

[2] Rec. ITU-R P.837-5, "Characteristics of precipitation for propagation modelling", 2008.

[3] ITU-R Study Group 3 Databanks - DBSG3, Available at: <http://saruman.estec.esa.nl/dbsg3/login.jsp> [Accessed at 01 August 2013].

[4] Kalnay E., Kanamitsu, M., Kistler, P. Collins, W. Deaven, D. Gandin, L. Iredell, M. Saha, S. White, G. Woollen, J. Zhu, Y. Cheillab, M, Ebsuzaki, W. Higgins, W. Janowiak, J. Mo, K. C. Ropelewski, C. Wang, J. Leetma, A. Reynolds, P. Jenne 1. and Joseph, D. "The NCEP/NCAP 40-year reanalysis project", Bull. Amer. Meteor. Soc., 1996, 77, pp 437-470.

[5] U. Schneider, A. B., A. Meyer-Christoffer, M. Ziese, B. Rudolf (2008). Global Precipitation Analysis Products of the GPCC. Germany, Global Precipitation Climatology Centre.

[6] K. S. Paulson, "The Effects of Climate Change on Microwave Telecommunication" 11th International Conference on Telecommunication, ConTell, Graz, Japan, 2011

[7] D. Bacon, "Modelling Rain Rate Maps for Fixed-Link frequency Assignment Procedures", Ofcom contract No: 796, 2012

APPENDIX C

A Method to Estimate Trends in Distributions of One-Minute Rain Rates, Globally

Kevin S. Paulson, *Member, IoP*, Channa Ranatunga, Timothy Bellerby

Abstract—**It is known that the rain rate exceeded 0.01% of the time in the UK, has experienced an increasing trend over the last twenty years. It is very likely that rain fade and outage experience a similar trend. This paper presents a globally applicable method to estimate these trends. The input data are parameters easily extracted from numerical weather prediction reanalysis data. The method is verified using rain gauge data from the UK.**

Index Terms—**rain fade, fade trends, climate change**

Dynamic fading due to rain and wet snow tends to be larger and longer lasting than that due to other mechanisms on terrestrial and Earth-space links at frequencies above approximately 5 GHz. The International Telecommunication Union (ITU-R) maintains a set of models for predicting average annual distributions of rain fade, with a one-minute integration time, on individual links. An important parameter in these models of rain fade is the one-minute rain rate exceeded for 0.01% of an average year (R0.01%). At the location of interest, this can be estimated from long term rain gauge records, sometimes requiring some statistical conversion to allow for different integration periods. If local data are not available then Rec. ITU-R P.837-6 provides a method to estimate this parameter at any point globally.

Several recent papers have suggested that temporal trends in climate parameters could be having significant effects on telecommunications systems over their lifetime. A satellite communications system has a typical life-cycle of 30 years, from initial conception to decommissioning. Any climate variation, either natural or anthropogenic, with a period of more than 60 years, may be experienced as a monotonic trend in fading over the system lifetime.

Paulson [1] examines data from 32 rain gauges situated in the Southern UK and operated by the UK Environment Agency. The tipping bucket gauges recorded the time to the nearest second whenever 0.2 mm of rain accumulated. These data showed a strongly increasing trend in the incidence of rain rates at outage levels, consistent with 99.99% and 99.999% availability outage rates, doubling or tripling each decade for the last two decades. A later paper [2] extends the analysis to 100 gauges in the Southern and North Western England with similar results. More recently, a research study by the UK spectrum regulator Ofcom, using over a thousand gauges, confirmed these results and extended their scope to the whole of the UK, [3]. These results are especially significant for the planning of high availability and security critical links. It is likely that other regions, outside the UK, will experience trends in the incidence of rain at outage levels. However, the UK is unusual in having historical data from a relatively dense network of gauges capable of estimating distributions of rain rate with a one-minute integration time. For most of the globe, this is not the case.

A further paper [4] identified global trends in rain height, mostly increasing in altitude over time, derived from NOAA NCEP/NCAR reanalysis data. The rain height is related to the zero-degree isotherm and is near the top of the melting layer when the atmosphere is stratified. Increases in zero-degree isotherm height are correlated with increasing surface temperature. Earth-space links are assumed to experience rain fade up to the rain height and so increasing rain height is another mechanism that is expected to lead to increasing fade intensity. The situation for terrestrial links is more complicated as increasing rain height can increase or decrease the incidence of wet snow along the link and so can either

increase or decrease annual fade levels dramatically, [5].

The objective of this work is to develop a method to estimate trends in the R0.01% parameter anywhere on earth, using readily accessible data. High resolution rain gauge data is available in only a very small proportion of the globe. By contrast, numerical weather models, particularly reanalysis data, spans the globe and assimilates large amounts of measured data, including rain data from gauges and rain radar networks. The major drawback is that rain data is averaged over very large areas, typically hundreds of kilometers across, and accumulated over long times, typically six hours or daily. A relationship needs to be found between these very low resolution rain parameters and the one-minute averaged, point rain rates required for radio regulation, spectral efficiency and performance optimization.

To some extent this relationship has already been developed. Before 1999, Rec. ITU-R P.837-1 provided R0.01% globally by dividing the world into rain zones, over which all regions were assumed to experience the same one-minute rain rate distributions. This was replaced by a new model, Rec. ITU-R P.837-2, where rain distributions were assumed to follow the Salonen - Poiares Baptista (SPB) double exponential model and associated method, [6,7&8]. The parameters of this distribution were linked to outputs from ERA15 reanalysis data, produced by the European Centre for Medium Range Weather Forecasting (ECMWF). The parameters for later versions of this Recommendation were extracted from the ERA40 database. The Rec. ITU-R P.837-6 model parameters are provided on global maps with a grid spacing of 1.125°. The SPB method is a transformation of the long term average (many years) of three reanalysis outputs to the average annual distribution of one-minute rain rates. The transformation is applied globally and assumed to be valid for all climates.

This paper explores a logical extension of this method. If a region experiences climate change, then the SPB method should be applicable to intervals both before and after the change, as long as the climates stay within the very wide global range, from desert to rain forest, over which the model has been verified. Quantifying this approach is limited by unanswered questions as to the rate of convergence of distributions of measured rain rates to average annual distributions, and the rate of convergence of

averages of reanalysis parameters to long term averages. Both these questions are further complicated by natural climate cycles of various periods and the possibility of anthropogenic climate change.

Section 1 introduces the SPB method and the input parameters. Section 2 describes the ECMWF ERA40 and the US National Oceanic and Atmospheric Administration (NOAA) NCEP/NCAR reanalysis datasets, calibration using Global Precipitation Climatology Centre (GPCC) data, and the extraction of the SPB input parameters. Section 3 presents time-series of SPB input parameters and the derived R0.01% rain rates for the UK. These are compared with R0.01% time series derived from rain gauges. Section 4 presents conclusions and a map of predicted, global R0.01% trend slopes.

I. SALONEN - POIARES BAPTISTA METHOD

This Section summarises the SPB distribution of one-minute rain rates and the method described in [6,7&8] for estimating the distribution parameters from reanalysis data.

The average annual one-minute rain rate complementary cumulative distribution function (CCDF) is assumed to have a distribution well described by the expression:

$$P(R) = P_0 \cdot e^{-aR\frac{1+bR}{1+cR}} \tag{1}$$

$P(R)$ is the probability of experiencing a rain rate greater than R and P_0 is the probability of a one-minute interval experiencing rain. Both probabilities are often expressed as percentages. The four parameters P_0, a, b, c; control the shape of the distribution and match the distribution to the local climate. Rec. ITU-R P.837-6 provides a method to calculate these parameters from three, long-integration time rain parameters. These parameters are:

M_S = mean annual stratiform rain accumulation (mm),

M_C = mean annual convective rain accumulation (mm),

P_{r6} = probability of rainy 6-hours periods (%).

The ITU-R model estimates the distribution parameters from these input parameters using:

$$P_0 = P_{r6h} \cdot \left(1 - e^{-\alpha_1 \frac{M_S}{P_{r6h}}} \right)$$

$$b = \frac{M_C + M_S}{\alpha_2 \times P_0} = \frac{M_T}{\alpha_2 \times P_0} \qquad (2)$$

$$c = \alpha_3 \cdot b$$

$$a = \alpha_4$$

The constants have changed with revisions of Rec. ITU-R P.837 and the current values are

$$\{\alpha_1, \alpha_2, \alpha_3, \alpha_4\} = \{0.0079, 21797, 26.02, 1.09\}$$

The transformation of reanalysis parameters to one-minute rain rate CCDF parameters has been optimized to provide the best fit to the database of the ITU-R Study Group 3: DBSG3, [9]. This contains the 743 experimental CCDF statistics, acquired from over the 139 locations. However, distributions derived from experiments lasting more than one year are often included both as individual year and multi-year results. We have selected 415 distributions derived from one-year experiments.

II. REANALYSIS AND GAUGE DATA

The original work by SPB used ERA15 and later ERA40 reanalysis data provided by the ECMWF. ERA40 data spans the interval 1957 to 2001, [10]. Similar data is also provided by NOAA NCEP/NCAR: reanalysis 1 spanning 1958 to 2011. The motivation for the NOAA NCEP/NCAR Reanalysis project was to remove the apparent climate change artefacts introduced by the occasional changes made to numerical weather models, Kalnay et al [11]. Kalnay et al further state: "The basic idea of the Reanalysis Project is to use a frozen state-of-the-art analysis/forecast system and perform data assimilation using past data". Although the NWP algorithm does not change, the data available for assimilation does. For ERA40 between 1973 and 1988, the amount of satellite data that were assimilated increases with time. After 1988 the amount of satellite data is large and the system can be considered stable, [7].

Precipitation data from reanalysis products require calibration to surface measurements. For example, ERA40 has known problems with the humidity scheme of the ECMWF assimilation system, [7]. Rain parameters over land used in Rec. ITU-R P.837-6 uses calibration factors derived from the GPCC rain gauge dataset maintained by the Global Precipitation Climatology Centre of the Germany's National Weather Service. Rain parameters over sea use a calibration factor derived from the "satellite-gauge precipitation product" produced by the Global Precipitation Climatology Project of the NASA Goddard Space Flight Center (USA). For this project the VASClimO dataset version 1.1 is used, [12]. This dataset provides daily precipitation accumulation derived from rain gauge measurements, integrated over regions of diameter 1°, over land. The dataset is based on time series from more than 9,300 gauge stations and covers more than 90% of the period between 1951-2000.

This project also refers to UK rain rate trends derived from rain gauge data acquired by the UK Environment Agency, [1], [2] and [3]. Each tipping bucket gauge records the time of each 0.2 mm accumulation to the nearest second. Most gauges started recording to this resolution in the mid 1990's although the earliest data started in 1989.

III. TIME SERIES OF PRCIPITATION PARAMETERS

Although the original work by SPB that lead to the current global ITU-R rain models was based on ERA-40 data; we have chosen to use NOAA NCEP/NCAR reanalysis data due to the temporal span of data up to 2011. For statistically significant trend identification, the length of interval is important. Furthermore, as underlying climate trends appear to be accelerating i.e. surface temperatures [13]; it is important to include the most recent data. Two precipitation parameters have been extracted from the NOAA reanalysis databases: total precipitation and convective precipitation, over 1.875° integration regions, over 6 hour periods. The three parameters M_T, M_C and P_{r6}; are estimated over each integration region and for each 365-day interval starting at midnight UTC. M_T and M_C are calculated as running sums of 4×365 consecutive values while P_{r6} is the percentage of 4×365 consecutive values for which the total precipitation is greater than 0.1 mm/6hr.

Three NOAA grid regions have been explored in detail. Each has a diameter of 1.825° and centered on the points listed in Table 1.

Name	Latitude	Longitude
North	54.3°	-0.9°
Midlands	52.4°	-0.9°
South	50.5°	-0.9°

Table 1: centers of NOAA grid regions spanning the UK

The accumulations need to be calibrated to VASClimO surface rain gauge measurements. Figure 1 provides a scatter plot of M_T derived from NOAA and VASClimO, for the NOAA grid region covering the southern UK. The corresponding VASClimO estimates are produced by forming weighted sums of the smaller 1° VASClimO regions where the weights are proportional to the region overlap areas.
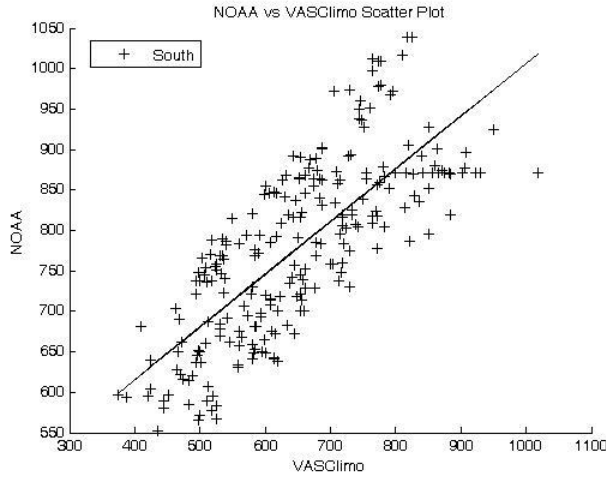

Figure 1: scatter plot of annual accumulation in mm (M_T) derived from NOAA and from VASClimO for the Southern UK.

These plots show high correlation between the accumulation estimates, with regressions lines with slope very close to one but a significant offset as large as 30% of the annual accumulation. This result is in marked contrast with that of [7] where a multiplicative calibration factor was required to match ERA40 accumulations with GPCC data. Table 2 lists the slope a, intercept b and Pearson correlation coefficient r; for the three NOAA regions.

Name	a	b (mm)	r
North	1.02	250	0.92
Centre	1.03	300	0.94
South	1.04	200	0.93

Table 2: regression slope, intercept and correlation coefficient for three NOAA grid regions spanning the UK.

Constant linear calibrations, such as those listed in Table 2, have been applied to all average annual NOAA accumulations, to make them consistent with the VASClimO database of gauge measurements. Assuming that the NOAA convective fraction:

$$\beta \equiv \frac{\text{annual convective accumulation}}{\text{total annual accumulation}}$$

(3)

remains unchanged then the same linear calibration can be applied to the annual convective accumulation, M_C. We assume the calibration does not change over time.

Figures 2a&b illustrate the time series of the three parameters M_T, M_C and P_{r6}; for the three UK NOAA grid cells. All parameters exhibit increasing temporal trends.
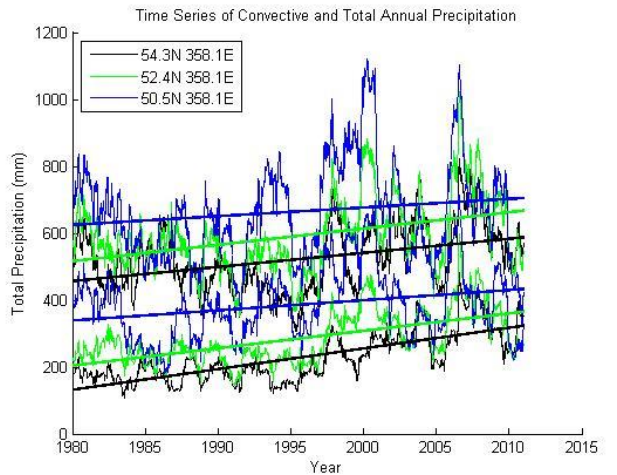

Figure 2a: time series of annual convective (lower) and total (upper) precipitation accumulation for three grid areas covering the UK.
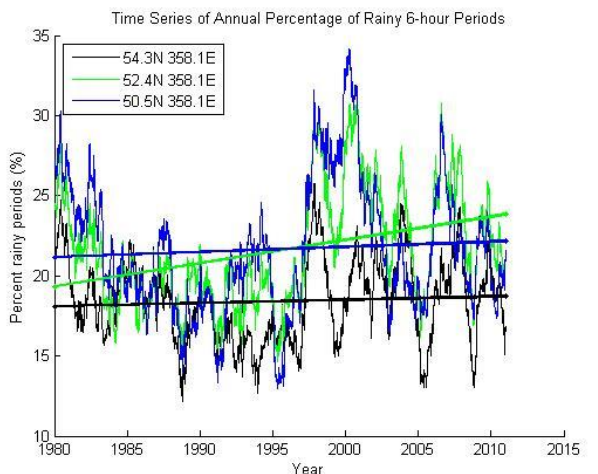

Figure 2b: time series of the percentage of annual 6-hour periods that experience rain for three grid areas covering the UK.

IV. Estimation of Rain Rate Distribution

SPB proposed a link between the three parameters M_T, M_C and P_{r6}; and the average annual distribution of one-minute rain rates. The four distribution parameters P_0, a, b, c; from (1), need to be determined from the three meteorological parameters; as in (2). The transformation defined by (2) is specific to ERA40 $1°$ reanalysis data. The form of the transformation is expected to remain but the constants with numerical values in (2) are likely to be different when using NOAA $1.824°$ data. These four numerical values have been recalculated to provide the best fit to the 4 experimental CCDF statistics derived from single years of observation, archived in DBSG3.

The data in the DBSG3 database can be used in different ways. SPB assumed stationarity and so used values of meteorological parameters, averaged over all ERA40 data from 1957 to 2001. We are looking for non-stationary trends in precipitation and so, in some cases, we used the meteorological parameters from the time interval (one year) over which the exceeded rain rates were measured. We expect this to yield a better fit as in wet years, with a larger M_T, we would also expect a higher R0.01%.

We have defined a number of cases using combinations of average annual and specific annual reanalysis parameters. The four constants α_j in the SPB method (2) are allowed to vary to optimise the fit between DBSG3 measured R0.01% values, and the prediction using equations (2) with inputs being either average or specific annual meteorological parameters. Two sets of annual accumulation data are available: NOAA and VasClimo. We either use VasClimo calibrated NOAA data or the VasClimo data directly. The data in the DBSG3 database is not from sites evenly distributed around the world. To partially address this bias, site data is assigned a weight which is inversely proportional to the number of sites in a specific country.

The four cases considered are:

Case 1: Specific annual M_T, M_C and P_{r6}; from VasClimo calibrated NOAA data;

Case 2: Average annual M_T, M_C and P_{r6}; from VasClimo calibrated NOAA data;

Case 3: Specific annual VASClimo, mean annual total precipitation M_T, and specific annual M_C and P_{r6} from NOAA;

Case 4: Average annual VASClimo, mean annual total precipitation M_T, and average annual M_C and P_{r6} from NOAA.

The error functional is defined in a way analogous to the definition in Rec. ITU-R P.311-14, but with a weighted sum to compensate for the distribution of sites:

$$Error \equiv \frac{1}{nCountry} \sum_{i=1}^{415} W_i \left| \log \left(\frac{R_i^{DBSG3}}{R_i^{S-B}} \right) \right|$$

(4)

In (4), W_i is the weight for the ith site, and R_i^{DBSG3} and R_i^{S-B} are the exceeded rain rates from DBSG3 and from the model with the test parameters respectively. In this paper, only the 0.01% exceeded rain rate was used. The constant $nCountry$ is the number of countries with sites used in the DBSG3 database. This normalization allows the error value to be interpreted as the average relative error per site. This functional has been minimized using the Nelder-Meade simplex method, starting from the current Rec. P.837 values. Numerical experiments showed that doubling any initial parameter yielded the same minimum.

	Optimal Solution				
	α_1	α_2	α_3	α_4	Error
Case 1	48.15	0.635	0.838	0.4603	0.2976
Case 2	19.50	0.609	1.391	0.7791	0.2418
Case 3	8.79	0.921	1.151	0.5866	0.3167
Case 4	10.47	0.961	1.078	0.5392	0.2789

Table 3: experiment results with optimal values and the minimum error.

The experimental results show that the case 2, which uses the stationary parameters, yields the minimum error value of 0.2418 compare to the other results. This result can be directly comparable with Castanet. *et al* study [15] which yielded average relative errors around 0.3. Figures 3 illustrate the DBSG3 R0.01% values for the 415 DBSG3 site-years with annual data, and the best fit predicted R0.01% values using the

optimal parameters from cases 1, 2 and 4. The data are in temporal order and the increasing trend in the rain rates is due to the increasing amounts of data from Asia and South America in recent decades. The best fit follows gross trends well but there is still considerable deviation for specific site-years.
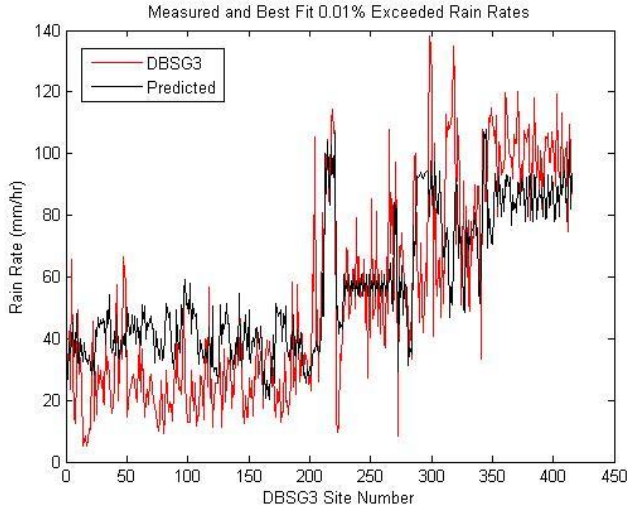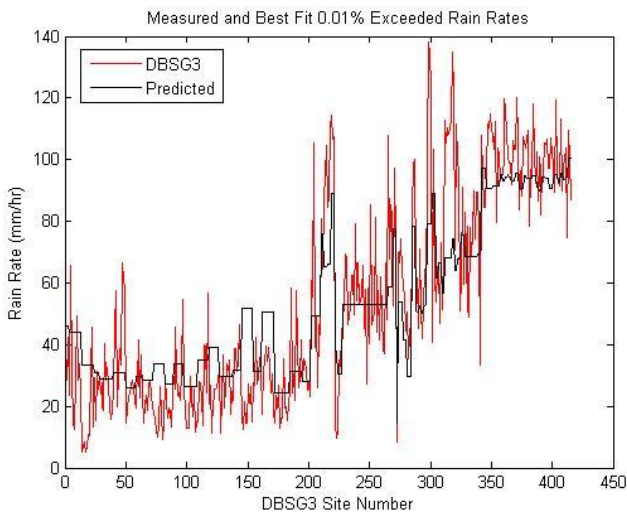

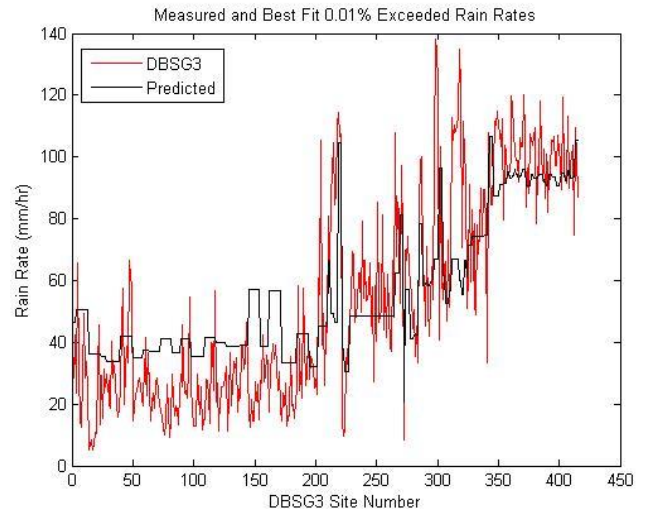Figure 3a: Case 1.

Figure 3b: Case 2.

Figure 3c: Case 4

Figure 3: Time series of measured annual 0.01% exceeded rain rates compared to the best fit prediction using: a) Case 1, b) Case 2 and c) Case 4.

Figure 3 illustrates some features of the problem. All the optimized fits follow the gross pattern of increasing R0.01% as DBSG3 sites have changed from being principally in Europe and North America to Asia and South America. The prediction methods based on average annual parameters, cases 2 and 3, yield one predicted distribution for each site. Measured 0.01% exceeded rain rates from a single site can show factors of four variation due to year-to-year variability. The use of specific annual input parameters yields some correlation between predicted and measured R0.01% in Europe, but doesn't perform better due to general over-estimation in Europe and under-estimation in Asia and South America. These biases are also present in the other cases and reflect an underlying problem with the transformation (2). In particular, the difference in convective fractions between temperate and tropical climates does not affect the distribution parameters a, b and c.

V. Time series of predicted rain rates

The calibrated NOAA data illustrated in Figs 1 and 2, allow the calculation of time series of 0.01% exceeded rain rates using the distribution (1) and the transformation (2) using Case 2 optimised constants. This is speculative as the input and output parameters to the SPB distribution and transformation are average annual values, as discussed in the Introduction. However, even if the method is a poor predictor of individual yearly rain rate distributions, it is

possible that long term trends will be reproduced. Figure 4 illustrates these 0.01% exceeded rain rate time-series for the three NOAA grid regions spanning the UK. All three time-series show large year-to-year variation, but also exhibit increasing trends of approximately 0.4, 1.0 and 0.1 mm/hr/year for the regions South, Midlands and North respectively.
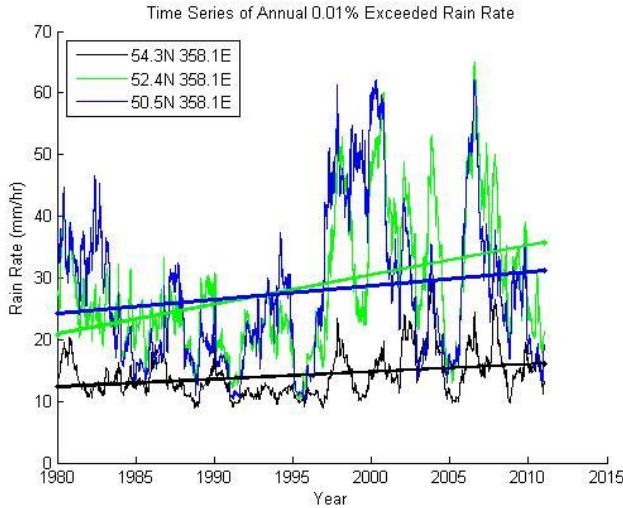

Figure 4: Time series of 0.01% exceeded rain rates derived from NOAA Reanalysis data using distribution (1) and the transformation (2)

Figure 5 shows the rain rates exceeded at annual time percentages of 0.005%, 0.01%, 0.03%, 0.05% and 0.1%, for the eighty rain gauges in Southern England, [2]. Error bars indicate the mean, upper and lower quartiles for the best fit Weibull distribution to all the available exceeded rain rates for each annual period. The gradient of the maximum likelihood (MLE) line fitted to the 0.01% exceedance data has a slope on 0.44 mm/hr/year.
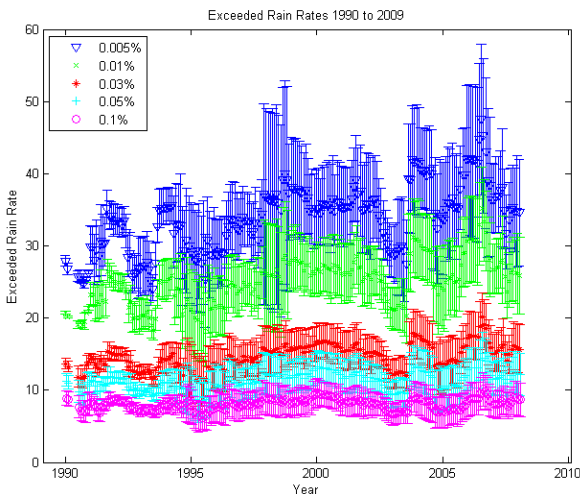

Figure 5: time-series of exceeded annual rain rates from 80 gauges in the Southern UK.

The slope of the 0.01% exceeded rain rate can also be compared to that found in the Ofcom study, based on 1350 high resolution rain gauges across the UK, [3]. This found increasing trends in 0.01% exceeded rain rates around 0.4 mm/hr/year in the north and 0.8 mm/hr/year in the south. Given the different time periods considered and the standard errors in the slopes, these results are consistent. Table 4 compares the 0.01% rain rate trend slopes predicted using the method in this Section and those from the Ofcom study. We have considered a simpler method where the transformation from rain parameters to 0.01% exceeded rain rate is linearised i.e.

$$\frac{dR_{0.01\%}}{dt} = \frac{dR_{0.01\%}}{dM_T}\frac{dM_T}{dt} + \frac{dR_{0.01\%}}{dM_C}\frac{dM_C}{dt} + \frac{dR_{0.01\%}}{dP_{r6h}}\frac{dP_{r6h}}{dt}$$

(3)

The derivatives of M_T, M_C and P_{r6}; were estimated by fitting linear regression lines to 21 year time-series, 1980 to 2001, of calibrated NOAA parameters. The derivatives of the transformation between rain parameters and the 0.01% exceeded rain rate were evaluated numerically around the 21 year average parameter value. From the chain rule (3), trend slopes in Figs. 2, the 0.01% rain rate was estimated for the three regions spanning the UK and results are shown in table 4.

Region	This Work	Ofcom Study
	Slope	Slope
North	0.6 mm/h/year	0.4 mm/h/year
Midlands	0.8 mm/h/year	0.6 mm/h/year
South	1 mm/h/year	0.8 mm/h/year

Table 4: Trend slopes of 0.01% exceeded rain rates over 3 UK regions.

VI. Global Trends in 0.01% rain rates

The time-series method applied to the estimation of 0.01% rain rate trends over the UK can be applied to the rest of the world. The GPCC data is only available for land areas and so the predictions are similarly constrained. From the calibrated NOAA/GPCC meteorological parameters, the time-series of 0.01% exceeded rain rates can then be calculated for each NOAA grid region. From the time-series, the slope of the trend line for each grid cell can be calculated. Figure 6 illustrates this trend slope.
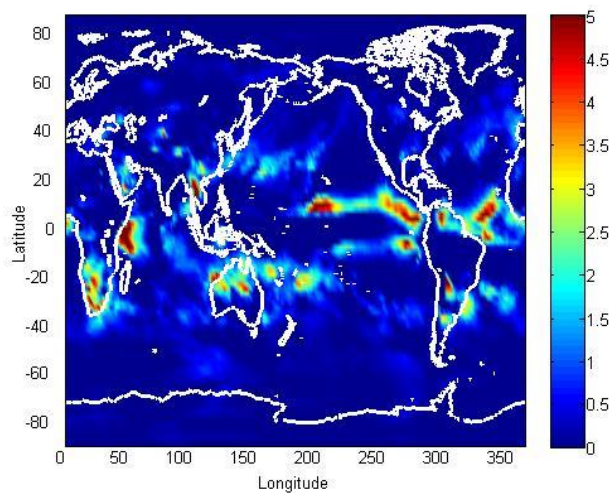
Figure 6: trend slope of 0.01% exceeded rain rates, in mm/hr/year, derived using the SPB distribution and transformation from NOAA/GPCC time series of precipitation parameters.

This approach is speculative as it has only been tested in the UK. However, it is better to have some estimate of 0.01% rain rate trends than none at all. For some regions the trend slopes are not reliable due to the low incidence of rain, particularly Saharan Africa and mountainous regions such as the Himalayas, Andes and Rockies. Of all the NOAA grid cells, 90% yielded trends that are statistically significant with a probability of occurring by chance of less than 1%. Of the trend slopes greater than 0.2 mm/hr/year, 40% are statistically significant. The results presented in Fig. 6 suggest many parts of the world are experiencing rapid increases in 0.01% rain rate; particularly tropical areas within 30° of the equator.

VII. Conclusions

A method has been developed for predicting the evolution of one-minute rain rate distributions, over land areas, globally. The method is based on the widely accepted Salonnen-Poiares-Baptista method that is integral to Rec. ITU-R P.836. We have extended the Salonnen-Baptista method by removing the implicit assumption of climate stationarity, and using GPCC calibrated NOAA reanalysis data rather than the ECMWF ERA40 data. The trend slope in 0.01% exceeded rain rates in three NOAA grid regions spanning the UK have been estimated with the new method and are consistent with results produced by two independent researchers analysing a large database of high resolution rain gauge data.

When climate trends lead to large changes in the underlying fade distributions, over the lifetime of a radio system, then these can have serious effects on system performance. Such changes can undermine the system the business model or make it not fit for purpose. These considerations are particularly important for expensive space based systems where hardware adaptation is difficult or impossible. Such systems are designed with wide margins to allow for climate variability. Introducing climate trends into the margin calculation may lead to more realistic estimates of the range of climates a system will encounter over its lifetime.

The assumption of climate stationarity is deeply embedded in the ITU-R recommendations and the processes controlling their evolution. Refinements of Recommendations are tested against the DBSG3 database of measurements, collected over the last 50 years. Removing the assumption of stationarity changes the way this database is used, as we have in the work described in this paper. When predicting the performance of systems several decades into the future, non-stationary recommendations are likely to produce more reliable results.

Acknowledgment

References

[1] K. S. Paulson, "Trends in the incidence of rain rates associated with outages on fixed links operating above 10 GHz in the southern United Kingdom", Radio Sci., 45, RS1011, doi:10.1029/2009RS004193, 2010.

[2] K. S. Paulson, "The Effects of Climate Change on Microwave Telecommunication" 11th International Conference on Telecommunication, ConTell, Graz, Japan, 2011

[3] D. Bacon, "Modelling Rain Rate Maps for Fixed-Link frequency Assignment Procedures", Ofcom contract No: 796, 2012

[4] K. S. Paulson, A, Al-Mreri, "Trends in the incidence of rain height and the effects on global stallite telecommunications", Microwaves, Antennas & Propagation, IET, vol 5, issue 14, 2011, pp. 1710-1713

[5] K. S. Paulson, A, Al-Mreri, "A rain height model to predict fading due to wet snow on terrestrial links", Radio Science, vol 46, issue 4, 2011

[6] E. T. Salonen and J. P. V. Poiares Baptisa, A new global rainfall rate model, 10th International Conference on Antennas and Propagation, 14-17 April 1997, Conference Publication No. 436 0 IEE 1997.

[7] [Poiares-Baptista and Salonen, 1998] Poiares-Baptista P., Salonen E., 1998: "Review of rainfall rate modelling and mapping", Proc. of URSI Commission F Open Symposium on Climatic Parameters in Radiowave Propagation Prediction (CLIMPARA'98), Ottawa, Ontario, Canada

[8] FASCICLE CONCERNING THE RAINFALL RATE MODEL GIVEN IN RECOMMENDATION ITU-R P.837-5.

[9] ITU-R Study Group 3 Databanks - DBSG3, Available at: <http://saruman.estec.esa.nl/dbsg3/login.jsp> [Accessed at 01 February 2014].

[10] ERA: ECMWF Re-analysis project report series, "ERA-40 Archive", December 2002, European Centre for Medium-Range Weather Forecasts.

[11] Kalnay E., Kanamitsu, M., Kistler, P. Collins, W. Deaven, D. Gandin, L. Iredell, M. Saha, S. White, G. Woollen, J. Zhu, Y. Cheillab, M, Ebsuzaki, W. Higgins, W. Janowiak, J. Mo, K. C. Ropelewski, C. Wang, J. Leetma, A. Reynolds, P. Jenne 1. and Joseph, D. "The NCEP/NCAP 40-year reanalysis project", Bull. Amer. Meteor. Soc., 1996, 77, pp 437-470.

[12] U. Schneider, A. B., A. Meyer-Christoffer, M. Ziese, B. Rudolf (2008). Global Precipitation Analysis Products of the GPCC. Germany, Global Precipitation Climatology Centre.

[13] S. Solomon, et al., "Climate Change 2007: The physical science basis. Contribution of Working Group I to the Fourth Assessment Report of the Intergovernmental Panel on Climate Change," Cambridge and New York 2007.

Kevin S. Paulson: received the B.Sc. degree in physics and the M.Sc. degree in atmospheric physics from the University of Auckland, New Zealand, and the Ph.D. degree in applied mathematics from Oxford Brookes University, Oxford, U.K., for work in medical electrical impedance tomography. From 1998 to 2004, he led research into terrestrial radio telecommunications in the Radio Communications Research Group of Rutherford Appleton Laboratory, U.K. His primary research interest is the mitigation of rain fading across radio networks. He initiated the Research Council funded Rainmap network coordinating research into the broad-scale modeling of rain for engineering applications. Currently he is a Senior Lecturer in Telecommunications at the University of Hull, U.K.

Channa Ranatunga: was born in Sri Lanka and received his BSc in Mobile Computer Technology from Manchester Metropolitan University, UK. Currently he is in his 3rd year of doctoral studies in Electronic Engineering at the University of Hull, UK.

Tim Bellerby: received BSc in Applied Mathematics from the University of Warwick and a PhD in Geophysics from the University of Sheffield. He was a Research Associate at the University of Bristol Centre for Remote Sensing and a contactor to the United States National Weather Service. Currently he is a Senior Lecturer in Geography at the University of Hull, UK

References

ARKIN, P. A. & XIE, P. 1994. The Global Precipitation Climatology Project: First Algorithm Intercomparison Project *Bulletin of Americal Meteorological Society,* 75, 401-419.

BACON, D. 2012. Modelling Rain Rate Maps for Fixed-Link Frequency Assignment Procedures. Ofcom. Contract No: 796. Web: http://stakeholders.ofcom.org.uk/binaries/research/technology-research/2012-2013/RainRateFinal.pdf

BECK, C., J. GRIESER & RUDOLF, B. 2004. A New Monthly Precipitation Climatology for the Global Land Areas for the Period 1951 to 2000. *Climate Status Report* Offenbach, Germany: German Weather Services

BECKER, A. 2012. High-Resolution Precipitation Dataset *GCOS/WCRP ATMOSPHERIC OBSERVATION PANEL FOR CLIMATE.* Geneva, Switzerland.

BELEN, M., O. CLAUDE, V. DANIELLE, P. ROBERTO & ANTONIO, M. Year. Review and Update of Mobile Data Processing for the Land Mobile Satellite Channel Modelling*:* Proceedings of the Fourth European Conference on Antennas and Propagation (EuCap), 12 – 16 April 2010 Barcelona, Spain. 1-4.

BRADLEY, R. S., KEIMIG, F. T., DIAZ, H. F. & HARDY, D. R. 2009. Recent changes in freezing level heights in the Tropics with implications for the deglacierization of high mountain regions. *Geophysical Research Letters,* 36.

CASTANET, L., CAPSONI, C., BLARZINO, G., FERRARO, D. & MARTELLUCCI, A. 2007. Development of a new global rainfall rate model based on ERA40, TRMM and GPCC products *:* Proceedings of ISAP07, Niigata, Japan. 1378-1381.

CHEN, K. S., CHU, C. Y. & TZENG, Y. C. 2011. A Semi-Empirical Model of Rain Atyenuation at KA-band in Northern Taiwan. *Progress In Electromagnetics Research M,* 16, 213-223.

CRANE, R. K. 1980. Prediction of Attenuation by Rain. *IEEE Transactions on Communications,* 28, 1717-1733.

CRANE, R. K. 1982. A two-component rain model for the prediction of attenuation statistics. *Radio Science,* 17, 1371-1387.

CRANE, R. K. 2003. *Propagation Handbook for Wireless Communication System Design*, CRC Press.

CRANE, R. K. & SHIEH, H. C. 1989. A two-component rain model for the prediction of site diversity performance. *Radio Science,* 24, 641-665.

DEEA, D. P., S. M. UPPALAA, A. J. SIMMONSA, P. BERRISFORDA, P. POLIA, S. KOBAYASHIB, U. ANDRAEC, M. A. BALMASEDAA, G. BALSAMOA, P. BAUERA, P. BECHTOLDA, A. C. M. BELJAARSA, L. VAN DE BERGD, J. BIDLOTA, N. BORMANNA, C. DELSOLA, R. DRAGANIA, M. FUENTESA, A. J. GEERA, L. HAIMBERGERE, S. B. HEALYA, H. HERSBACHA, E. V. H´OLMA, L. ISAKSENA, P. KALLBERGC, M. K¨OHLERA, M. MATRICARDIA, A. P. MCNALLYA, B. M. MONGE-SANZF , J.-J. MORCRETTEA, B.-K. PARKG, C. PEUBEYA, P. DE ROSNAYA, C. TAVOLATOE, THEPAUTA, J.-N. & VITARTA, F. 2011. The ERA-Interim reanalysis: configuration and performance of the data assimilation system. *Royal Meteorological Society,* 137, 553-597.

DIAZ, H. & GRAHAM, N. 1996. Recent changes in tropical freezing heights and the role of sea surface temperature. *Nature*, 152–155.

EASTERBROOK, B. J. & TURNER, D. 1967. Prediction of attenuation by rainfall in the 10.7–11.7 GHz communication band. *In:* Proceedings of the Institution of Electrical Engineers, IET, 557-565.

EBERT, E. E. & MANTON, M. J. 1998. Performance of Satellite Rainfall Estimation Algorithms during TOGA COARE. *Jouurnal of The Atmospheric Sciences,* 55, 1537-1557.

FIELD, C. B., V.R. BARROS, D.J. DOKKEN, K.J. MACH, M.D. MASTRANDREA, T.E. BILIR, M. CHATTERJEE, K.L. EBI, Y. O., ESTRADA, R. C., GENOVA, B. G., E.S. KISSEL, A. N. L., S. MACCRACKEN, P.R. MASTRANDREA & (EDS.)., L. L. W. 2014. IPCC, 2014: Summary for policymakers. In: Climate Change 2014: Impacts, Adaptation, and Vulnerability. Part A: Global and Sectoral Aspects. Contribution of Working Group II to the Fifth Assessment Report of the Intergovernmental Panel on Climate Change. Cambridge University Press, Cambridge, United Kingdom and New York, NY, USA.

GIBSON, J. K., P. KALLBERG, S. UPPALA, A. HERNANDEZ, A. NOMURA & SERRANO, E. 1999. ECMWF Re-Analysis Project Report Series: ERA-15 Description. European Centre for Medium-Range Weather Forecasts.

GOES-R: Benefits of Next-Generation Environmental Monitoring. [Online]. Available:http://stream2.cma.gov.cn/pub/comet/SatelliteMeteorology/G OESRBenefitsofNextGenerationEnvironmentalMonitoring/comet/goes_r /envmon/print.htm [Accessed 11 June 2014].

GROISMAN, P. Y. & LEGATES, D. R. 1994. The accuracy of United States precipitation data. *Bulletin of Americal Meteorological Sociery,* 75, 215-227.

HARRIS, J. R., GETTYS, N., KENNETH, P. B. & DONG-BIN, S. 2000. Comparison of Freezing-Level Altitudes from the NCEP Reanalysis with TRMM Precipitation Radar Bright Band Data. *Journal of Climate*, 4137-4148.

HERTZOG, A., BASDEVANT, C. & VIAL, F. 2006. An Assessment of ECMWF and NCEP–NCAR Reanalyses in the Southern Hemisphere at the End of the Presatellite Era: Results from the EOLE Experiment (1971–72). *American Meteorological Society,* 134, 3367- 3383.

HUFFMAN, G. J. & BOLVIN, D. T. 2013. GPCP Version 2.2 SG Combined Precipitation Data Set Documentation. Frankfurt: Deutscher Wetterdienst.

HUFFMAN, G. J., R. F. ADLER, B. RUDOLF, U. SCHNEIDER & P. R. KEEHN 1995. Global precipitation estimates based on a technique for combining satellite-based estimates, rain gauge analysis, and NWP model precipitation information. *Journal of Climate,* 8, 1284-1295.

HUFFMAN, G. J., R. F. ADLER, P. ARKIN, A. CHANG, R. FERRARO, A. GRUBER, J. JANOWIAK, A. MCNAB, B. RUDOLF & SCHNEIDER, U. 1997. The Global Precipitation Climatology Project (GPCP) Combined Precipitation Dataset. *Bulletin of the American Meteorological Society 5,* 78, 5-20.

HULST, H. C. V. D. 1981. *Light Scattering by Small Particles,* New York, USA, Dover Publications.

HUNTER, S. M. 1996. WSR-88D Radar Rainfall Estimation: Capabilities, Limitations and Potential Improvements. *National Weather Service Dig. ,* 20, 26-38.

ITU-R. *DBSG3* [Online]. Available: http://saruman.estec.esa.nl/dbsg3/login.jsp [Accessed 15/01/2014].

ITU-R:STUDYGROUP3 2012. Fascicle concerning the rainfall rate model given in Annex 1 to Recommendation. *ITU-R P.837-6, International Telecommunication Union Radiocommunication*

ITU:REC.P.311-14 2013. Acquisition, presentation and analysis of data in studies of tropospheric propagation *P Series* Geneva, Switzerland: International Telecommunication Union.

ITU:REC.P.530-15 2013. Propagation data and trediction methods required for the design of terrestrial line-of-sight systems *P Series* Geneva, Switzerland: International Telecommunication Union.

ITU:REC.P.618-11 2013. Propagation data and prediction methods required for the design of Earth-Space telecommunication system. *P Series* Geneva, Switzerland: International Telecommunication Union.

ITU:REC.P.837-6 2012. Characteristics of precipitation for propagation modelling

P Series Geneva, Switzerland: ITU Recommendation Sector

ITU:REC.P.838-3 2005. Specific attenuation model for rain for use in prediction methods. *P Series* Geneva, Switzerland: International Telecommunication Union

JENKINS, G. J., PERRY, M. C. & PRIOR, M. J. 2009. The climate of the United Kingdom and recent trends. *In:* CENTRE, M. O. H. (ed.). Exeter.

JENNE, R. 1999. GLOBAL OBSERVATIONS FOR REANALYSIS, 1948 – ON. *Proceeding of 2nd International Reanalysis Conference* Waterfield Park, Reading, United Kingdom.

JOSS, J. & WALDVOGEL, A. 1977. Comments onSome Observations on the Joss-Waldvogel Rainfall Disdrometer'. *Journal of Applied Meteorology,* 16, 112-112.

KALNAY, E., M. KANAMITSU, R. KISTLER, W. COLLINS, D. DEAVEN, L. GANDIN, M. IREDELL, S. SAHA, G. WHITE, J. WOOLLEN, Y. ZHU, M. CHELLIAH, W. EBISUZAKI, W. HIGGINS, J. JANOWIAK, K. C. MO, C. ROPELEWSKI, J. WANG, A. LEETMAA, REYNOLDS, R., ROY JENNE & JOSEPH, D. 1996. The NCEP/NCAR 40-Year Reanalysis Project. *Bulletin of Americal Meteorological Sociery,* 77, 437-471.

KISTLER, R., E. KALNAY, W. COLLINS, S. SAHA, G. WHITE, J. WOOLLEN, M. CHELLIAH, W. EBISUZAKI, M. KANAMITSU, V. KOUSKY, H. DEN DOOL, R. JENNE & FIORINO, M. 2001. The NCEP–NCAR 50-Year Reanalysis: Monthly Means CD-ROM and Documentation. *Bulletin of the American Meteorological Society,* 82.

KITCHEN, M. & JACKSON, P. M. 1993. Weather radar performance at long range - Simulated and observed. *Journal of Applied Meteorology,* 32, 975-985.

KOUROGIORGA, C., L. FERAL, V. FABBRO, N. JEANNIN & LEMORTON, J. 2010. Use of the HYCELL Model for Predicting Rain Attenuation on UAS Low Elevation Data links. *In:* Proceedings of the Fourth European Conference on Antennas and Propagation (EuCap), 12 – 16 April 2010 Barcelona, Spain. 1-5.

LAWS, J. O. & PARSONS, D. A. 1943. The relation of raindrop-size to intensity. *Transactions, American Geophysical Union,* 24, 452-460.

LEMPIO, G., BUMKE, K. & MACKE, A. 2007. Measurement of solid precipitation with an optical disdrometer. *Advances in Geosciences,* 10, 91-97.

LIN, S. H. 1973. Statistical Behavior of Rain Attenuation. *Bell System Technical Journal,* 52, 557-581.

LUINI, L. & CAPSONI, C. 2010. A Physically Based Methodology For The Evaluation Of The Rain Attenuation On Terrestrial Radio Links. *In:* Proceedings of the Fourth European Conference on Antennas and Propagation (EuCAP), 12 – 16 April 2010 Barcelona, Spain. 1-5.

MANDEEP, J. S. 2009. Comparison of rainfall models with Ku-band beacon measurement. *Acta Astronautica,* 64, 264-271.

MARAUN, D., OSBORN, T. J. & GILLETT, N. P. 2008. United Kingdom daily precipitation intensity: Improved early data, error estimates and an update from 2000 to 2006. *International Journal of Climatology,* 28, 833 - 842.

MARAUN, D., RUST, H. W. & OSBORN, T. J. 2009. The annual cycle of heavy precipitation across the United Kingdom: a model based on extreme value statistics. *International Journal of Climatology,* 29, 1731-1744.

MARSHALL, J. S. & PALMER, W. M. K. 1948. The distribution of raindrops with size. *Journal of meteorology,* 5, 165-166.

MEEHL, G. A., STOCKER, T. F., COLLINS, W. D., FRIEDLINGSTEIN, P., GAYE, A. T., GREGORY, J. M., KITOH, A., KNUTTI, R., MURPHY, J. M., NODA, A., RAPER, S. C. B., WATTERSON, I. G., WEAVER, A. J. & ZHAO, Z. C. Climate change 2007: The physical science basis, Contribution of Working Group I to the Fourth Assessment Report of the Intergovernmental Panel on Climate Change, Chapter Global Climate Projections. Cambridge, New York.

MO, K. C., WANG, X. L., KISTLER, R., KANAMITSU, M. & KALNAY, E. 1995. Impact of Satellite Data on the CDAS-Reanalysis System. *Monthly Weather Review* 123, 124-139.

MYERS, W. 1999. Comparison of Propagation Models *In:* IEEE Transaction P802.16cc-99/13.

NCAR/UCAR. 2014. *JRA-25* [Online]. Available: https://climatedataguide.ucar.edu/climate-data/jra-25 [Accessed 01/06/2014].

ONOGI, K. J., J. TSUTSUI, H. KOIDE, M. SAKAMOTO, S. KOBAYASHI, H. HATSUSHIKA, T. MATSUMOTO, N. YAMAZAKI, H. KAMAHORI, K. TAKAHASHI, S. KADOKURA, K. WADA, K. KATO, R. OYAMA, T. OSE, MANNOJI, N. & TAIRA, R. 2007. The JRA-25 Reanalysis *Journal of Meteorological Society of Japan,* 82, 369-432.

OSBORN, T. J., HULME, M., JONES, P. D. & BASNETT, T. A. 2000. Observed trends in the daily intensity of United Kingdom precipitation. *International Journal of Climatology,* 20, 347-364.

PARKER, D., GOOD, E. & CHADWICK, R. 2011. Reviews of Observational Data Available over Africa for Monitoring, Attribution and Forecast Evaluation *Hadley Centre Technical Note 86.* Exeter Met Office Hadley Centre.

PASAGOPOULOS, A. D., ARAPOGLOU, P.-D. M. & COTTIS, P. G. 2004. Satellite communications at KU, KA, and V bands: Propagation impairments and mitigation techniques. *IEEE, Communications Surveys & Tutorials,* 6, 2-14.

PAULSON, K. . The Effects of Climate Change on Microwave Telecommunications. *In:* CONTEL, ed. International Conference on Telecommunications 2011a Graz, Austria. 157-160.

PAULSON, K. & AL-MRERI, A. 2011a. A Rain Height Model to Predict Fading due to Wet Snow on Terrestrial Links. *RADIO SCIENCE,* 46.

PAULSON, K. & AL-MRERI, A. 2011b. Trends in the incidence of rain height and the effects on global satellite telecommunications. *IET Microwaves, Antennas & Propagation,* 5, 1710-1713.

PAULSON, K. & GIBBINS, C. 2000. Rain models for the prediction of fade durations at millimetre wavelengths: Microwaves, Antennas and Propagation, IEE Proceedings, IET, 431-436.

PAULSON, K. S. 2010. Trends in the incidence of rain rates associated with outages on fixed links operating above 10 GHz in the southern United Kingdom. *Radio Science,* 45, 9.

PAULSON, K. S. The Effects of Climate Change on Microwave Telecommunications. *In:* Proceedings of the 11th International Conference on Telecommunications (ConTEL), June 2011b Graza, Austria. 157-160.

PECK, E. L. 1997. QUALITY OF HYDROMETEOROLOGICAL DATA IN COLD REGIONS. *JOURNAL OF THE AMERICAN WATER RESOURCES ASSOCIATION,* 33, 125-134.

POIARES BAPTISTA, J. P. V & SALONEN, E. T. 1998. Review of rainfall rate modelling and mapping*:* Proceedings of USRI-F Open Symposium, CLIMAPARA, 1998. 35-44.

RUDOLF, B. & FUCHS, T. 2006. Monthly rain gauge-based monitoring and assessment of global precipitation on Earth's land surface. Global Precipitation Climatology Centre (GPCC).

SALONEN, E. T & POIARES BAPTISTA, J. P. V 1997. A new global rainfall rate model. *In:* Antennas and Propagation, Tenth International Conference on (Conf. Publ. No. 436), IET, 182-185.

SCHNEIDER, U., A. BECKER, A. MEYER-CHRISTOFFER, M. ZIESE & RUDOLF, B. 2011. Global Precipitation Analysis Products of the GPCC. Deutscher Wetterdienst, Offenbach a. M., Germany.

SCOFIELD, R. A. & KUIGOWSKI, R. J. 2003. Status and Outlook of Operational Satellite Precipitation Algorithms for Extreme-Precipitation Events. *National Environmental Satellite, Data, and Information Service,,* 18, 1037-1051.

SIMMONS, A. J. & GIBSON, J. K. 2000. The ERA-40 Project Plan. ERA-40 Project Report. Series 1. Shinfield Park, Reading, United Kingdom: ECMWF

SMITH, J. A., A. A. BRADLEY & BAECK, M. L. 1994. The Space-Time Structure of Extreame Storm Rainfall in the Southern Plains *Journal of Applied Meteorology,* 33, 1402, 1417.

SMITH, J. A., D. J. SEO, M. L. BAECK & HUDLOW, M. D. 1996. An intercomparison study of NEXRAD precipitation estimates. *WATER RESOURCES RESEARCH,* 32, 2035-2045.

SOLOMON, S., QIN, D., MANNING, M., MARQUIS, M., AVERYT, K. B., TIGNOR, M. & MILLER, H. L. 2007. Climate Change 2007: The physical science basis. Contribution of Working Group I to the Fourth Assessment Report of the Intergovernmental Panel on Climate Change: IPCC (ed.). Cambridge and New York.

STOCKER, T.F., D. QIN, G.-K. PLATTNER, M. TIGNOR, S.K. ALLEN, J. BOSCHUNG, A. NAUELS, Y. XIA, V. BEX and P.M. MIDGLEY (eds.). IPCC, 2013: Summary for Policymakers. In: Climate Change 2013: The Physical Science Basis. Contribution of Working Group I to the Fifth Assessment Report of the Intergovernmental Panel on Climate Change Cambridge University Press, Cambridge, United Kingdom and New, NY, USA.

TRENBERTH, K. E., JONES, P. D., AMBENJE, P., BOJARIU, R., EASTERLING, D., TANK, A. K., PARKER, D., RAHIMZADEH, F., RENWICK, J. A., RUSTICUCCI, M., SODEN, B. & ZHAI, P. 2007. Climate change 2007: the physical science basis. *Contribution of Working Group I to the Fourth Assessment Report of the Intergovernmental Panel on Climate Change, Chapter Observations: Surface and Atmospheric Climate Change.* New York.

TURNER, D. & TURNER, D. 1970. Attenuation due to rainfall on a 24 km microwave link working at 11, 18 and 36 GHz. *Electronics Letters,* 6, 297-298.

ULBRICH, C. W. 1983. Natural variations in the analytical form of the raindrop size distribution. *Journal of Climate and Applied Meteorology,* 22, 1764-1775.

UPPALA, S. M., P. W. KALLBERG, A. J. SIMMONS, U. ANDRAE, V. DA COSTA BECHTOLD, M. FIORINO, J. K. GIBSON, J. HASELER, A. HERNANDEZ, G. A. KELLY, LI, X., K. ONOGI, S. SAARINEN, N. SOKKA, R. P. ALLAN, E. ANDERSSON, K. ARPE6, BALMASEDA, M. A., A. C. M. BELJAARS, L. VANDE BERG, J. BIDLOT, N. BORMANN, S. CAIRES, F. CHEVALLIER, A. DETHOF, M. DRAGOSAVAC, M. FISHE, M. FUENTES, S. HAGEMANN, E. HO´ LM, B. J. HOSKINS, L. ISAKSEN, P. A. E. M. JANSSEN, R. JENNE, A. P.MCNALLY, J.-F. MAHFOUF, J.-J. MORCRETTE, N. A. RAYNER, R. W. SAUNDERS, P. SIMON, A. STERL, K. E. TRENBERTH, A. UNTCH, D. VASILJEVIC, VITERBO, P. & WOOLLEN13, J. 2005. The ERA-40 re-analysis. *Quarterly Journal of The Royal Meteorological Society,* 131, 2961-3012.

USMAN, I. S. 2005. *Development of point to multipoint models for available and fade mitigation in the millimeter wave frequency range.* University of Bath, UK.

WALDVOGEL, A. 1974. The N 0 jump of raindrop spectra. *Journal of The Atmospheric Sciences,* 31, 1067-1078.

WATERHISTORY.ORG. *The Nilometer in Cairo* [Online]. Available: http://www.waterhistory.org/histories/cairo/ [Accessed 01/06/2014 2014].

XIE, P. & ARKIN, P. A. 1997. Global Precipitation: A 17-Year Monthly Analysis Based on Gauge Observations, Satellite Estimates, and Numerical Model Outputs. *Bulletin of the American Meteorological Society,* 78, 2539-2558.